

INFORMATION TO USERS

This manuscript has been reproduced from the microfilm master. UMI films the text directly from the original or copy submitted. Thus, some thesis and dissertation copies are in typewriter face, while others may be from any type of computer printer.

The quality of this reproduction is dependent upon the quality of the copy submitted. Broken or indistinct print, colored or poor quality illustrations and photographs, print bleedthrough, substandard margins, and improper alignment can adversely affect reproduction.

In the unlikely event that the author did not send UMI a complete manuscript and there are missing pages, these will be noted. Also, if unauthorized copyright material had to be removed, a note will indicate the deletion.

Oversize materials (e.g., maps, drawings, charts) are reproduced by sectioning the original, beginning at the upper left-hand corner and continuing from left to right in equal sections with small overlaps.

Photographs included in the original manuscript have been reproduced xerographically in this copy. Higher quality 6" x 9" black and white photographic prints are available for any photographs or illustrations appearing in this copy for an additional charge. Contact UMI directly to order.

ProQuest Information and Learning
300 North Zeeb Road, Ann Arbor, MI 48106-1346 USA
800-521-0600

UMI[®]

**DYNAMIC ANALYSIS AND BUCKLING OF VARIABLE
THICKNESS LAMINATED COMPOSITE BEAMS USING
CONVENTIONAL AND ADVANCED FINITE ELEMENT
FORMULATIONS**

Abd EL-Maksoud, Mohamed A.

A Thesis
in
The Department
of
Mechanical Engineering

Presented in Partial Fulfillment of the requirement
for the Degree of Master of Applied Science at
Concordia University
Montreal, Quebec, Canada

December 2000

© Abd EL-Maksoud, Mohamed A.



National Library
of Canada

Acquisitions and
Bibliographic Services

395 Wellington Street
Ottawa ON K1A 0N4
Canada

Bibliothèque nationale
du Canada

Acquisitions et
services bibliographiques

395, rue Wellington
Ottawa ON K1A 0N4
Canada

Your file Votre référence

Our file Notre référence

The author has granted a non-exclusive licence allowing the National Library of Canada to reproduce, loan, distribute or sell copies of this thesis in microform, paper or electronic formats.

The author retains ownership of the copyright in this thesis. Neither the thesis nor substantial extracts from it may be printed or otherwise reproduced without the author's permission.

L'auteur a accordé une licence non exclusive permettant à la Bibliothèque nationale du Canada de reproduire, prêter, distribuer ou vendre des copies de cette thèse sous la forme de microfiche/film, de reproduction sur papier ou sur format électronique.

L'auteur conserve la propriété du droit d'auteur qui protège cette thèse. Ni la thèse ni des extraits substantiels de celle-ci ne doivent être imprimés ou autrement reproduits sans son autorisation.

0-612-59313-4

Canada

ABSTRACT

Dynamic Analysis and Buckling of Variable Thickness Laminated Composite Beams Using Conventional and Advanced Finite Element Formulations

Abd EL-Maksoud, Mohamed A.

The use of uniform composite beams has been ever growing since the 1940s. Recently, the tapered composite beams formed by terminating or dropping off some of the plies in some primary structures have received much attention since the mid-1980s because of their structural tailoring capabilities, damage tolerance, and their potential for creating significant weight savings in engineering applications. Design of mechanical components using composite beams requires a better understanding of their behavior in the static and dynamic analyses. The behavior of variable thickness laminated composite beams has not so far been fully understood. In the present thesis, a finite element formulation is established for uniform and variable thickness composite beams (externally and mid-plane tapered composite beams). First the conventional formulation is used to establish the stiffness, geometric stiffness (for constant axial load, uniformly distributed axial load, and non-uniformly distributed axial load), and mass matrices. Second a new formulation (advanced formulation) is established, which considers not only the geometric boundary conditions, but also the natural boundary conditions. This means that at each node there will be four degrees of freedom, that are deflection, slope,

bending moment, and shear force, such that all physical parameters that can be encountered in any practical situation can be included in the element formulation. The new stiffness, geometric stiffness, and mass matrices corresponding to the new formulation are set up. These matrices are provided into the MATLAB[®] environment to obtain the natural frequencies and the critical buckling load. The results show that the new formulation provides higher accuracy with lesser number of elements. The dynamic response and the buckling of variable thickness composite beams are investigated using both the conventional and advanced finite element formulations. A parametric study encompassing the influences of boundary conditions, laminate configuration, taper angle and type, and beam discretization on the response of the beam is conducted. The NCT-301 graphite epoxy composite material is employed in the analysis and in the parametric study.

Acknowledgments

The author wishes to express his gratitude to his thesis supervisor Dr. Rajamohan Ganesan for his great support and encouragement throughout the journey of the development of the thesis. Also, special thanks to the Mechanical Department of Concordia University for the different facilities they offered.

The author extends his gratefulness to his family and his friends for their continuous kindness.

List of Contents

Abstract	iii
List of Figures	xi
List of Tables	xvi
Nomenclature	xviii
Chapter 1 Introduction	1
1.1 Dynamic Analysis and Buckling in Mechanical Design	1
1.2 Composite Material and Structures in Mechanical Design	2
1.3 Analysis and Solution Methods in Mechanical Design	5
1.4 Literature Survey	6
1.4.1 Literature Survey on Vibration Analysis	6
1.4.2 Literature Survey on Elastic Stability	13
1.4.3 Literature Survey on Finite Element Method	15
1.5 Objective of the Thesis	19
1.6 Layout of the Thesis	20
Chapter 2 Dynamic Analysis of Variable Thickness Composite Beams Using Conventional Finite Element Formulation	23
2.1 Introduction	23
2.2 Weak Formulation Based on Euler-Bernoulli Theory	25

2.3	Weak Formulation of the Problem	29
2.3.1	Weak Formulation for Uniform and Externally Tapered Composite Beams	29
2.3.2	Weak Formulation for Mid-Plane Tapered Composite Beams	38
2.3.3	Assembly of Elements and Imposing the Boundary Conditions	40
2.4	Modeling Variable Thickness Composite Beams	41
2.4.1	Modeling Externally Tapered Composite Beams	41
2.4.2	Modeling Mid-Plane Tapered Composite Beams	42
2.5	Solution of Equilibrium Equations in Dynamic Analysis	44
2.6	Program Development For Vibration and Buckling Analyses	46
2.6.1	Subroutines of the Program	49
	2.6.1.1 Subroutine TRANMAT	49
	2.6.1.2 Subroutine ELEFREX	49
	2.6.1.3 Subroutine ELESTF	49
	2.6.1.4 Subroutine ELEMAS	50
	2.6.1.5 Subroutine CONTRN	50
	2.6.1.6 Subroutine EIGZF	50
	2.6.1.7 Subroutine FORVNM	50
	2.6.1.8 Subroutine FORVWT	51
2.7	Example Problems and Validations	53
2.7.1	Beams Made of Metals	53

2.7.2	Example Problems and Validation for Composite Beams	67
2.8	Conclusions and Discussion	79
Chapter 3	Dynamic Analysis of Variable Thickness Composite Beams Using Advanced Finite Element Formulations	80
3.1	Introduction	80
3.2	Formulation Based on Euler-Bernoulli Theory	82
3.3	Weak Formulation of the Governing Equation	82
3.2.1	Weak Formulation for Uniform and Externally Tapered Composite Beams	82
3.2.2	Weak Formulation for Mid-Plane Tapered Composite Beams	109
3.4	Assembly of Elements and Imposing the Boundary Conditions	
3.4.1	Assembly of Element Equations	112
3.4.2	Imposing Boundary Conditions	116
3.5	Modeling Variable Thickness Composite Beams	117
3.5.1	Modeling Externally Tapered Composite Beams	117
3.5.2	Modeling Mid-Plane Tapered Composite Beams	118
3.6	Program Development For Vibration and Buckling Analyses	120
3.6.1	Subroutine ELESTF8	120

3.6.2	Subroutine ELEMAS8	120
3.7	Example Problems and Validations	121
3.7.1	Example Problems Involving Metallic Materials	121
3.7.2	Example Problems and Validation for Composite Beams	124
3.8	Conclusions and Discussions	129
Chapter 4	Parametric Study on Variable Thickness Composite Beams	141
4.1	Introduction	131
4.2	Parametric Study on Externally Tapered Composite Beams	133
4.2.1	The Effect of Boundary Conditions on the Natural Frequencies	134
4.2.2	The Effect of Fiber Orientations on the Natural Frequencies	142
4.2.3	The Effect of the Beam Discretization on the Natural Frequencies	148
4.3	Parametric Study on Mid-Plane Tapered Composite Beams	157
4.3.1	The Effect of Boundary Conditions on the Natural Frequencies	157
4.3.2	The Effect of Fiber Orientations on the Natural Frequencies	163

4.3.3	The Effect of Taper Angles on the Natural Frequencies	167
4.3.4	The Effect of the Beam Discretization on the Natural Frequencies	173
4.4	Parametric Study on Buckling of Externally Tapered Composite Beams	176
4.5	Overall Conclusions and Discussion	179
4.6	Summary	182
Chapter 5	Recommendations and Future Work	183
References		187
Appendix I		194

List of Figures

Figure 2.1	Basic types of tapers in composite beams	24
Figure 2.2	A beam-column with static axial force and dynamic lateral load	25
Figure 2.3	Typical rod or beam	27
Figure 2.4	Finite-Element Discretization and a Typical Element	30
Figure 2.6	Modeling of Externally Tapered Composite Beam	41
Figure 2.7	Modeling of Mid-plane Tapered Composite Beam	43
Figure 2.8	Six-Degrees-Of-Freedom Frame Element	47
Figure 2.9	The structure of MATLAB [®] program for determining the natural frequencies and the dynamic response of metallic and composite beam	52
Figure 2.10	Free vibration analysis of a simply supported beam	54
Figure 2.11	Free Vibration Analysis of a Portal Frame with Both Ends Fixed	57
Figure 2.12	Fixed-Free Beam Subjected to its own weight	60
Figure 2.13	Formulation for an element under linearly varying axial load	61
Figure 2.14	Modeling the Fixed-Fixed Beam for Forced Vibration Analysis	65
Figure 2.16	Tapered Cantilever Beam Modeled by Two Tapered Elements	67
Figure 2.17	Modeling Fixed-Fixed Externally tapered Composite Beam	75
Figure 3.1	Variations of N_1 and N_5 With Respect To x	92
Figure 3.2	Variations of N_2 and N_6 With Respect To x	92
Figure 3.3	Variations of N_3 and N_7 With Respect To x	93

Figure 3.4	Variations of N_4 and N_8 With Respect To x	94
Figure 3.5	Variations of $\frac{d^2 N_1}{dx^2}$ and $\frac{d^2 N_5}{dx^2}$ With Respect To x	94
Figure 3.6	Variations of $\frac{d^2 N_4}{dx^2}$ and $\frac{d^2 N_8}{dx^2}$ With Respect To x	95
Figure 3.7	Variations of $\frac{d^3 N_3}{dx^3}$ and $\frac{d^3 N_7}{dx^3}$ With Respect To x	96
Figure 3.8	Variation of Z_p with x -axis	110
Figure 3.9	Assembling Two Elements in Advanced Finite Element Formulation	114
Figure 3.10	Modeling of Externally Tapered Composite Beam	117
Figure 3.11	Modeling of Mid-plane Tapered Composite Beam	119
Figure 4.1	The Variations of the Natural Frequencies with Different Boundary Conditions Obtained Using Conventional Formulation	135
Figure 4.2	The Variations of the Natural Frequencies with Different Boundary Conditions Obtained Using the Advanced Formulation	137
Figure 4.3	The Natural Frequencies Obtained Using Conventional Formulation and Advanced Formulation for the Fixed-Fixed Support	139
Figure 4.4	A Comparison Between the Natural Frequencies Obtained Using Conventional Formulation and Advanced Formulation for Free-Fixed Support	140
Figure 4.5	The Lowest Three Natural Frequencies for Different Laminate Configurations of an Externally Tapered Composite Beam Based on Conventional Formulation	143

Figure 4.6	The Variation of the Flexural Rigidity in the Finite Element Mesh of an Externally Tapered Composite Beam for Different Ply Orientations	145
Figure 4.7	The Lowest Three Natural Frequencies for Different Laminate Configurations of an Externally Tapered Composite Beam Obtained Using Advanced Formulation	146
Figure 4.8	A Comparison Between the Natural Frequencies Obtained Using Conventional Formulation and Advanced Formulation for Cross-Ply Laminate	147
Figure 4.9	The Variations in the Natural Frequencies for Different Meshes of an Externally Tapered Composite Beam Obtained Using Conventional Formulation	149
Figure 4.10	The Variations in The Natural Frequencies for Type A and Type B Meshes of An Externally Tapered Composite Beam Obtained Using Conventional Formulation	150
Figure 4.11	The Variations in The Natural Frequencies of Type C and Type D Meshes of An Externally Tapered Composite Beam Obtained Using Conventional Formulation	151
Figure 4.12	The Variations in The Natural Frequencies of Type A and Type B Meshes of An Externally Tapered Composite Beam Obtained Using Advanced Formulation	153
Figure 4.13	The Variations in The Natural Frequencies of Type C and Type D Meshes of An Externally Tapered Composite Beam Obtained Using Advanced Formulation	154

Figure 4.14	A Comparison Between the Natural Frequencies Obtained Using Conventional Formulation and Advanced Formulation for Type A Beam Discretization	155
Figure 4.15	The Variations of the Natural Frequencies with Different Boundary Conditions Obtained Using the Conventional Formulation	158
Figure 4.16	The Variations of the Natural Frequencies with Different Boundary Conditions Obtained Using the Advanced Formulation	159
Figure 4.17	Comparison Between the Natural Frequencies Obtained Using Conventional and Advanced Formulations for Mid-Plane Tapered Fixed-Free Composite Beam	160
Figure 4.19	The Lowest Three Natural Frequencies for Different Laminate Configurations of a Mid-plane Tapered Composite Beam Obtained Using the Advanced Formulation	165
Figure 4.20	Comparison Between the Natural Frequencies Obtained Using Conventional and Advanced Formulations for Mid-Plane Tapered Composite Beam with $[\pm 45]_s$ Ply Groups	166
Figure 4.21	The Variations of the Natural Frequencies of a Mid-Plane Tapered Composite Beam with Different Taper Angles Obtained Using the Conventional Formulation	168
Figure 4.22	The Variations of the Natural Frequencies of a Mid-Plane Tapered Composite Beam with Different Taper Angles Obtained Using the Advanced Formulation	169

Figure 4.23	Comparison Between the Natural Frequencies Obtained Using Conventional and Advanced Formulations for Mid-Plane Tapered Composite Beam with Two Degrees Taper Angle	171
Figure 4.24	The Variations in the Natural Frequencies for Beam Meshes Type B and Type D of a Mid-plane Tapered Composite Beam Obtained Using Conventional Formulation	173
Figure 4.25	The Variations in the Natural Frequencies for Beam Meshes Type A and Type C of a Mid-plane Tapered Composite Beam Obtained Using Conventional Formulation	174
Figure 4.26	The Critical Buckling Loads for Different Fiber Orientations Obtained Using the Conventional and Advanced Formulations	178
Figure 4.27	The Variations in the Natural Frequencies for External and Mid-Plane Tapered Composite Beams Obtained Using Conventional Formulation	179

List of Tables

Table 2.1	Percentage of Errors in Natural Frequencies	56
Table 2.2	Percentage of Errors in Natural Frequencies that Correspond to Constant End Axial Loading	59
Table 2.3	Comparison of the Maximum Displacement	66
Table 2.4	Percentage of Error in Deflection and Slope at the Free End of a Tapered Cantilever Beam	68
Table 2.5	Percentage of Errors Associated with the Natural Frequencies for Different Boundary Conditions	71
Table 2.6	Percentage of Error in Natural Frequencies of $[0/90]_s$ Composite Beam	73
Table 2.7	Maximum Displacement of the Fixed-Fixed $[0/90]_s$ Composite Beam	75
Table 3.1	Geometric and Natural Boundary Conditions For Different Supports	116
Table 3.2	Comparison Between the Percentage of Error in the Natural frequencies Obtained Using the Advanced Formulation and the Conventional Formulation	123
Table 3.3	Comparison of the Percentages of Error in Lowest Three Natural Frequencies Obtained Using Conventional and Advanced Formulations	125
Table 4.1	Comparison of the Natural Frequencies Obtained Using Conventional and Advanced Formulations for Different Boundary Conditions	141
Table 4.2	Comparison of the Natural Frequencies Obtained Using Conventional Formulation and Advanced Formulation for Different Fiber Orientations	148

Table 4.3	Comparison Between the Natural Frequencies Obtained Using Conventional and Advanced Formulations For Different Element Discretizations	156
Table 4.4	Comparison Between the Natural Frequencies That Correspond to Different Boundary Conditions and for Different Formulations	162
Table 4.5	Comparison Between the Natural Frequencies for Different Fiber Orientations Obtained Using the Conventional and Advanced Formulations	167
Table 4.6	Comparison Between the Natural Frequencies for Different Taper Angles for A Fixed-Free Mid-plane Composite Beam Obtained Using the Conventional and Advanced Formulations	172
Table 4.7	The Natural Frequencies for Different Beam Meshes Obtained Using Conventional Formulation	175
Table 4.8	The Critical Buckling Load for an Externally Tapered Composite Beam for Different Fiber Orientations Obtained Using Conventional and Advanced Formulations	178

Nomenclature

E	Young's modulus
I	mass moment of inertia
W	transverse deflection, as a function of x only
θ	slope of the beam (function of x)
w	transverse deflection, as a function of x and time 't'
b	laminate width
N_x	axial load per unit width in the axial direction
M_x	bending moment per unit width in the axial direction
ϵ_{x0}	strain component in the x direction on the reference plane
κ_x	curvature in the x direction
ρ	density of the laminate material
A	cross-sectional area of the laminate
q	distributed transverse load (function of x and t)
L	beam span
l	beam element length
τ	arbitrary function of time
v	weight function
$[N]$	the matrix of interpolation functions
Q_i	generalized force matrix
$[K]$	beam element global stiffness matrix

[n]	beam element global geometric stiffness matrix in conventional formulation
[M]	beam element global mass matrix
[F]	the equivalent nodal force vector
[Q]	the laminate stiffness in the laminate coordinates
$[\bar{Q}]$	transformed laminate stiffness matrix
[D]	bending or flexural laminate stiffness matrix (that relates bending moment M_x to curvature κ_x)
[A]	axial laminate stiffness matrix (that relates bending moment N_x to strain ε_{x0})
[B]	bending-stretching coupling matrix
bD_{11}	the laminate flexural rigidity
G	the shear rigidity of the laminate
t_p	ply thickness
m	slope of the centerline of a ply in the mid-plane tapered laminate
g	intercept of the centerline of a ply in the mid-plane tapered laminate
ν_{12}	Poisson's ratio between the fiber direction (1) and matrix direction (2)
ω	natural frequency of the beam
{d}	the global degrees of freedom vector
[T]	the transformation matrix
h	laminate height
P	total axial load accumulated over an element
p	distributed axial load in an element

u_i	common variable for all nodal variables (degrees of freedom) in local coordinates
U_i	common variable for all nodal variables (degrees of freedom) in global coordinates
P_{cr}	critical buckling load
α, δ	parameters to determine the accuracy and stability of Newmark direct integration method
α	index to express the nature of the variation of the axial load (in finite element modeling for buckling due to variable axial load)
r	coefficient used to evaluate the intensities of the axial loads at the top and bottom nodes (in finite element modeling for buckling due to variable axial load)
[nc]	beam element global geometric stiffness matrix for constant axial load in advanced formulation
[nd]	beam element global geometric stiffness matrix for variable axial load in advanced formulation

Chapter 1

Introduction

1.1 Dynamic Analysis and Buckling in Mechanical Design

Mechanical components and structures are subjected to forces of a time-dependent nature. Analysis and design of such components and structures subjected to dynamic loads involve consideration of time-dependent inertial forces. Hence, the term 'dynamic' may be defined simply as 'time-varying'. Thus a dynamic load is any load the magnitude, direction, or position of which varies with time. Similarly, the structural response to a dynamic load, i.e., the resulting deflections and stresses, is also 'time-varying', or dynamic. Hence, it is evident that a dynamic problem does not have a single solution, as a static problem does, instead the analyst must establish a succession of solutions corresponding to all times of interest in the response history.

There are several ways in which a component or structure can become damaged or useless; one of them is through a dynamic response to time-dependent loads, resulting in too large deflections or too high stresses, or fatigue damage, and another way is through the occurrence of an elastic instability (buckling). In the former case, the dynamic

loading on a structure can vary from a reoccurring cyclic loading of the same repeated magnitude, such as a structure supporting an unbalanced motor that is rotating at one hundred revolutions per minute, for example, to the other extreme of a short time intense, non-reoccurring load, termed as shock or impact loading, such as a bird striking an aircraft component during flight. A number of different types of dynamic loads exists between these two extremes of harmonic oscillation and impact. In both the cases, the free vibration response of the component becomes a controlling aspect.

A simple way to describe the buckling phenomenon is to use an example of an ideally straight bar with uniform and axisymmetrical cross section subjected to a compressive force along the center axis of the bar. Under such force, the bar will be slightly shortened but remains straight with no bending. If a small lateral load is applied, the beam will be bent infinitesimally but return to its original straight form when the lateral load is removed. If the axial force is gradually increased, a condition will be reached in which a small lateral force will cause a deflection, which remains when the lateral force disappears. Such an unstable phenomenon is called buckling and the critical force is called the buckling load or Euler load. Buckling usually occurs when the compressive stress is well below the material stress limit.

Buckling can happen in components and structures in many forms, such as columns, truss members, components of thin-walled beams and plate girders, walls, arches, and shell roofs. Buckling can also happen to torispherical shells under internal pressure. In aerospace structures, minimum-weight design is an important criterion so

that the structures are made of skins and thin members. Buckling is a predominant failure mode in these structures.

1.2 Composite Materials and Structures in Mechanical Design

In the most general terms, a composite is a material that consists of two or more constituent materials or phases. Traditional engineering materials (steel, aluminum, etc.) contain impurities that can represent different phases of the same material and fit the broad definition of a composite, but are not considered composites because the elastic modulus or strength of the impurity phase is nearly identical to that of the pure material. In the present thesis, a composite material is considered to be one that contains two or more distinct constituents with significantly different macroscopic behavior and a distinct interface between each constituent (on the microscopic level). This includes the continuous fiber-reinforced laminated composites that are of primary concern herein, as well as a variety of composites not specifically addressed.

Composite materials have been in existence for many centuries. No record exists as to when people first started using composites. Some of the earliest records of their use date back to the Egyptians, who are credited with the introduction of plywood, papier-mâché, and the use of straw in mud for strengthening bricks. Similarly, the ancient Inca and Mayan civilizations used plant fibers to strengthen bricks and pottery. Swords and armor were plated to add strength in medieval times.

The composites have experienced steady growth since about 1960 and are projected to continue to increase through the next several decades, and they are considered now as one of the great technological advances of the last half of the twentieth century. By the term composite it is usually referred to materials that are combinations of two or more organic or inorganic components, of which one serves as a matrix and the other as reinforcement. The purpose of the matrix is to bind the fibers together and keep them in proper orientation, transfer the load to and between them and distribute it evenly, protect the fibers from hazardous environments and handling, provide resistance to crack propagation and damage, provide all the interlaminar shear strength of the composite, and offer resistance to high temperatures and corrosion. The individual fiber is usually stiffer and stronger than the matrix. The most powerful concept behind composites is that the fibers and the matrix can blend into a new material with properties that are better than those of the constituent parts. In addition, by changing the orientation of the fibers, the composites can be optimized for strength, stiffness, fatigue, heat and moisture resistance, etc. It is therefore feasible to tailor the material to meet specific needs. Furthermore, a preferred fiber orientation may be used to increase the modulus and strength well above isotropic values; the resulting lightweight material may have much higher strength / weight ratios than the conventional materials.

Modern composite materials are used in weight sensitive structures, and in applications where high stiffness / weight ratios are required. Fiberglass was widely used in the 1950s for boats, and for automobiles such as the Chevrolet Corvette. The aircraft industry uses composites to meet performance requirements beyond the capabilities of

metals. The first large, commercial aircraft to use composites extensively was the Boeing 777. It uses approximately 760 ft³ of composites in its body and wing components, with an additional 361 ft³ used in rudder, elevator, edge panels, and tip fairings. The B-2 bomber contains carbon and glass fibers, epoxy resin matrices, and high-temperature polyamides as well as other materials in more than 10,000 composite components. The British Aerospace-McDonnell Douglas Av-8B Harrier has 25 % of its structural weight in composites.

1.3 Analysis and Solution Methods in Mechanical Design

The analysis of laminated composite beams is usually based on three approaches, classical theory of elasticity, theory of mechanics of materials, and variational methods and strain energy statements. In general, laminated composite beams have been studied to a lesser degree than isotropic beams, and laminated plates and shells as well. Work is still needed to understand the behavior of these structures under complicated loading and harsh environmental conditions and to maintain active control of these structures, which may be suffering degradation.

The governing equations of motion of the dynamic systems are generally nonlinear partial differential equations, which are extremely difficult to be solved in a closed form. The availability and sophistication of modern digital computers has made possible the extensive use of the finite element method for analyzing complex structures. This method consists of representing a complex structure by an assembly of simple discrete

elements, such as rods, beams, plates, or two-force truss members. Finite Element Method (FEM) is one of the most powerful numerical analysis tools in the engineering and physical sciences. It is widely accepted as a mathematical technique for the numerical solution of the partial differential equations.

1.4 Literature Survey

1.4.1 Literature Survey on Vibration Analysis

The mathematical Theory of Elasticity is occupied with an attempt to calculate the state of strain, or relative displacement, within a solid body which is subject to the action of an equilibrating system of forces, or is in a state of slight internal relative motion, and with endeavors to obtain results which shall be practically important in applications to architecture, civil and mechanical engineering, and all other fields in which the material of construction is solid.

The first mathematician that considered the nature of the resistance of solids to rupture was Galileo in his initial inquiries in 1638. In the history of the theory, started by the question of Galileo, undoubtedly the two great landmarks are the discovery of Hooke's Law in 1660, and the formulation of the general differential equations by Navier in 1821. Hooke's Law provided the necessary experimental foundation for the theory. When the general equations had been obtained, all questions of the small strain of elastic bodies were reduced to a matter of mathematical calculation. In the interval between the

discovery of Hooke's Law and that of the general differential equations of Elasticity by Navier, the attention of those mathematicians who occupied themselves with our science was chiefly directed to the solution and extension of Galileo's problem, and the related theories of the vibrations of bars and plates, and the stability of columns.

Side by side with the statical developments of Galileo's enquiry there were discussions of the vibrations of solid bodies. In 1744 Euler and in 1751 Daniel Bernoulli obtained the differential equation of the lateral vibrations of bars by variation of the function by which they had previously expressed the work done in bending. They determined the forms of the functions, which are called the "*normal functions*", and the equation, which is called the "*frequency equation*" in the six cases of boundary conditions, which arise from free, clamped, or simply supported conditions. Chladni investigated these modes of vibration experimentally, and also the longitudinal and torsional vibrations of bars. James Bernoulli's attempt in (published in 1787) appears to have been made with the view of discovering a theoretical basis for the experimental results of Chladni concerning the nodal figures of vibrating plates. These results were still unexplained when in 1809 the French Institute proposed as a subject for a prize the investigation of the tones of a vibrating plate. After several attempts the prize was adjudged in 1815 to Mdlle Sophie Germain, and her work was published in 1821. She assumed that the sum of the principal curvatures of the plate when bent would play the same part in the theory of plates as the curvature of the elastic central-line in the theory of rods, and she proposed to regard the work done in bending as proportional to the integral of the square of the sum of the principal curvatures taken over the surface. From this

assumption and the principle of virtual work she deduced the equation of flexural vibration in the form now generally admitted. Later investigations have shown that the formula assumed for the work done in bending was incorrect.

During the first period in the history of our science (1638 till the end of the year 1820), the fruit of all the ingenuity expended on elastic problems might be summed up as: an inadequate theory of flexure, an erroneous theory of torsion, an unproved theory of the vibrations of bars and plates, and the definition of Young's modulus. But such an estimate would give a very wrong impression of the value of the older researches. The recognition of the distinction between shear and extension was a preliminary to a general theory of strains, and the recognition of forces across the elements of a section of a beam, producing a resultant, was a step towards a theory of stress, the use of differential equations for the deflection of a bent beam and the vibrations of bars and plates was a foreshadowing of the employment of differential equations of displacement.

Navier in 1827 was the first to investigate the general differential equations of equilibrium and vibration of elastic bodies. He set out from the Newtonian conception of the constitution of bodies, and assumed that the elastic reactions arise from variations in the intermolecular forces, which result from changes in the molecular configuration. He deduced, by an application of the Calculus of Variations, not only the differential equations of equilibrium and vibration, but also the boundary conditions that hold at the surface of the body. The material is assumed to be isotropic. Objection has been raised against Navier's expression for the forces between two molecules, and to his method of

simplifying the expressions for the forces acting on a single molecule. These expressions involve triple summations, which Navier replaced by integrations, and the validity of this procedure has been disputed. This dispute was over when Cauchy in 1828 verified Navier's equations, and Poisson in 1829 got equations of equilibrium and motion of isotropic elastic solids, which are identical to Navier's, but by the aid of a different assumption. Clausius in 1849 held that both Poisson's and Cauchy's methods could be presented in unexceptionable forms.

The theory of elasticity established by Poisson and Cauchy on the then accepted basis of material points and central forces was applied by them and also by Lamé and Clapeyron to numerous problems of vibrations and of statical elasticity.

The theory of the vibrations of thin rods was brought under the general equations of vibratory motion of elastic solid bodies by Poisson. He regarded the rod as a circular cylinder of small section, and expanded all the quantities that occur in powers of the distance of a particle from the axis of the cylinder. When terms above certain order (the fourth-order power of the radius) are neglected, the equations for flexural vibrations are identical with Euler's equations of lateral vibration. The equation found for the longitudinal vibrations had been obtained by Navier. The equation for the torsional vibrations was first obtained by Poisson. The application of Poisson's theory has been extended to the vibrations of curved bars, the first problem to be solved being that of the flexural vibrations of a circular ring, which vibrates in its own plane.

The theory of the free vibrations of solid bodies requires the integration of the equations of vibratory motion in accordance with prescribed boundary conditions of stress or displacement. Poisson gave the solution of the problem of free radial vibrations of a solid sphere, and Clebsch founded the general theory on the model of Poisson's solution. The analysis of the general problem of the vibrations of a sphere was first completely given by P. Jaerisch, who showed that the solution could be expressed by means of Bessel's functions of order *integer* + $\frac{l}{2}$. H. Lamb obtained the result independently, and gave an account of the simpler modes of vibration and of the nature of the nodal division of the sphere, which occurs when any normal vibration is executed. He also calculated the more important roots of the frequency equation. L. Pochhammer has applied the method of normal functions to the vibrations of cylinders, and has found modes of vibration analogous to the known types of vibration of bars.

In 1889 Lord Rayleigh published his celebrated work on the vibration of an infinite elastic plates [1]. He formalized the idea of normal functions, as introduced by Daniel Bernoulli and Clebsch, and also the ideas of generalized forces and generalized coordinates. He, further, introduced systematically the concepts of potential energy and the approximate methods in vibration analysis, without solving differential equations. Rayleigh improved the classical theory by allowing for the effects of rotary inertia of the cross-sections of a beam. In 1921 Timoshenko extended the theory to include the effects of shear deformation [2]. The resulting equations are known as the *Timoshenko beam equations*. Sutherland and Goodman [3] have given solutions of Timoshenko equations for a cantilever beam of rectangular cross section. In 1951 Mindlin included the

transverse shear and rotary inertia effects [4]. This made the Timoshenko's and Mindlin's beam and plate theories capable to handle much higher frequencies than the classical theories. Mindlin further compared and coordinated the results for an infinite plate given by his plate theory and those derived from the exact elasticity theory by Rayleigh. This was the first attempt to establish a connection between an engineering plate theory and the exact elasticity theory.

The innocent-looking frequency equation of the infinite plate given by Rayleigh was not fully explored until almost 70 years later, again by Mindlin when he in 1960 gave a thorough treatment of Rayleigh's exact frequency equation of an isotropic plate [5]. On the other hand, Mindlin in 1955 had started developing approximate plate theories so that problems involving high frequencies in finite-sized crystal plates can be solved [6]. Mindlin's results on anisotropic plates have a close bearing upon laminated composites [7].

In the early years in the history of laminated composites, the transverse shear effect was usually neglected, and laminated composite plates were generally treated as anisotropic plates of the classical type. Thus, for instance, solutions for vibration of orthotropic plates, such as given by Hearmon [8], become immediately applicable to composite plates. Recently, Toledano and Murakani developed a new laminated composite plate theory for an arbitrary laminate configuration [9].

In the dynamic theory of elasticity, the variational equation of motion is the end result obtained by carrying out the variation process in Hamilton's principle. The Euler's equation written from the variational equation constitutes the governing equation in elasticity. The variational equation has been applied to a variety of linear and nonlinear dynamic and vibration analysis of structures including layered plates and shells [10], which can be applied to laminated composites.

Several investigators have studied the free vibration of fiber-reinforced composite beam structures. In 1977, Teoh and Huang [11] presented a theoretical analysis of free vibrations of fiber-reinforced composite beams. Natural frequencies and mode shapes of a cantilevered composite beam (glass/epoxy) were determined. In the analysis, a continuous model was used and both shear and rotary inertias were included. The effects of shear deformation and fiber orientation on the free vibrations were given. Teh and Huang [12] formulated a finite element approach to determine the natural frequencies of generally orthotropic composite beams (graphite/epoxy) with the cantilevered boundary conditions. Earlier, Abarcar and Cunniff [13] developed a numerical method to analyze the free vibration of a cantilevered beam, which also includes both shear deformation and rotary inertia, using a discrete model based on Myklestad's method.

In 1980, Crawley and Dugundji [14] studied free vibrations of composite cantilevered plates (beams) based on a partial Ritz (Kantorovich) analysis, in which the mode shapes are assumed only in the cord-wise direction. Thus, the problem is reduced to a set of uncoupled ordinary differential equations. Their efforts were concentrated on

the estimation of both the bending and torsional frequencies and the development of non-dimensionalizing frequency data. The resulting non-dimensional frequencies are not only more consistent than the original data, but also are in better agreement with the eigenvalues of the Ritz analysis. Later, Jensen and Crawley [15] developed frequency determination techniques for cantilevered plates with bending-torsion coupling. These techniques include partial Ritz analysis, Rayleigh- Ritz analysis assuming mode shapes both in span-wise and cord-wise directions, and the finite element analysis.

In view of the important roles of the individual layers in overall performance of composite laminates, a layer-wise approach was presented by Barbero and Reddy [16,17] in 1989. By assuming both translational and rotational displacement components for each composite layer, the displacement of the whole laminate is nothing but the assembly of the individual components. Lu and Liu [18], and Lee and Liu [19] further employed the continuity conditions of interlaminar shear stresses and interlaminar normal stress for composite layer assembly. Di Sciuva [20] evaluated a new displacement model for bending, vibration, and buckling of simply supported thick multilayered orthotropic plates.

1.4.2 Literature Survey on Elastic Stability

Whenever very thin rods or plates are employed in mechanical components or structures it becomes necessary to consider the possibility of buckling, and thus there

arises the general problem of *elastic stability*. The work on elastic stability started by Daniel Bernoulli when he suggested to Euler (in a letter in 1742) that the differential equation of the *elastica* could be found by making the integral of the square of the curvature taken along the rod a minimum; and Euler, acting on this suggestion, was able to obtain the differential equation of the curve and to classify the various forms of it. One form is a curve of sines of small amplitudes, and Euler pointed out (in 1757) that in this case the line of thrust coincides with the unstrained axis of the rod, so that the rod, of sufficient length and vertical when unstrained, may be bent by a weight attached to its upper end. Further investigations led him to assign the least length of a column in order that it may bend under its own or an applied weight. In 1773 Lagrange followed and used his theory to determine the strongest form of column. These two writers found a certain length which a column must attain to be bent by its own or an applied weight, and they concluded that for shorter lengths it will be simply compressed, while for greater lengths it will be bent. These constitute the earliest research in the field of elastic stability. Then a number of isolated problems have been solved. In all of them two modes of equilibrium with the same type of external forces are considered to be possible, and the ordinary proof of the determinacy of the solution of the equations of elasticity is employed. G. H. Bryan has proposed a general theory of elastic stability. He arrived at the result that in all cases where two modes of equilibrium are possible the criterion for determining the modes that will be adopted is given by the condition that the energy must be a minimum.

The failure of Euler's formula in the case of short and medium-length columns was the primary cause of its almost complete abandonment, together with the reasoning by which it was derived. In 1921, Salmon gives a lively account to reconcile Euler's theory with the observations of column buckling tests [21].

The first buckling analysis of cylindrically orthotropic circular plates of uniform thickness has been presented by Woinowsky-Krieger in 1958 [22]. Patel and Broth have given the first buckling analysis of cylindrically orthotropic circular plates of variable thickness in 1970 [23]. A broad literature survey on buckling of laminated composites is given in Ref. [24] up to the year 1985. More recently, studies of dynamic buckling of anisotropic shells have received much attention, as given in detail in Ref. [25].

1.4.3 Literature Survey on Finite Element Method

An analysis of complex structures and other systems in a matrix formulation is now unthinkable without the finite element method. It is believed that the origins of such a rich and applicable method cannot be attributed solely to one person or a school of thought but rather to a synergy of various scientific developments at various research establishments. The notion of geometrical division can be tracked back to the Greek natural philosopher Archimedes who in order to compute the area of a complex shape divided it into triangles and quadrilaterals whose areas could be easily computed as the assembly of the individual areas provided the total area of the complex shape. More

recently, Courant used variational and minimization arguments for the solution of physical problems. Courant [26], and Prager and Synge [27] had both proposed the concept of regional discretization that is essentially equivalent to the assumption of constant strain fields within the elements. The adaptation, however, and development of these concepts for structural analysis and other physical and technical problems were not conceptually achieved until during and shortly after World War II.

During World War II the demand for more efficient aeronautical structures and methods for the analysis of complex structural systems provided John Argyris with the incentive for developing the *matrix displacement method*, a concise matrix presentation of the equilibrium equations governing a skeletal structure. It was wartime that necessitated this sudden explosion of knowledge, and it was published later after the war in 1954 [28]. By 1945 the breakdown of the continuum into triangular elements had been accomplished, and engineers had started to apply the matrix displacement method to the analysis of swept-back wings. It was not immediately realized that these developments had led to the birth of the finite element method.

Essential contributions to the finite element method were made at Boeing during the summer of 1952 and 1953 under the direction of M. J. Turner. He saw the need for an improved way taking into account of the contributions of the wing skin to the stiffness of airplane wings or arbitrary configurations, and he recognized that Ritz-type procedure could be used to evaluate the contributions of individual skin elements if the wing was represented as an assemblage of such discrete structural components [29]. At Boeing

they were inspired to name this method as finite element method, and that name appeared first in a paper presented at the 1960 ASCE Conference.

Most of the numerical methods developed before the era of electronic computers are now adapted for use with these machines. Perhaps the best known is the finite difference method. It was used by Thomas [30] to obtain frequencies of vibration of uniform, tapered and pre-twisted Timoshenko beams with fixed-free end conditions. Other types of classical methods are the method of least squares and such variational methods as the Ritz method. In addition to the direct and variational approaches, the finite element equation can be formulated by employing the residual methods such as collocation, least squares, and Galerkin's methods.

It might be of interest to mention that the Finite Element Method now has three approaches, displacement method (in which displacements are assumed as primary unknowns in it), equilibrium method (in which stresses are assumed as primary unknowns in it), and mixed method (in which some displacements and some stresses are assumed as primary unknowns in it).

A number of finite element models have been presented for the analysis of Euler-Bernoulli and Timoshenko beams by various investigators. Just the main points on the literature survey of higher-order finite element formulation will be mentioned here, as a comprehensive and very recent survey is given in Ref. [31].

Cook, Malkus and Plesha [32] have mentioned that for achieving the minimally acceptable degree of inter-element compatibility, it is necessary to define *essential degrees of freedoms* as the particular nodal degrees of freedoms (more details about essential nodal degrees of freedoms are discussed in chapter 3). Pestel studied the effect of imposing nodal continuity of successively higher derivatives of deflection and noted that such family of elements can be formulated simply by the use of Hermitian polynomials of orders higher than the fourth [33].

Many authors have shown the desirability of using higher order finite element for vibration problems. The development of higher order tapered beam element was carried out to study first the vibration analysis of uniform beams by Fried [34] in 1971, and the transverse impact problems by Sun and Huang [35]. They all claim that improved accuracy can be obtained more efficiently with an increase in the number of degrees of freedom in the element. Thomas and Dokumaci have shown that the higher order finite element-modeling yields improved results for the vibration of tapered beams [36]. In 1979, C. S. To had developed expressions for mass and stiffness matrices of two higher order tapered beam elements for vibration analysis [37].

Four years earlier Thoinas and Abbas developed an element model that is capable of incorporating all the forced and natural boundary conditions associated with various end conditions, deflection, slope, bending slope and the first derivative of bending slope as nodal co-ordinates [38]. Again, this model is proven for dynamic analysis of Timoshenko beam element only.

Akin has developed a more accurate solution by using a fifth order Hermite polynomial [39]. Reddy suggested that if higher order (higher than cubic) approximation of deflection w is desired, one must identify additional dependent (primary) unknowns at each of the two nodes [40]. Houmat presented a 2-node Timoshenko beam finite element with variable degrees of freedom [41]. Hou, Tseng, and Ling developed a new finite element model of a Timoshenko beam to analyze the free vibration of uniform beams [42]. The results of the above-mentioned two models show that using one or two-variable order Timoshenko beam element with a few trigonometric terms yields better accuracy with fewer degrees of freedom than using many polynomials. R. Ganesan, J. A. Selliah, and R. B. Bhat formulated a finite element model that involves all boundary conditions for vibration analysis of structures [43].

1.5 Objective of the Thesis

The objective of the present thesis is to consider two aspects: (i) The dynamic analysis and buckling of variable thickness composite beams (externally tapered and mid-plane tapered composite beams) using the conventional formulation, a formulation that takes into account the geometric (essential) degrees of freedom (deflection and slope). (ii) Development of an efficient and powerful method to obtain the natural frequencies and the critical buckling load of these composite beams; a method that is called herein as *advanced formulation*. In the advanced formulation both categories of degrees of freedom are considered, the geometric and the natural (shear force and bending moment)

degrees of freedom. The interpolation polynomial was chosen such that it adapts with the new definition of the nodal degrees of freedom matrix. It is an algebraic equation of the seventh order. The stiffness, geometric stiffness, and mass matrices are established. These matrices are provided to the MATLAB[®] environment to obtain the eigenvalues, which are the natural frequencies or the critical buckling load of the beam. The superiority of this method is illustrated by comparing the results with the conventional finite element model.

The present study aims at modifying the conventional finite element model such that it accepts the natural boundary conditions right in the element formulation. Thus, this model fully represents all the physical situations involved in any practical case. This development is hoping to achieve higher accuracy by increasing the degrees of freedom rather than increasing the number of elements. This was obvious in the output of the MATLAB[®] program when its results were converging with the results of the exact solution faster than the results obtained using the conventional formulation.

1.6 Layout of the Thesis

The present chapter provides a brief introduction and a literature survey regarding the dynamic analysis and buckling of variable thickness composite beams that are studied using finite element methods.

Chapter 2 develops the basic finite element mathematical formulations including free vibration, forced vibration, and buckling for externally tapered and mid-plane tapered composite beams. The finite element formulation consists of the determination of the equation of motion and its solution. The finite element formulation is basically to determine the stiffness, geometric stiffness, and mass matrices for each element in local coordinates using the geometric degrees of freedom at the nodes (deflection and slope), which is called the “*conventional formulation*”. Then, these matrices in global coordinates are assembled, and the eigenvalues of the dynamic matrix are obtained in order to get the natural frequencies of the structure, or the critical buckling load.

Chapter 3 gives a basic and reasonably complete development of higher order beam finite elements and interpolation functions. In this new method of formulation, natural (force) degrees of freedom (shear force and bending moment) along with the geometric boundary conditions are embedded in the interpolation functions, which is called “advanced formulation”. Also, the applications of the advanced formulation to the transverse vibration and buckling of variable thickness composite beams are explained.

Chapter 4 is devoted to the parametric study, which includes the effects of the boundary conditions, the laminate configuration, the beam element discretization, and the taper angle on the natural frequencies of the beam for both types of tapers. Both the conventional and advanced finite element formulations are employed. In addition, the buckling of externally tapered composite beams is considered.

The thesis ends with chapter 5, which provides the conclusions of the present thesis work and some recommendations for future work.

CHAPTER 2

Dynamic Analysis of Variable Thickness Composite Beams Using Conventional Finite Element Formulation

2.1 Introduction

Composite materials are increasingly used in aerospace, mechanical, and automotive structures. The application of composite materials to engineering components has resulted in a major effort to analyze structural components made from them. Composite materials provide unique advantages over their metallic counterparts, but they also present complex and challenging problems to analysts and designers.

Variable thickness composite structures (see Figure 2.1) are a natural choice because of the saving in material and hence cost. Since most composite laminates are composed of a number of layers, it is possible to construct variable thickness composite structures by terminating each ply in such a way as to meet the design requirements [54].

Design of such structures requires an understanding of their dynamic behavior, which involves the determination of their natural frequencies. Accordingly, the dynamic response, dynamic bending moments, and dynamic stresses can be evaluated as final steps of design process.

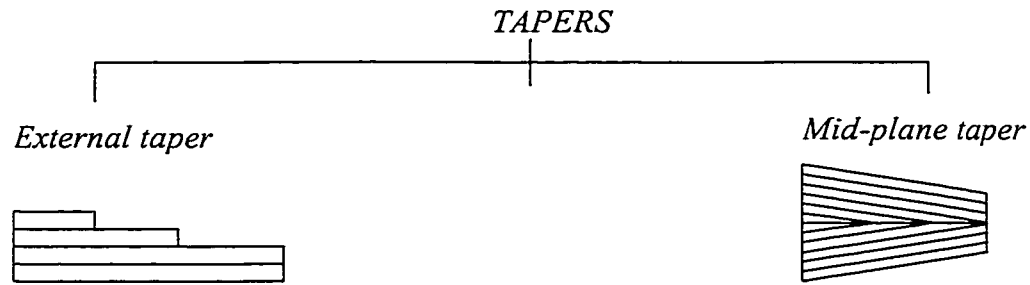


Figure 2.1 Basic types of tapers in composite beams

Tapered composite beams have not so far been analyzed for their dynamic response using exact analytical methods, since they require solutions to more complex mathematical problems. Hence, it is necessary to employ the approximate methods to study the dynamic behavior of such beams. In this regard, the finite-element method provides a powerful, convenient and reliable idealization of the composite system and further, it is particularly effective in digital-computer analyses [55].

In this chapter, a weak formulation based on the Euler-Bernoulli theory of bending of composite beams is developed first for both uniform and externally tapered composite beams. The formulation is then modified so as to be appropriate and applicable for mid-plane tapered composite beams. These formulations are based on the

conventional method. That is, two degrees of freedom are considered at each node, which are, the deflection (w) and the slope (θ). The analysis considers the coupling of bending and axial deformations due to the axial forces. Based on the above-mentioned formulations, the stiffness, geometric stiffness, and mass matrices are determined for variable thickness composite beams.

The MATLAB[®] computer program that incorporates the above-mentioned formulations is developed and demonstrated using example laminates. Also, the aspects related to the input data and the subroutines that form this program are described in detail.

2.2 Weak Formulation Based on Euler-Bernoulli Theory

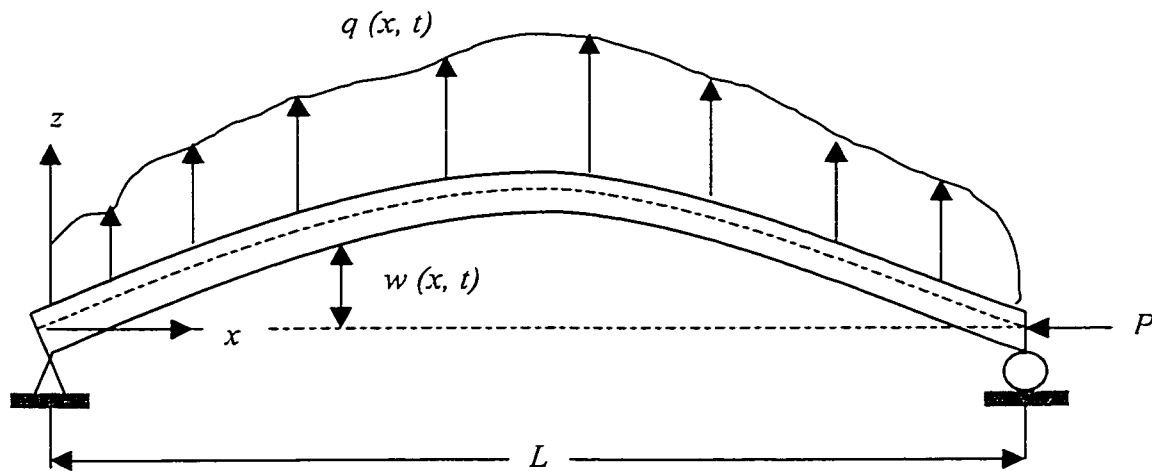


Figure 2.2 A beam-column with static axial force and dynamic lateral load

The differential equation of motion for a beam (shown in Figure 2.2) made of an isotropic material with lateral loading and axial load, based on the assumption that the transverse shear deformations are negligible, is given below:

$$\frac{\partial^2}{\partial x^2} \left(EI \frac{\partial^2 w}{\partial x^2} \right) + P \frac{\partial^2 w}{\partial x^2} + \rho A \frac{\partial^2 w}{\partial t^2} = q(x, t) \quad (2.1)$$

The significant physical properties of this beam are assumed to be the flexural rigidity (stiffness) $EI(x)$ and the mass per unit length $\rho A(x)$, both of which may vary arbitrarily with position x along the span L . The transverse loading $q(x, t)$ is assumed to vary arbitrarily with position x and time t , and the transverse-displacement response $w(x, t)$ also is a function of these variables. The axial force, P , is parallel to the beam axis before deformation and is assumed to be constant with respect to both time and position (in principle, it could vary as an arbitrary function, but the case of constant P will be considered here). The end-support conditions for the beam are arbitrary, although they have been shown as simple supports for illustrative purposes. The case of uniform cross-section can then be given as:

$$EI \frac{\partial^4 w}{\partial x^4} + P \frac{\partial^2 w}{\partial x^2} + \rho A \frac{\partial^2 w}{\partial t^2} = q(x, t) \quad (2.2)$$

The assumption of neglecting the transverse shear strains is valid if the thickness of the beam, h , is ‘small’ relative to the length, L . The difference between a beam and a plate is that the width, b , of the beam is ‘small’ compared with the span L .

This one-dimensional structural element is called a beam-column when lateral loads act upon it. When this element is loaded only by an axial loading, it is called as a rod if the loading is tensile, and a column if the loading is compressive.

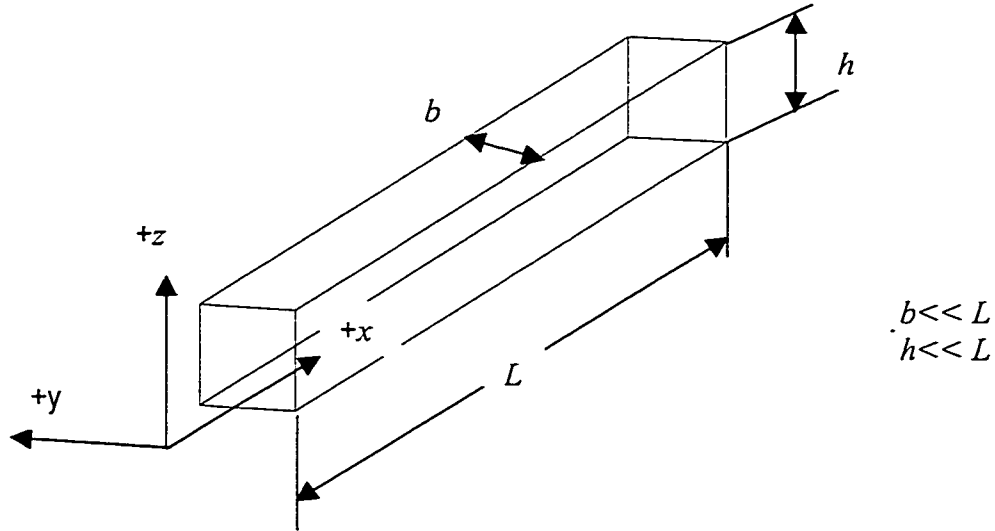


Figure 2.3 Typical rod or beam

Consider a beam made of composite material under lateral loading acting in the x - z plane. The overall dimensions are shown in Figure 2.3. For simplicity, the thermal and hygrothermal effects are ignored. Since the composite beam is so narrow, all Poisson's effects are neglected, conforming to the classical beam theory. With these assumptions, the force-displacement equations are reduced to [52]:

$$\begin{bmatrix} N_x \\ M_x \end{bmatrix} = \begin{bmatrix} A_{11} & B_{11} \\ B_{11} & D_{11} \end{bmatrix} \begin{bmatrix} \epsilon_{xo} \\ \kappa_x \end{bmatrix} \quad (2.3)$$

In the above equation, N_x denotes the normal force in the x direction per unit width, M_x denotes the bending moment in the x direction per unit width, ε_{x0} denotes the strain component in the x direction on the reference plane, and κ_x denotes the curvature in x direction.

If the beam has mid-plane symmetry, there is no bending-stretching coupling so that $B_{II} = 0$, and equation 2.3 becomes

$$N_x = A_{II} \varepsilon_{x0} \quad (2.4)$$

$$M_x = D_{II} \kappa_x \quad \text{or,} \quad (2.5)$$

$$M_x = D_{II} \frac{d^2 w}{dx^2} \quad (2.6)$$

Then from equations 2.3 - 2.6, equation 2.1 can be written as:

$$\frac{\partial^2}{\partial x^2} \left(b D_{II} \frac{\partial^2 w}{\partial x^2} \right) + b N_x \frac{\partial^2 w}{\partial x^2} + \rho A \frac{\partial^2 w}{\partial t^2} = q(x, t) \quad (2.7)$$

This is the governing equation of motion for the variable thickness composite beam.

The static buckling load of a column, $(b N_x)_{cr}$, is obtained from equation 2.7 after setting the lateral load, $q(x, t)$, to be zero, and dropping out the inertia term. For free vibration analysis, the relevant equation can be written as:

$$\frac{\partial^2}{\partial x^2} \left(b D_{II} \frac{\partial^2 w}{\partial x^2} \right) + b N_x \frac{\partial^2 w}{\partial x^2} + \rho A \frac{\partial^2 w}{\partial t^2} = 0 \quad (2.8)$$

2.3 Weak Formulation of the Problem

2.3.1 Weak Formulation for Uniform and Externally Tapered Composite Beams

In the finite element formulation an integral statement is to be established to develop algebraic relations among the coefficients w_j of the approximation [53]:

$$w(x, t) \approx \sum_{j=1}^n w_j(t) N_j(x) \quad (2.9)$$

Here $w(x, t)$ represents the solution of the governing differential equation in hand. The use of an integral statement equivalent to the governing differential equation is necessitated by the fact that substitution of equation (2.9) into the differential equation of motion does not always result in the required number of linearly independent algebraic equations for the unknown coefficients $w_j(t)$. One way to insure that there are exactly the same number ‘ n ’ of equations as there are unknowns is to require that the “*weighted integrals*” of the error involved in approximating the equation have to be zero.

There are three basic steps in the development of the weak form, if it exists, of any differential equation.

STEP 1:

In order to facilitate the mathematical modeling, move all expressions of the governing differential equation to one side, multiply the entire equation with a function $v(x, t)$ which is called as the “*weight function*”, and integrate over the domain $\Omega = (0, L)$ of the problem. The domain is divided into a set (say, n) of line elements. In this step a typical

element $\Omega^e = (x_e, x_{e+l})$ is isolated (see Figure 2.4) and the variational form of equation 2.7 over the element is constructed. For simplifying the analysis, the axes are taken at the first node so x_e equals to zero, and the element length $(x_{e+l} - x_e)$ is denoted by ' l_e ' or ' l '. Therefore, the limits of integration are 0 and l . For the case of forced vibration, the variational formulation leads to the following equation. For simplicity, $q(x,t)$ will be written as q .

$$0 = \int_0^l \left[bD_{II} \frac{\partial^4 w}{\partial x^4} + bN_x \frac{\partial^2 w}{\partial x^2} + \rho A \frac{\partial^2 w}{\partial t^2} - q \right] dx \quad (2.10)$$

Then multiplying equation 2.10 by the weight function v ,

$$0 = \int_0^l v \left[bD_{II} \frac{\partial^4 w}{\partial x^4} + bN_x \frac{\partial^2 w}{\partial x^2} + \rho A \frac{\partial^2 w}{\partial t^2} - q \right] dx \quad (2.11)$$

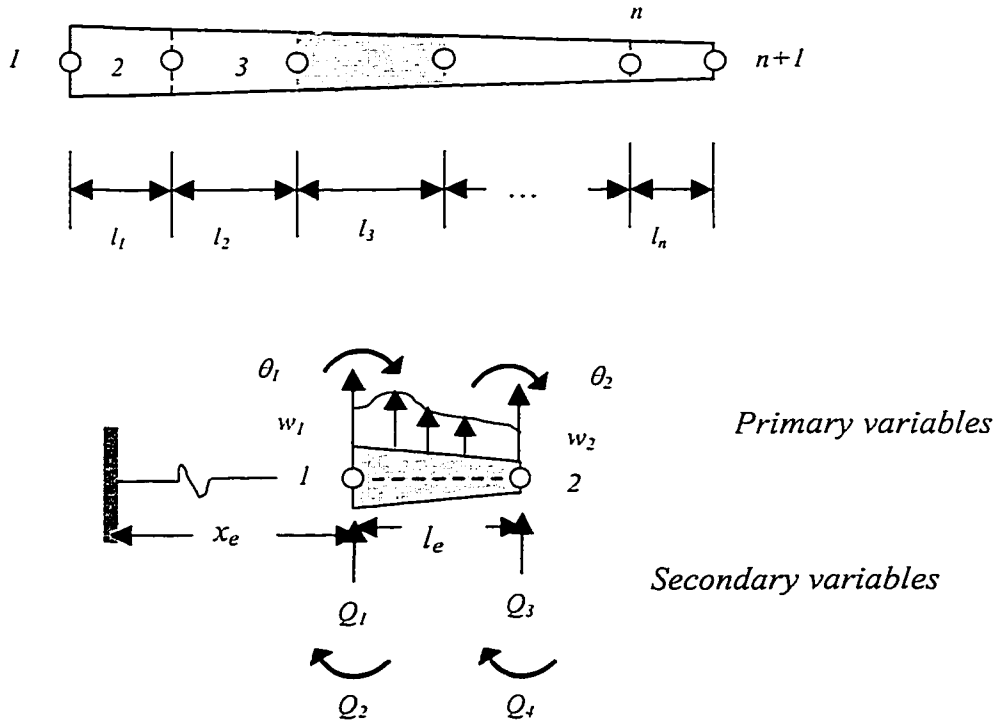


Figure 2.4 Finite-Element Discretization and a Typical Element

The statement 2.11 is called as the “*weighted-integral*”, or “*weighted-residual statement*” equivalent to the equation 2.9. It may be noted here that for uniform composite beam and for each uniform segment of an externally tapered composite beam, bD_{II} is constant.

STEP 2:

i) Integration by parts the weighted integral statement twice, one can get the following equation:

$$0 = \int_0^l \left[v \frac{\partial^2}{\partial x^2} (bD_{II} \frac{\partial^2 w}{\partial x^2}) + vbN_x \frac{\partial^2 w}{\partial x^2} + v\rho A \frac{\partial^2 w}{\partial t^2} - vq \right] dx \quad (2.12)$$

The approach of separation of variables is being applied for $w(x, t)$, and it can be expressed as the product of two functions one in displacement ‘ x ’ and the other in time ‘ t ’ as

$$w(x, t) = W(x)\tau(t) = W(x)e^{i\omega t} \quad (2.13)$$

where ω is the natural frequency of the transverse motion and $W(x)$ is the mode shape of this transverse motion. Substituting equation 2.13 into equation 2.12, and noting that

$$\frac{\partial^2 w(x, t)}{\partial t^2} = -\omega^2 W(x) e^{i\omega t} \text{ and that } e^{i\omega t} \text{ can never be zero, then}$$

$$0 = e^{i\omega x} \int_0^l \left[v \frac{\partial^2 W}{\partial x^2} (bD_{11} \frac{\partial^2 W}{\partial x^2}) + v b N_x \frac{\partial^2 W}{\partial x^2} - v \rho A \omega^2 W - v q \right] dx \quad (2.14)$$

$$0 = - \int_0^l \frac{dv}{dx} \frac{d}{dx} \left(bD_{11} \frac{d^2 W}{dx^2} - \lambda \rho A v W + v q \right) dx + v \frac{d}{dx} \left(bD_{11} \frac{d^2 W}{dx^2} \right) \Big|_0^l - \int_0^l b N_x \frac{dv}{dx} \frac{dW}{dx} dx + v b N_x \frac{dW}{dx} \Big|_0^l \quad (2.15)$$

In the above equations $\lambda = \omega^2$

$$0 = - \left[- \int_0^l \left(bD_{11} \frac{d^2 v}{dx^2} \frac{d^2 W}{dx^2} - \lambda \rho A v W + v q \right) dx + \frac{dv}{dx} bD_{11} \frac{d^2 W}{dx^2} \Big|_0^l \right] - \int_0^l b N_x \frac{dv}{dx} \frac{dW}{dx} dx + \left[v \frac{d}{dx} \left(bD_{11} \frac{d^2 W}{dx^2} \right) + v b N_x \frac{dW}{dx} \right]_0^l \quad (2.16)$$

$$0 = \int_0^l \left(\frac{d^2 v}{dx^2} bD_{11} \frac{d^2 W}{dx^2} - b N_x \frac{dv}{dx} \frac{dW}{dx} - \lambda \rho A v W - v q \right) dx + \left[v \frac{d}{dx} \left(bD_{11} \frac{d^2 W}{dx^2} \right) - \frac{dv}{dx} bD_{11} \frac{d^2 W}{dx^2} + v b N_x \frac{dW}{dx} \right]_0^l \quad (2.17)$$

Note that, the first term of the differential equation is integrated twice by parts to trade two differentiations to the weight function v , while retaining two derivatives of the dependent variable W , i.e. the differentiation is distributed equally between v and W .

ii) Boundary conditions:

An important part of step 2 is to identify the two types of boundary conditions associated with the governing differential equation.

Examination of the boundary terms indicates that the essential boundary conditions involve the specification of the deflection W , and slope dW/dx , and the natural boundary conditions involve the specification of the bending moment $b D_{11} \frac{d^2W}{dx^2}$ and the shear force $\frac{d}{dx}(b D_{11} \frac{d^2W}{dx^2})$ at the end points of the element (see Figure 2.4). The following notation is introduced:

$$Q_1^e \equiv \left[\frac{d}{dx} \left(b D_{11} \frac{d^2W}{dx^2} \right) + b N_x \frac{dW}{dx} \right]_{x=0} \quad Q_2^e \equiv \left[b D_{11} \frac{d^2W}{dx^2} \right]_{x=0} \quad (2.18)$$

$$Q_3^e \equiv - \left[\frac{d}{dx} \left(b D_{11} \frac{d^2W}{dx^2} \right) + b N_x \frac{dW}{dx} \right]_{x=l} \quad Q_4^e \equiv - \left[b D_{11} \frac{d^2W}{dx^2} \right]_{x=l} \quad (2.19)$$

iii) Interpolation Functions:

Since there are four boundary conditions in an element (two per node) a four-parameter polynomial is selected as:

$$W(x) = c_1 + c_2 x + c_3 x^2 + c_4 x^3 \quad (2.20)$$

This approximation is needed in order to satisfy the essential boundary conditions, and further this approximation automatically satisfies the continuity conditions (i.e. the existence of a non-zero second derivative of W in the element).

First, let us define the slope $\theta(x)$ as:

$$\theta(x) = \frac{dW(x)}{dx} = c_2 + 2c_3x + 3c_4x^2 \quad (2.21)$$

Now it is needed to express c_i in terms of primary variables, W_1 , θ_1 , W_2 , and θ_2 , and secondary variables (generalized displacements and forces) in the following manner.

$$W(0) = W_1 = c_1 \quad (2.22)$$

$$\theta(0) = \theta_1 = c_2 \quad (2.23)$$

$$W(l) = W_2 = c_1 + c_2l + c_3l^2 + c_4l^3 \quad (2.24)$$

$$\theta(l) = \theta_2 = c_2 + 2c_3l + 3c_4l^2 \quad (2.25)$$

In matrix form, the above four equations can be given as:

$$\begin{Bmatrix} W_1 \\ \theta_1 \\ W_2 \\ \theta_2 \end{Bmatrix} = \begin{bmatrix} 1 & 0 & 0 & 0 \\ 0 & 1 & 0 & 0 \\ 1 & l & l^2 & l^3 \\ 0 & 1 & 2l & 3l^2 \end{bmatrix} \begin{Bmatrix} c_1 \\ c_2 \\ c_3 \\ c_4 \end{Bmatrix} \quad (2.26)$$

Inverting this matrix equation so as to express c_j in terms of W_1 , θ_1 , W_2 , and θ_2 , and substituting the results into equation 2.20, one can show that:

$$W(x) = N_1 W_1 + N_2 \theta_1 + N_3 W_2 + N_4 \theta_2 \quad (2.27)$$

To sum up:

From (2.12), $[W(x)]_{1 \times 1} = [x]_{1 \times 4} \times [c]_{4 \times 1}$;

But from (2.26), $[d]_{4 \times 1} = [I]_{4 \times 4} \times [c]_{4 \times 1}$;

And from (2.27) $[W(x)]_{1 \times 1} = [N]_{1 \times 4} \times [d]_{4 \times 1}$;

Therefore, $[x]_{1 \times 4} \times [c]_{4 \times 1} = [N]_{1 \times 4} \times [I]_{4 \times 4} \times [c]_{4 \times 1}$, and hence

$$[N]_{1 \times 4} = [x]_{1 \times 4} \times [I]_{4 \times 4}^{-1}$$

The interpolation (shape) functions denoted by N_1 , N_2 , N_3 , and N_4 are given as:

$$[N] = \left[\left(1 - \frac{3x^2}{l^2} + \frac{2x^3}{l^3} \right) \quad \left(x - \frac{2x^2}{l} + \frac{x^3}{l^2} \right) \quad \left(\frac{3x^2}{l^2} - \frac{2x^3}{l^3} \right) \quad \left(-\frac{x^2}{l} + \frac{x^3}{l^2} \right) \right] \quad (2.28)$$

which satisfy the following interpolation properties:

$$N_1|_{x=0} = 1, \quad N_i|_{x=0} = 0 \quad (i \neq 1) \quad (2.29)$$

$$N_3|_{x=l} = 1, \quad N_i|_{x=l} = 0 \quad (i \neq 3) \quad (2.30)$$

$$\frac{dN_2}{dx}|_{x=0} = 1, \quad \frac{dN_i}{dx}|_{x=0} = 0 \quad (i \neq 2) \quad (2.31)$$

$$\frac{dN_4}{dx}|_{x=l} = 1, \quad \frac{dN_i}{dx}|_{x=l} = 0 \quad (i \neq 4) \quad (2.32)$$

$$i = 1 \dots 4$$

STEP 3: Finite Element Model

The Finite Element Model of the governing differential equation 2.7 is obtained by substituting the finite element interpolation functions for W , and the interpolation functions N_i in equation 2.28 for the weight function v in the weak form given by equation 2.13. Since there are four nodal variables W_i , four different choices are used for v , that is $v = N_{1...4}$ to obtain a set of four algebraic equations. The i -th algebraic equation of the finite element model (for $v = N_i$) is:

$$0 = \sum_{j=1}^4 \left(\int_0^l b D_{11} \frac{d^2 N_i}{dx^2} \frac{d^2 N_j}{dx^2} - b N_x \frac{dN_i}{dx} \frac{dN_j}{dx} - \lambda \rho A v W \right) u_j dx - \int_0^l N_i q dx - Q_i \quad (2.33)$$

$$\text{or, } \sum_{j=1}^4 (K_{ij} - n_{ij} - M_{ij}) u_j - F_i = 0 \quad (2.34)$$

Here u is a common variable for all nodal variables such that,

$$u_1 = W(0) \quad u_2 = \frac{dW}{dx} \Big|_{x=0} \quad (2.35)$$

$$u_3 = W(l) \quad u_4 = \frac{dW}{dx} \Big|_{x=l} \quad (2.36)$$

$$K_{ij} = \int_0^l b D_{11} \frac{d^2 N_i}{dx^2} \frac{d^2 N_j}{dx^2} dx \quad (2.37)$$

$$n_{ij} = \int_0^l b N_x \frac{dN_i}{dx} \frac{dN_j}{dx} dx \quad (2.38)$$

$$M_{ij} = \int_0^l \rho A N_i N_j dx \quad (2.39)$$

$$F_i = \int_0^l N_i q dx + Q_i \quad (2.40)$$

$$Q_i = \begin{bmatrix} \left[\frac{d}{dx} \left(bD_{11} \frac{d^2 W}{dx^2} \right) + bN_x \frac{dW}{dx} \right]_{x=0} \\ bD_{11} \frac{d^2 W}{dx^2} \Big|_{x=0} \\ - \left[\frac{d}{dx} \left(bD_{11} \frac{d^2 W}{dx^2} \right) + bN_x \frac{dW}{dx} \right]_{x=l} \\ - bD_{11} \frac{d^2 W}{dx^2} \Big|_{x=l} \end{bmatrix} \quad (2.41)$$

Here K_{ij} is the stiffness matrix coefficient, n_{ij} is the geometric stiffness matrix coefficient, and M_{ij} is the mass matrix coefficient.

As one can see, the forms of K_{ij} , n_{ij} , and M_{ij} are the same as for isotropic materials, and further, EI is replaced by bD_{11} and P by bN_x . The stiffness, geometric stiffness, and mass matrices are now given:

$$[K] = \frac{bD_{11}}{l^3} \begin{bmatrix} 12 & 6l & -12 & 6l \\ & 4l^2 & -6l & 2l^2 \\ & & 12 & -6l \\ sym & & & 4l^2 \end{bmatrix} \quad (2.42)$$

$$[n] = \frac{bN_x}{10} \begin{bmatrix} \frac{12}{l} & 1 & -\frac{12}{l} & 1 \\ & \frac{4l}{3} & -1 & -\frac{l}{3} \\ & & \frac{12}{l} & -1 \\ sym & & & \frac{4l}{3} \end{bmatrix} \quad (2.43)$$

$$[M] = \frac{\rho Al}{420} \begin{bmatrix} 156 & 22l & 54 & -13l \\ & 4l^2 & 13l & -3l^2 \\ & & 156 & -22l \\ sym & & & 4l^2 \end{bmatrix} \quad (2.44)$$

For the case of constant ‘ q ’ over an element, the element matrix of generalized forces F_i will be:

$$F_i = -\frac{ql}{12} \begin{bmatrix} 6 \\ -l \\ 6 \\ l \end{bmatrix} + \begin{bmatrix} Q_1 \\ Q_2 \\ Q_3 \\ Q_4 \end{bmatrix} \quad (2.45)$$

It can easily be verified that the term $-\frac{ql}{12} \begin{bmatrix} \cdot \\ \cdot \\ \cdot \\ \cdot \end{bmatrix}$ in F_i represents the “work equivalent” forces and moments at nodes 1 and 2 due to the uniformly distributed load over the element. When q is an algebraically complicated function of x , the mechanics of materials type approach becomes less appealing, whereas equation 2.40 provides a straightforward way of computing the generalized “work equivalent” force components.

2.3.2 Weak Formulation for Mid-plane Tapered Composite Beams

The classical lamination theory states that [57]:

$$D_{II} = \sum_{p=1}^n \left[t_p \bar{Z}_p^2 + \frac{t_p^3}{12} \right] (\bar{Q}_{II})_p \quad (2.46)$$

where D_{II} is the bending or flexural laminate stiffness relating the bending moment M_x to curvature κ_x , $(\bar{Q}_{II})_p$ is the transformed stiffness coefficient of a ply, t_p is the ply thickness, \bar{Z}_p is the distance between the centerline of the ply and the centerline of the

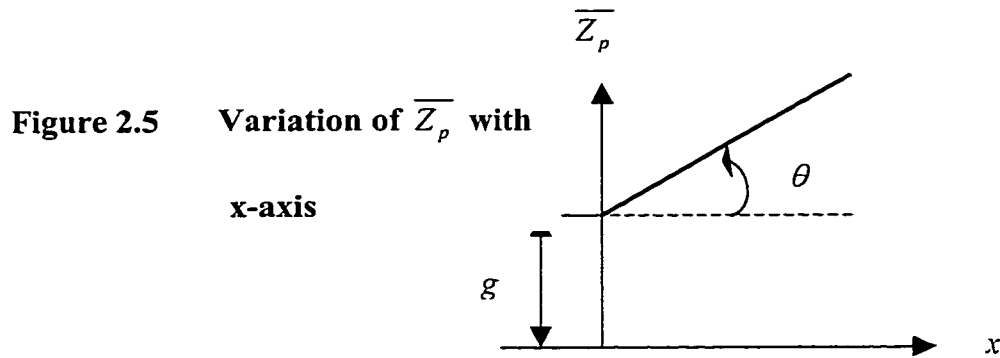
whole laminate, and n is the total number of plies. The derivation of equation 2.46 is summarized in Appendix II.

For tapered composite beams the height of the centerline of each ply (\bar{Z}_p) is a function of x (as shown in Figure 2.5). The equation for \bar{Z}_p is:

$$\bar{Z}_p = mx + g \quad (2.47)$$

In equation 2.47 ' m ' is the slope of the straight line ($= \tan \theta$), and ' g ' is its intercept at $x = 0$. Then equation 2.46 can be written as:

$$D_{II} = \sum_{p=1}^n \left[t_p (\overline{mx + g})_p^2 + \frac{t_p^3}{12} \right] (\bar{Q}_{II})_p \quad (2.48)$$



Hence, the ply stiffness coefficient D_{II} will be a function of x too. In the previous section the three matrices, $[K]$, $[n]$, and $[M]$ required for the dynamic analysis of composite beams were established (equations 2.42, 2.43, and 2.44). By examining them one can find that only the stiffness matrix $[K]$ will be affected by this change because it is a function of bD_{II} . Mathematically, this involves the calculation of the integration (equation 2.37) after replacing D_{II} in the integration by the equation 2.48. This

integration is performed using the software Maple[®] V Release 4, and the stiffness matrix for the mid-plane tapered composite beam has been obtained as:

$$[K] = H \begin{bmatrix} 0.2A & 0.1B & -0.2A & 0.1C \\ \frac{8m^2l^2 + 30glm + 60g^2 + 5t_p^2}{15l} & -0.1B & \frac{26m^2l^2 + 60glm + 60g^2 + 5t_p^2}{30l} & \\ & 0.2A & -0.1C & \\ sym & & \frac{38m^2l^2 + 90glm + 60g^2 + 5t_p^2}{15l} & \end{bmatrix} \quad (2.49)$$

where

$$A = \frac{24m^2l^2 + 60glm + 60g^2 + 5t_p^2}{l^3} \quad (2.50)$$

$$B = \frac{14m^2l^2 + 40glm + 60g^2 + 5t_p^2}{l^2} \quad (2.51)$$

$$C = \frac{34m^2l^2 + 80glm + 60g^2 + 5t_p^2}{l^2} \quad (2.52)$$

$$H = b(\overline{Q_{11}})_p t_p \quad (2.53)$$

2.3.3 Assembly of Elements and Imposing the Boundary Conditions

As there is no change in the number of degrees of freedom at each node, the procedures for assembling the elements and imposing the boundary conditions on the

structure will be the same, as in the case of metallic beams. The relevant details are available in chapter 4 of Ref. [53], and they are not repeated here.

2.4 Modeling Variable Thickness Composite Beams

2.4.1 Modeling Externally Tapered Composite Beams

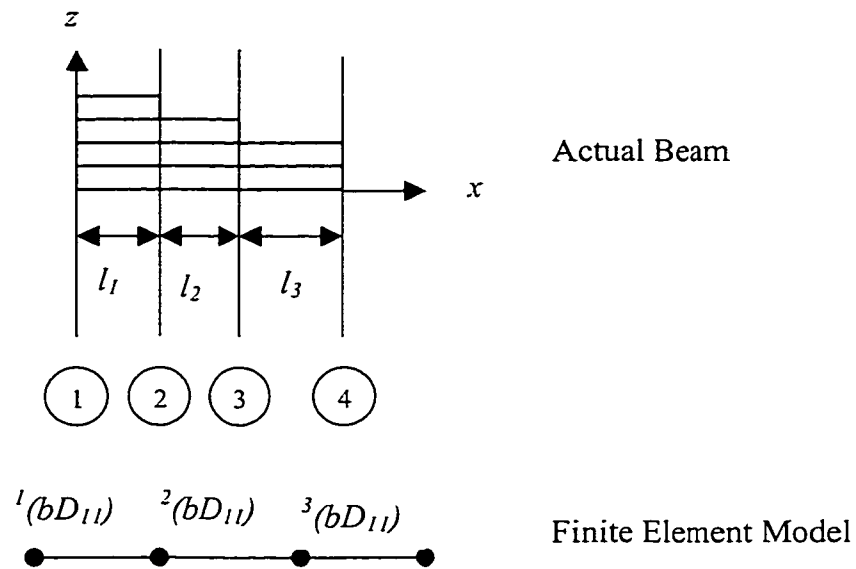


Figure 2.6 Modeling of Externally Tapered Composite Beam

This type of beams is modeled using uniform one-dimensional finite elements. In the present case, the geometry requires selecting the locations of nodes, and consequently the elements where the thickness changes. Therefore, the beam shown in Figure 2.6 is divided into three elements with a total of four nodes, and eight global degrees of freedom (before imposing the boundary conditions). The actual beam is represented

using homogenous beam elements. The bD_{II} values for different elements corresponding to the actual beam are shown in Figure 2.6. The numbering of plies starts from the bottom, so the common ply in all elements will have the same number. To simplify the analysis the coordinates are taken at the first node, so the x-coordinate of node 1 is zero.

The present configuration is merely an example, but the number of plies for each element, the number of elements, and the length of each element can be modified according to the structures used in industry.

One should note that the finite element solution of a similar problem for metals is also defined element-wise (because of the discontinuity in the flexural rigidity). In other words, this way of modeling is not far from the solution employed for similar metallic beams of variable thickness.

2.4.2 Modeling Mid-plane Tapered Composite Beams

This type of beams is modeled using non-uniform one-dimensional finite elements that are made of symmetric type of laminate. Again, the geometry of the present case requires selecting the locations of nodes, and consequently the elements where the plies are terminated (see Figure 2.7). Therefore, the beam shown in Figure 2.7 is divided into three elements with a total of four nodes, and eight global degrees of freedom (before imposing the boundary conditions). The numbering of plies starts from

the top ply, so that the common ply in all elements will have the same number. The origin of the coordinates is located at the first node, and so the x-coordinate of node 1 is zero.

The present configuration is merely an example, but the number of plies for each element, the number of elements, and the length of each element can be modified according to the structures used in the industry.

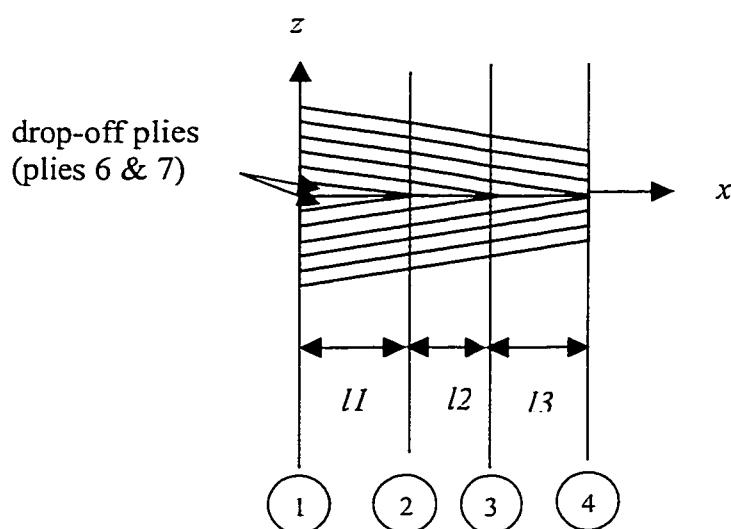


Figure 2.7 Modeling of Mid-plane Tapered Composite Beam

There are two approximations that are involved in the modeling. First, by examining the configuration shown in Figure 2.7, one can notice that the terminated plies (plies 4, 5, 6, 7, 8, and 9) have larger cross-sectional areas at the axis of symmetry. The effect of this on the bending and shear response is ignored. Secondly, the cross-sectional

area of each drop-off ply (plies 6 & 7) is approximated by the cross-sectional area of a ply that is common to all elements.

It is believed that these two approximations in the modeling do not violate any of the basics of the governing differential equation or its weak form for the following reason. The slight change in thickness is very small. It is of the order of 10^{-5} m; hence its effect on the calculations will be of minor significance.

2.5 Solution of Equilibrium Equations in Dynamic Analysis

The equations of equilibrium governing the linear dynamic response of an undamped system of finite elements are [49]:

$$M\ddot{w} + Kw = q \quad (2.54)$$

where M and K are the mass and stiffness matrices, q is the vector of externally applied loads, and w and \ddot{w} are the displacement and acceleration vectors of the finite element assemblage. Mathematically, equation 2.54 represents a system of linear differential equations of second order. In practical finite element analysis two methods of solutions are employed: direct integration method and mode superposition method.

In direct integration method the equation 2.54 is integrated using a numerical step-by-step procedure. The term “direct” means that prior to the numerical integration, no transformation of the equations into a different form is carried out.

One of the direct integration methods is the Newmark method where its scheme can also be understood to be an extension of the linear acceleration method. The following assumptions are used:

$${}^{t+\Delta t}\dot{w} = {}^t\dot{w} + [(1-\delta){}^t\ddot{w} + \delta {}^{t+\Delta t}\ddot{w}]\Delta t \quad (2.55)$$

$${}^{t+\Delta t}w = {}^tw + {}^t\dot{w}\Delta t + \left[\left(\frac{1}{2} - \alpha\right){}^t\ddot{w} + \alpha {}^{t+\Delta t}\ddot{w}\right]\Delta t^2 \quad (2.56)$$

where α and δ are parameters that can be determined so as to obtain the desired integration accuracy and stability. In Newmark method values of $\delta = 1/2$ and $\alpha = 1/4$ are proposed to obtain an unconditionally stable scheme.

Another method of direct integration methods is the Wilson- θ method, which is essentially an extension of the linear acceleration method. In this method a linear variation of acceleration from time t to time $t + \theta\Delta t$ is assumed, where $\theta \geq 1$. A value of $\theta = 1.4$ is used for unconditional stability in the Wilson- θ method.

Let τ denote the increase in time, where $0 \leq \tau \leq \theta\Delta t$. Then for the time interval t to $t + \theta\Delta t$, it is assumed that:

$${}^{t+\tau}\ddot{w} = {}^t\ddot{w} + \frac{\tau}{\theta\Delta t} \left({}^{t+\theta\Delta t}\ddot{w} - {}^t\ddot{w} \right) \quad (2.57)$$

The two methods are employed in the MATLAB[®] program to obtain the dynamic response of the structures. The subroutines for both methods are included in the MATLAB[®] program in Appendix I under the names FORVNM and FORVWT, respectively.

2.6 Program Development For Vibration Analysis

In this section a detailed description of the program that computes the natural frequencies of a variable-thickness composite beam using finite element modeling will be given. Furthermore, the program can also compute the structural dynamic response (for the forced vibration case) using two different methods that are, the Newmark method and the Wilson- θ method.

The program can analyze structures made of metals and composites. Further, both the uniform and the tapered laminates can be analyzed.

The following types of analyses can be performed using the developed program: free vibration analysis, forced vibration analysis, and buckling due to constant and variable axial loads.

It is based on the use of the six-degrees-of-freedom frame element described in Figure 2.8.

This program has been developed using MATLAB[®] software. The program structure is shown in Figure 2.9 and the complete code is given in Appendix I.

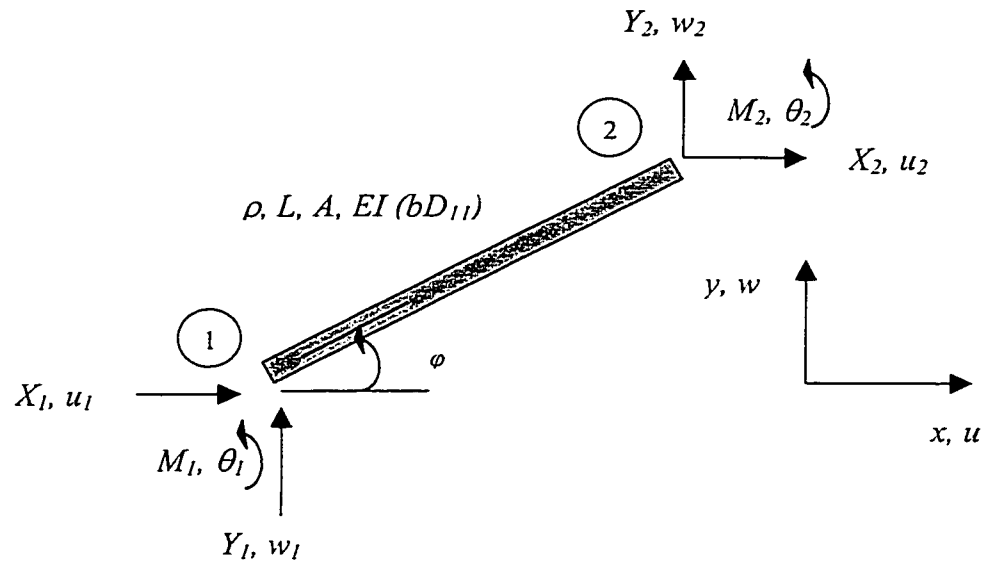


Figure 2.8 Six-Degrees-Of-Freedom Frame Element

The one-dimensional beam element and truss bar element are treated as special cases of the general plane frame element. Provision is given for inextensible members with relatively large axial stiffness. Further, options are provided for both the lumped and the consistent mass matrix formulations.

Here is a description of Input Data:

NNOD - Number of nodal points

NELE - Number of elements

NMOD - Desired number of modes to be printed

Flag to select lumped or consistent mass matrix:

LMAS = 1 for lumped mass matrix

LMAS = 2 for consistent mass matrix

Flag to select type of element:

ICAS = 1 for truss bar element

ICAS = 2 for general frame element

ICAS = 3 for inextensible frame element with infinite axial rigidity.

N - Nodal point number

Boundary condition for axial displacement in x direction:

IBOU (N, 1) = 1 free to move

IBOU (N, 1) = 0 restrained

Boundary condition for lateral displacement in y direction:

IBOU (N, 2) = 1 free to move

IBOU (N, 2) = 0 restrained

Boundary condition for rotation in xy plane:

IBOU (N, 3) = 1 free to rotate

IBOU (N, 3) = 0 restrained

X coordinate [XNOD (N)]

Y coordinate [YNOD (N)]

Mass in x direction [CMAS (N, 1)]

Mass in y direction [CMAS (N, 2)]

Mass moment of inertia [CMAS (N, 3)]

N - Element number

First-end nodal point number [NODN (N, 1)]

Second-end nodal point number [NODN (N, 2)]

Cross-sectional area [AREA (N)]

[SMOI (N)] Moment of inertia of a metal beam (I)

[EMOD (N)] Modulus of elasticity of a metal beam (E)

Mass density per unit volume [EROW (N)]

QT- Laminate stiffness matrix for an element (Q)

FLRI-Flexural Rigidity of composite beam (bD_{11})

The following subroutines constitute the program:

2.6.1 Subroutines of the Program

2.6.1.1 Subroutine TRANMAT

This subroutine is to compute the transformation matrix. This matrix will transform the element stiffness and mass matrices from local coordinates into global ones. It is stored as [T].

2.6.1.2 Subroutine ELEFEX

The function of this subroutine is the computation of the transformed ply stiffness matrix \bar{Q} . Also, it computes the laminate stiffness matrices: A , B , and D . From these computations one can get the flexural rigidity of the laminate.

2.6.1.3 Subroutine ELESTF

The function of this subroutine is to calculate the entries of the element stiffness matrix (in local coordinates). This matrix is named “ESTF”.

2.6.1.4 Subroutine ELEMAS

This subroutine is to compute lumped or consistent element mass matrix (in local coordinates). It is named “EMAS”.

2.6.1.5 Subroutine CONTRN

The function of this subroutine is to perform the congruent transformation. In other words, the element stiffness and mass matrices in local coordinates corresponding to

different elements in the frame structure are converted to their corresponding element stiffness and mass matrices in the global coordinate system. Mathematically, this transformation can be expressed as $C = (\text{Transpose of } T) \times G \times T$, where G is either stiffness or mass matrix.

2.6.1.6 Subroutine EIGZF

This subroutine calculates the eigenvalues, the eigenvectors, and the square root of eigenvalues, which are the natural frequencies, rearranges them in an increasing order of magnitude, and prints all these values for each node and for each mode.

2.6.1.7 Subroutine FORVNM

This subroutine computes the dynamic displacements and rotations of a structure using Newmark method, which is one of the direct integration methods. Provisions are made to calculate the maximum displacement, maximum velocity, and maximum acceleration at each node.

2.6.1.8 Subroutine FORVWT

The function of this subroutine is the same as the previous one. It just differs in the assumptions employed for obtaining the solution. It is based on the Wilson- θ method. It is added to verify the results of the previous subroutine, as explained in the next section.

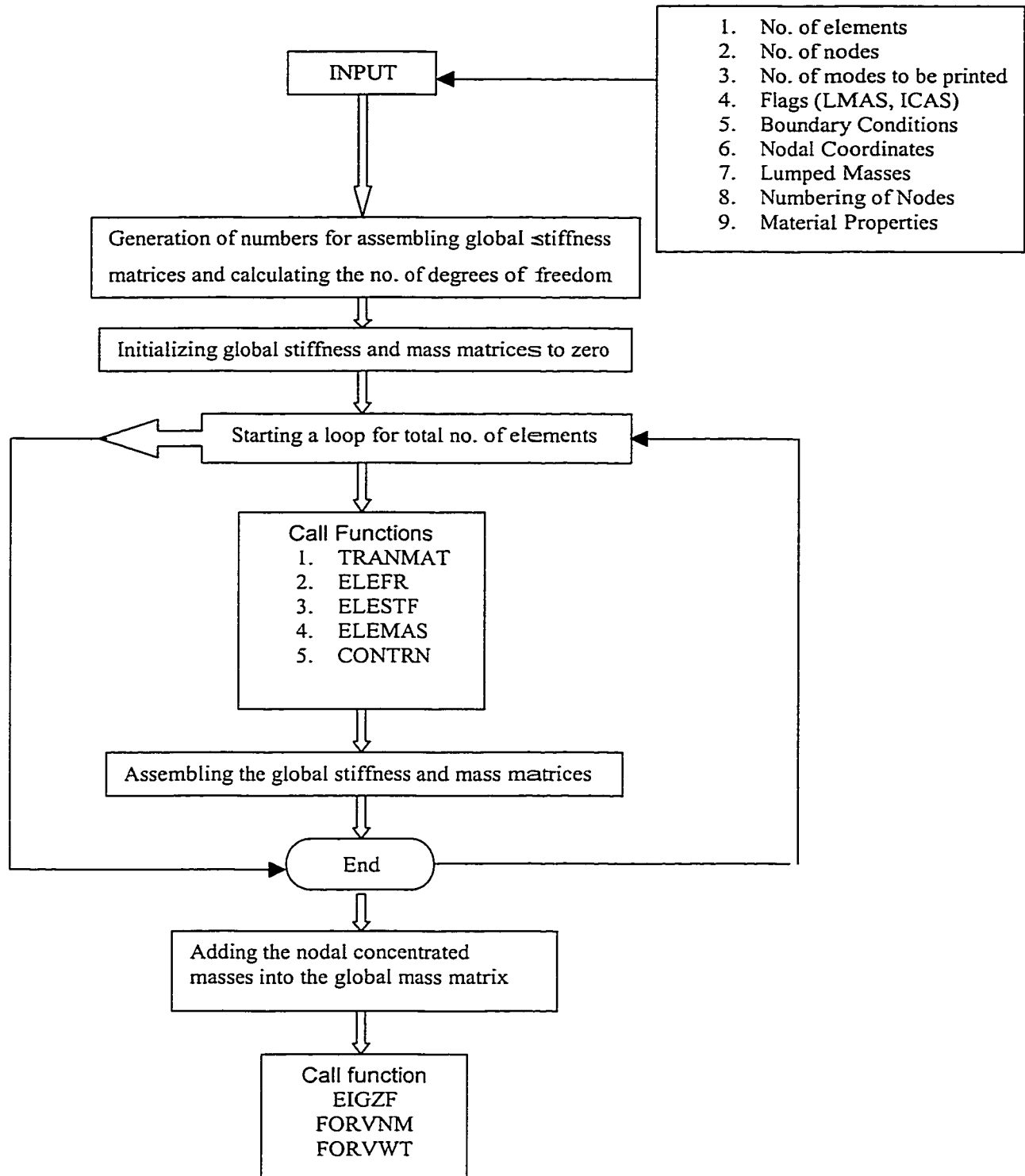


Figure 2.9 The structure of the MATLAB[®] program for determining the natural frequencies and the dynamic response of metallic and composite beams

2.7 Example problems and Validation

In this section a complete set of all example problems that were solved using the developed program will be covered. It will be divided into two sub-sections, one for problems involving metals, and the other one for problems involving composites. Solutions are validated by comparing them with existing results and the results obtained using the exact solution or other approximate methods.

2.7.1 Beams Made of Metals

2.7.1.1 Free Vibration of Simply Supported Beam

Problem description [43]:

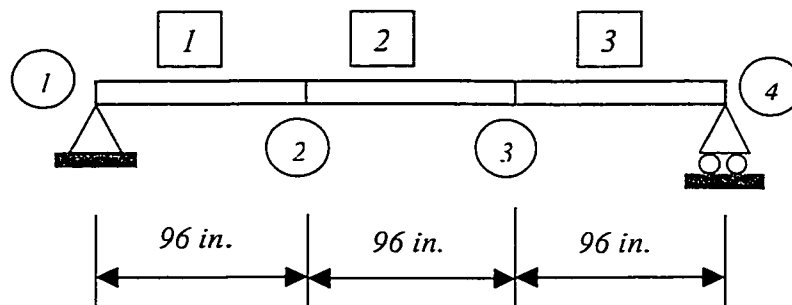


Figure 2.10 Free vibration analysis of a simply supported beam

Figure 2.10 shows an A-36 steel I beam with a cross section of 8I23 [43] and with both ends simply supported. The problem is defined by the following parameters: cross-sectional area $A = 6.71 \text{ in.}^2$, cross-section moment of inertia $I = 64.2 \text{ in.}^4$, modulus of elasticity $E = 30 \text{ Mpsi}$, and mass density of the beam $\rho = 0.0002734 \text{ lb / in.}^3$. The beam is modeled using three beam elements. The natural frequencies and corresponding mode shapes are sought. The input data necessary for a free vibration analysis of this beam were provided into the MATLAB[®] program and the results were obtained. The first three natural frequencies are obtained to be: 74.52, 301.37, and 743.81 rad./sec respectively.

Validation of the results:

There is an exact solution for this type of structure and loading, which is [43]:

$$\omega_i = \left(\frac{i\pi}{L} \right)^2 \sqrt{\frac{EI}{\rho A}} \quad (2.58)$$

in which $i = 1, 2, 3, \dots$ is the mode number, and L is the span of the beam.

The results obtained using the program were compared with the closed form solution, and the percentage of errors (The error is calculated as follows:

$$\text{error} = \left(\frac{\omega - \omega_{\text{exact}}}{\omega_{\text{exact}}} \right) \times 100$$

) is tabulated in Table 2.1 below. Also, the percentage of

errors for the same problem solved by FORTRAN program given in Ref. [43] is shown in the same table.

It was noticed that the percentage of error in the third mode is relatively high (10.99 %). It was suggested to increase the number of elements from three to six to make sure that this high percentage of error is due to the approximation in the modeling and not in the program codes themselves. The percentage of error in the third mode was significantly reduced (from 10.99% to 0.4 %) as shown in the same table. The table also shows that the results obtained from MATLAB[®] program are as accurate as they are from FORTRAN program given in Ref. [43].

Table 2.1 Percentage of Errors in Natural Frequencies

Number of elements	Mode	MATLAB [®] program results	FORTTRAN program results
3	1	0.08	0.08
	2	1.18	1.18
	3	10.99	11.00
6	1	0.01	0.01
	2	0.08	0.08
	3	0.40	0.39

2.7.1.2 Free Vibration of a Portal Frame

Figure 2.11 shows a four-node, three-element steel portal frame with both ends fixed and with a cross section of 315.7 [43]. The problem is thus defined by the following

parameters: $A = 1.64 \text{ in.}^2$, $I = 2.5 \text{ in.}^4$, $E = 30 \text{ Mpsi}$, and $\rho = 0.0002734 \text{ lb / in.}^3$. The frame is assumed to be inextensible with very large axial stiffness for each member.

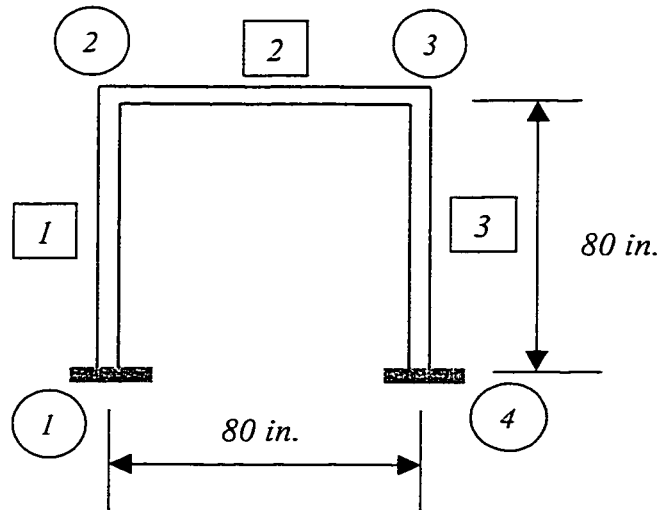


Figure 2.11 Free Vibration Analysis of a Portal Frame with Both Ends Fixed

The natural frequencies and modes are sought. The input data necessary for the free vibration analysis of this frame were provided into the MATLAB[®] program and the results are obtained. The first two natural frequencies are: 125.30 and 590.72 rad./sec., respectively.

Validation of the results:

From the eigenvectors printed, it is seen that the first mode is of antisymmetrical shape. That is, the axial displacement at node 2 (u_2) is equal to the axial displacement at node 3 (u_3) and further, the rotation at node 2 (θ_2) is equal to the rotation at node 3 (θ_3). The

second mode is of symmetrical shape. That is, θ_2 is equal to $-\theta_3$. The results for the same problem obtained in Ref. [43] based on FORTRAN program were 125.30 and 590.72 rad./sec., respectively. Obviously, they both match with the results obtained using the MATLAB[®] program.

2.7.1.3 Elastic Buckling of Columns

2.7.1.3.1 Simply Supported Beam Under Constant Axial Force

Solving the same problem of section 2.7.1.1 with the addition of an axial force of magnitude 320 lbf., the results are obtained to be: 74.42, 301.30, and 743.75 rad./sec., respectively. It is noted that there is a slight difference between these values and their corresponding ones in case of no buckling. Accordingly, an axial force of a higher value was tried to see the effect of the axial force on the natural frequencies. So another value of the axial force (1000 lbf) was tried and the results are: 74.39, 301.12, and 743.60 rad./sec., respectively.

Validation of the results:

The closed-form solution for such a problem is given as [45]:

$$\omega_i^2 = \frac{I}{m} \left(\frac{i\pi}{L} \right)^2 \left[\frac{i^2 \pi^2 EI}{L^2} - P \right] \quad (2.59)$$

**Table 2.2 Percentage of Errors in Natural Frequencies that Correspond to
Constant End Axial Loading**

No. of elements	Mode	For P = 320 lbf	For P = 1000 lbf
3	1	0.09	0.12
	2	1.17	1.15
	3	10.99	10.99
6	1	0.25	0.76
	2	0.08	0.09
	3	0.39	0.39

Table 2.2 shows the percentage of errors obtained by comparing the results obtained using the MATLAB[®] program with that obtained using the closed-form solution for both values of the axial load. Again the percentage of error in the third mode is high. This was improved by increasing the number of elements from three to six. Notably, the accuracy is improved in the case of six-element model.

Validation of the results using static buckling analysis

Applying equation 2.34 for static buckling analysis (i.e. neglecting the terms associated with the mass matrix and considering no external forces ($F_i = 0$)) the following equation is obtained:

$$0 = [K - n]\{u_i\} \quad (2.60)$$

But the axial force in $[n]$ is a common factor for all its entries as it is shown in equation 2.38. The matrix $[n]/P$ is denoted as $[n']$. Then equation 2.60 can be written as:

$$0 = [K - Pn']u_i \quad (2.61)$$

This is an eigenvalue problem, in which the buckling load P is the eigenvalue λ_i . The problem was solved again with this approach and the lowest eigenvalue, i.e. the critical buckling load, was obtained.

The exact solution for the critical buckling load is [45]:

$$P_{cr} = \frac{\pi^2 EI}{L^2} \quad (2.62)$$

The error is calculated as follows: $error = \left(\frac{\omega - \omega_{exact}}{\omega_{exact}} \right) \times 100$. The error associated with the critical buckling load is equal to 0.01029 %.

2.7.1.3.2 Fixed-Free Beam Under Linearly Varying Axial Force

Let the intensity of the distributed axial load be represented as [43]:

$$p(x) = p_o \left[1 + r \left(\frac{x}{l} \right)^\alpha \right] \quad (2.63)$$

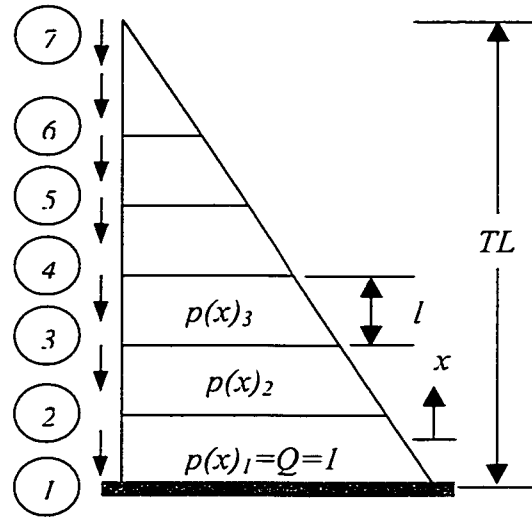
in which x is measured from node 1, and $p(x)$ acts in the direction from node 2 to node 1.

Comments:

- 1) This way of expressing the intensity of axial force is the most appropriate one for the finite element modeling for a common loading case because it is based on an element-wise representation.

- 2) Always x is measured from the node i of the element and l is the element length.
- 3) p_o is always the intensity at the node i of the element.

**Figure 2.12 Fixed-Free Beam
Subjected to its Own Weight**



- 4) α is expressing the nature of how the load is varying. For example:

$\alpha = 0$ for uniformly distributed axial load.

$\alpha = 1$ for linearly varying axial load.

$\alpha = 2$ for parabolically varying axial load,

and so on.

5) Calculation of the coefficient 'r'

As this coefficient is a function of the intensities of the axial load at the node j and node i of each element, and since these intensities differ from one element to another, the coefficient 'r' should be evaluated generally for any element under general intensities of axial loads. This formulation is done as follows (see Figure 2.13):

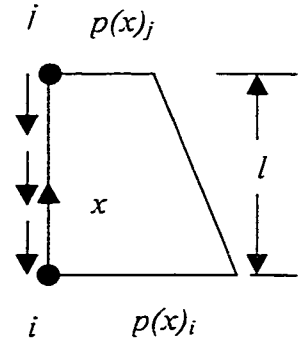
The intensity at the node i (bottom) of the element = $p(x)_i$, and at $x = l$, $p(x) = p(x)_j$.

Then,

$$p(x)_j = p(x)_i \left[1 + r \left(\frac{l}{l} \right)^r \right] \quad (2.64)$$

$$r = \left(\frac{p(x)_j}{p(x)_i} \right)^{\frac{1}{r}} - 1 \quad (2.65)$$

Figure 2.13 Formulation for an element under linearly varying axial load



For example, for analytical solutions where a one-element modeling can be considered, for a linearly varying axial load, $p(x) = 0$ at $x = l$, and $p(x) = p_o$ at $x = 0$. Substituting these values into equation 2.40, one concludes that $r = -1$.

- 6) As it might be noticed that for modeling using more than one element, a pile of axial forces will be accumulated at the top of each element from the elements above it. The axial load at the top node j is denoted as P_o . This was taken into consideration, and hence the final form of the axial forces is given as:

$$P(x) = P_o + P_d(x) \quad (2.66)$$

$$\text{where } P_d(x) = p_o l \left\{ 1 - \frac{x}{l} + \frac{r}{l + \alpha} \left[1 - \left(\frac{x}{l} \right)^{\alpha + 1} \right] \right\} \quad (2.67)$$

This new form of the axial forces was substituted into the equation 2.38, and the new geometric stiffness matrix was set up.

Solution Process:

1) Generally, the geometric stiffness matrix can be expressed as:

$$n_{ij} = c_1 P_o + c_2 p_o \quad (2.68)$$

in which c_1 and c_2 are constants of the element ($f(l, r, \alpha)$). Now let us multiply and divide n_{ij} by ' Q ', where Q is the intensity of the axial load at the base of the structure.

Then equation 2.68 can be written as:

$$n_{ij} = Q \left[\frac{c_1 P_o}{Q} + \frac{c_2 p_o}{Q} \right] \quad (2.69)$$

Then equation 2.34 can be written as:

$$0 = \left[K - Q \left[\frac{c_1 P_o}{Q} + \frac{c_2 p_o}{Q} \right] \right] \{u_i\} \quad (2.70)$$

This is again an eigenvalue problem, where Q is the eigenvalue λ_i . So if Q is given a value of unity, it will not affect the values inside the brackets, and the resulting eigenvalue λ_i is a scale factor of Q . Accordingly, the total axial load will be $0.5 \times \lambda_i \times \text{total length of the structure (TL)}$.

2) The material constants are chosen as in the problem described in section 2.7.1.1. The beam is modeled using six elements. From Figure 2.12, the following relation can be deduced, which is used in solving the problem. At any node i :

$$\frac{p(x)_i}{Q} = \frac{TL - x_i}{TL} \quad (2.71)$$

Finally, the critical buckling load (the lowest eigenvalue) was found to be 373912.2 lbf.

Validation of the results:

The closed-form solution for the beam with the loading and boundary conditions shown in Figure 2.12 is [47]:

$$P_{cr} = \frac{16.1EI}{l^2} \quad (2.72)$$

The percentage of error associated with the calculated critical buckling load was then calculated to be 0.02 %.

2.7.1.3.3 Fixed-Free Beam Under Uniformly Distributed Axial Force

The same problem as in the last section was solved for a different loading condition, that is, the uniformly distributed axial force (here $r = \alpha = 0$). The exact solution is given by an equation similar to the equation 2.47 wherein the constant 16.1 is replaced by the constant 7.84. The percentage of error in the present case was then calculated to be 0.09 %.

2.7.1.4 Dynamic Response of a Fixed-Fixed Beam

Problem description:

For the fixed-fixed beam shown in Figure 2.14, a) the natural frequencies and mode shapes, and b) the response to a concentrated force of 10000 lb suddenly applied at the center of the beam for 0.1 sec. and removed linearly as shown in Figure 2.15 are sought. A time step of integration $\Delta t = 0.01$ sec. [48] is used. The properties of the beam are: $L = 200$ in., $I = 100$ in⁴, $E = 6.58$ Mpsi, and mass per unit length $\bar{m} = 0.037$ lb / in. The beam is divided into four elements of equal length as shown in Figure 2.14.

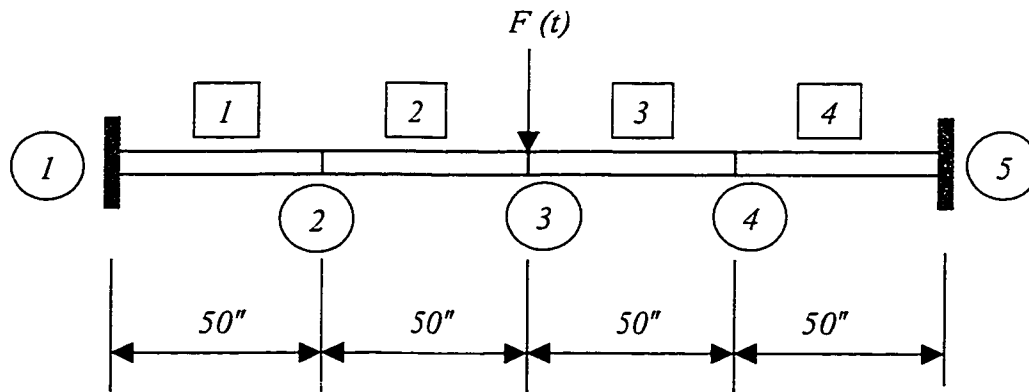


Figure 2.14 Modeling the Fixed-Fixed Beam for Forced Vibration Analysis

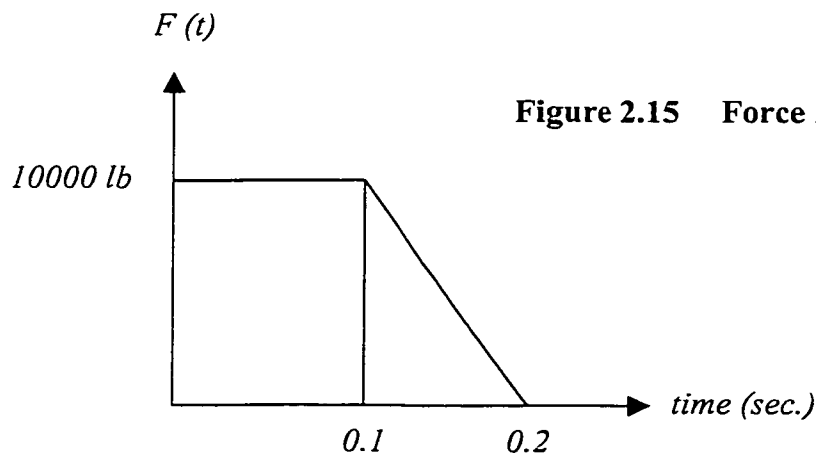


Figure 2.15 Force Applied on the Beam

Validation of the results:

Table 2.3 Comparison of the Maximum Displacement

Node No.	Results given in Ref. [48]	Present solution with Newmark Method	Present solution with Wilson- θ method
1	0.654	0.6551	0.6505
2	0.019	0.0186	0.0187
3	1.243	1.2426	1.2332
4	0.000	0.0000	0.0000
5	0.654	0.6551	0.6505
6	0.019	0.0186	0.0187

- 1) A Newmark method was used to find the dynamic response with $\delta = 0.5$ and $\alpha = 0.25$. The results for the maximum displacement in inches at nodes 1 to 6 are 0.654, 0.019, 1.243, 0.000, 0.654, and 0.019, respectively. These results of the MATLAB[®] program are compared to the results given in Ref. [6] as shown in Table 2.3 above. Obviously, they are almost identical as they start to differ in the third decimal place.
- 2) Another validation was done by using another method of direct integration methods which is the *Wilson- θ method*, with $\theta = 1.4$. The results for the maximum displacements in inches at nodes 1 to 6 are 0.6505, 0.0187, 1.2332, 0.000, 0.6505, and 0.0187, respectively. Again, these results of the MATLAB[®] program are compared

to the results given in Ref. [48] and the ones obtained by the Newmark Method as shown in Table 2.3. Apparently, they converge with the other two sets of results.

2.7.1.5 Application To Tapered Beam

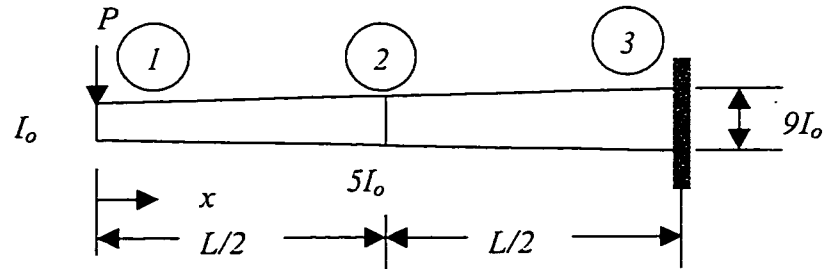


Figure 2.16 Tapered Cantilever Beam Modeled by Two Tapered Elements

A tapered cantilever beam is shown in Figure 2.16. The moment of inertia is assumed as defined by the following equation [43]:

$$I(x) = I_o \left[1 + r \left(\frac{x}{L} \right)^\alpha \right] \quad (2.73)$$

This is similar to equation 2.63, with replacing the axial force $p(x)$ by the moment of inertia $I(x)$. In the present case, $r = 8$ and $\alpha = 1$. Let it be desired to find the deflection and slope at the free end by finite element modeling and compare it with the exact solution.

Validation of the results:

The percentage of error in the response obtained using the MATLAB[®] program in comparison with the exact solution mentioned in Ref. [43] is shown in Table 2.4. As can be observed from the table, there is an excellent agreement between the results.

**Table 2.4 Percentage of Error in Deflection and Slope at the Free End of a
Tapered Cantilever Beam**

No. of Elements	Error in Tip Deflection (%)	Error in Tip slope (%)
1	-0.62	2.82
2	-0.17	0.77

2.7.2 Example Problems and Validation for Composite Beams

2.7.2.1 Example Problems and Validation for Uniform Composite Beams

2.7.2.1.1 Free Vibration of Simply Supported and Fixed-Fixed Composite Beams

A composite beam, shown in Figure 2.10, made up of NCT-301 graphite/epoxy material with the following ply material properties is considered: $E_{11} = 113.9 \text{ GPa}$, $E_{22} = 7.985 \text{ GPa}$, $\nu_{12} = 0.288$, $\nu_{21} = 0.018$, and $\rho = 1480 \text{ kg/m}^3$. The laminate is cross-ply symmetric $[0/90]_s$ and the number of plies is 30. Both the simply supported and the fixed-fixed boundary conditions are considered.

Validation of the results:

The closed-form solution for simply supported composite beam is [50]:

$$\omega_i = \left(\frac{i\pi}{L} \right)^2 \sqrt{\frac{bD_{II}}{\rho A}} \quad (2.74)$$

The results for the natural frequencies obtained using the MATLAB® program are 615.81, 2490.32, and 6146.46 rad./ sec., respectively. These results were compared with the closed form solution in equation 2.74, and the percentage of error is calculated as 0.08 %, 1.18 %, and 10.99 %, respectively. Clearly, the MATLAB® program results are of high accuracy, except in the third mode. This can be quickly understood by the fact that it is a matter of modeling. In other words, the approximation in the MATLAB® program is not reduced enough by modeling using three elements. To confirm what was just mentioned, let us check Table 2.5 below. One can see that the percentage of error in the third mode is significantly reduced from 10.99 % to 1.83 % by modeling using four elements instead of three.

The closed-form solution for the fixed-fixed composite beam is [45]:

$$\omega_i = \left(\frac{k_i}{L} \right)^2 \sqrt{\frac{bD_{II}}{\rho A}} \quad (2.75)$$

in which $k_1 = 4.730041$, $k_2 = 7.853205$, and $k_3 = 10.995607$.

The results for the natural frequencies obtained using the MATLAB® program are 1400.54, 3921.67, and 9121.16 rad./ sec., respectively. These results were compared with the closed form solution in equation 2.75, and the percentage of error is calculated

as 0.41 %, 2.00 %, and 21.01 %, respectively. Noticeably, the MATLAB[®] program results are of acceptable accuracy, except in the third mode. This can be reasoned by the fact that for this type of boundary conditions with just three-element modeling, the beam has just four degrees of freedom (at nodes 2 and 3). Hence, the solution of the MATLAB[®] program will have a significant amount of approximation. Consequently, the results starting from the third mode will show high percentage of error. This can be assured by checking Table 2.5 below, where it is shown that the percentage of error is drastically reduced from 21.01 % to 2.14 % by modeling using four elements instead of three.

Table 2.5 below shows the percentage of errors associated with the natural frequencies obtained using the MATLAB[®] program in comparison with the closed-form solutions, for different number of elements and different boundary conditions.

**Table 2.5 Percentage of Errors Associated with the Natural Frequencies for
Different Boundary Conditions**

No. of Elements	Mode	MATLAB® program results	
		Simply supported	Fixed-fixed
2	1	0.3947	1.6209
	2	10.9918	32.9201
	3	23.9942	- ¹
3	1	0.0810	0.4091
	2	1.1820	1.9965
	3	10.9918	21.0095
4	1	0.0260	0.1327
	2	0.3947	0.9250
	3	1.8273	2.1357
5	1	0.0107	0.0548
	2	0.1657	0.3991
	3	0.7942	1.3838
6	1	0.0052	0.02656
	2	0.0810	0.1963
	3	0.3947	0.7166

¹ For the case of fixed-fixed beam modeled by two elements, there will be two degrees of freedom (at the node in the middle). Hence, there will be only two modes (two values of natural frequencies).

2.7.2.1.2 Free Vibration of A Fixed-Fixed [0/90]_s Composite Beam

A beam (see Figure 2.14) made of T 300/5208 graphite/epoxy material with the following mechanical properties at 70° F is considered: $E_1 = 21 \text{ Mpsi}$, $E_2 = 1.76 \text{ Mpsi}$, $G_{12} = 0.65 \text{ Mpsi}$, $\nu_{12} = 0.21$, $\nu_{21} = 0.017$, and the mass density $\rho = 0.06 \text{ lb/in}^3$. The beam is considered to be made of a 0/90 lay up, with 4 plies each 0.006" thick. The beam is one inch wide ($b = 1''$) and twelve inches long ($L = 12''$). The beam is fixed at both ends. The lowest natural frequencies are to be determined.

The beam was modeled using four elements and the lowest three natural frequencies are: 9.00, 25.00, and 49.59 rad./sec., respectively. They can also be expressed as circular frequencies: 1.43, 3.98, and 7.89 cycles/sec., respectively.

Validation of the results:

- 1) The results for the natural frequencies obtained using the MATLAB[®] program are compared with the exact solution given by equation 2.75, and the percentage of error associated with the natural frequencies are 0.13 %, 0.92 %, and 2.14 %. Apparently, the results of the MATLAB[®] program are accurate enough to rely on. Furthermore, it is noticed that the percentage of error in the third mode is relatively low, which was not the case for the same problem in the last sub-section. This is because of the difference in the material used and the number of plies, which means that the material

properties as well as the number of plies have their remarkable effect on the results of the natural frequencies.

- 2) The results were validated again based on the results obtained using the software ANSYS® 5.4. The results for the circular frequencies using software ANSYS® 5.4 are 1.43, 3.94, and 6.97 cycles/sec., respectively. The percentage of error is calculated as -0.13 %, -0.14 %, and -9.81 %, respectively. As one can see, the percentage of error in the results obtained using software ANSYS® 5.4 are very close to the ones obtained using the MATLAB® program. It may be of importance to mention that the results of the ANSYS® software are always of lower values than the exact solution, which explains the negative sign in the results. On the contrary, the results of the MATLAB® program are always higher than the exact solution.

Below is given Table 2.6, which summarizes the above-mentioned results.

Table 2.6 Percentage of Error in Natural Frequencies of [0/90]_s Composite Beam

No. Of Elements	Mode	MATLAB® program result	ANSYS® software result
3	1	0.1327	-0.1347
	2	0.924	-0.1426
	3	2.1357	-9.8145

2.7.2.1.3 Buckling of Uniform Composite Beams

Problem description:

A composite beam, shown in Figure 2.10, made up of the same material used in section 2.7.2.1.1 with the same mechanical properties and the same laminate configuration, but with 100 plies instead of 30 is considered. The critical buckling load is to be determined. The beam was modeled using six elements. The method of solution was identical to the method used for metals (given in section 2.7.1.3.1). The critical buckling load was calculated as 8790.8 N.

Validation of the result:

1) The closed-form solution for such a structure and loading is [50]:

$$P_{cr} = \frac{n^2 \pi^2}{L^2} b D_{11} \quad (2.76)$$

So the exact value of critical buckling load is 8789.9 N. Correspondingly the percentage of error is 0.01 %.

2) The second validation was done using ANSYS® software. First with free mesh tool, P_{cr} is obtained to be 8543.8 N, which gives a percentage of error of 2.8 %. With mapped mesh on 3 or 4 sides, P_{cr} is 8546.4 N, and correspondingly the percentage of error is 2.77 %.

2.7.2.1.4 Dynamic Response of Composite Beams (Forced Vibration Case)

The same problem of last sub-section is considered with a concentrated force of 1000 N applied at the mid-span of the beam (see Figure 2.15). The same way of modeling the last problem was followed. The Newmark method was used to find out the maximum displacement at each node (with $\alpha = 0.32$ and $\delta = 0.5$), and further, the Wilson- θ method (with $\theta = 1.4$) was used to verify the results.

Table 2.7 Maximum Displacement of the Fixed-Fixed [0/90]_s Composite Beam

Node No.	Result corresponding to Newmark method	Result corresponding to Wilson- θ method
1	0.0005	0.0006
2	0.0084	0.0704
3	0.0010	0.0040
4	0.0000	0.0000
5	0.0005	0.0006
6	0.0084	0.0704

2.7.2.2 Example Problems and Validation for Tapered Composite Beams

2.7.2.2.1 Free Vibration of Fixed-Fixed $[0/90]_s$ Externally Tapered Composite Beams

An externally tapered composite beam of the same material used in section 2.7.2.1.1 with the same mechanical properties and the same laminate configuration is considered to determine its natural frequencies. The number of plies in each element is 4 and 2 respectively (see Figure 2.17). The beam is modeled using two elements. The MATLAB[®] program provided the following results for the first two natural frequencies: 322.34 and 1457.00 rad./sec., respectively.

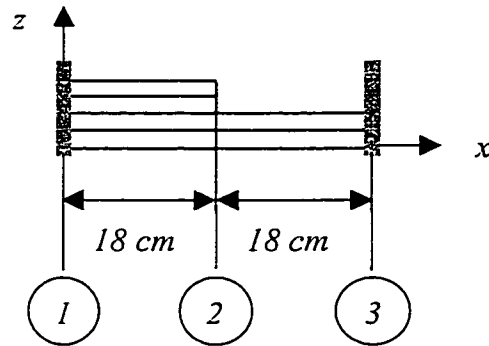


Figure 2.17 Modeling Fixed-Fixed Externally Tapered Composite Beam

Validation of the results:

As there is no exact solution, nor any other solution in any reference for such a problem, the validation for this problem was done by hand calculation. Therefore, the beam was modeled using two elements each of 18 cm length to facilitate the calculations. The

subroutine ELEFREX was used to obtain the flexural rigidity (bD_{II}) for each element, and the results are $6.113 \text{ N} / \text{m}^2$ and $0.954 \text{ N} / \text{m}^2$, respectively. Then the stiffness and mass matrices were calculated for each element using equations 2.41 and 2.43 as follows:

$${}^1K = \frac{6.113}{(0.18)^3} \begin{bmatrix} 12 & 1.08 & -12 & 1.08 \\ & 0.1296 & -1.08 & 0.0648 \\ & & 12 & -1.08 \\ \text{sym} & & & 0.1296 \end{bmatrix}$$

$${}^2K = \frac{0.954}{(0.18)^3} \begin{bmatrix} 12 & 1.08 & -12 & 1.08 \\ & 0.1296 & -1.08 & 0.0648 \\ & & 12 & -1.08 \\ & & & 0.1296 \end{bmatrix}$$

With $\rho = 1480 \text{ Kg} / \text{m}^3$ and the cross-sectional areas are $'A_1' = 6.096 \times 10^{-4} \text{ m}^4$ and $'A_2' = 3.048 \times 10^{-4} \text{ m}^4$, the mass matrices are given by:

$${}^1M = \frac{1480 \times 6.096 \times 10^{-4} \times 0.18}{420} \begin{bmatrix} & & & \\ & 156 & -3.96 & \\ & -3.96 & 0.1296 & \\ & & & \end{bmatrix}$$

$${}^2M = \frac{1480 \times 3.048 \times 10^{-4} \times 0.18}{420} \begin{bmatrix} 156 & 3.96 \\ 3.96 & 0.1296 \\ & & \end{bmatrix}$$

In the mass matrices only the entries that will be used in the assembly of the elements are mentioned.

Assembling these matrices after considering the fact that for this structure there are only two degrees of freedom at node 2, the results are as follows:

$$K = \begin{bmatrix} 14540.65 & -955.305 \\ -955.305 & 157.04 \end{bmatrix}$$

$$M = \begin{bmatrix} 0.0905 & -7.655 \times 10^{-4} \\ -7.655 \times 10^{-4} & 7.51 \times 10^{-4} \end{bmatrix}$$

These two matrices were inputted into the MATLAB[®] software, to get the dynamic matrix 'a' which is:

$$a = \text{inv}(M) \times K$$

$$\text{The matrix 'a' will be given by } a = \begin{bmatrix} 0.0058 & 0.0008 \\ -1.2128 & 0.2171 \end{bmatrix} \times 10^7$$

Then the eigenvalues of this matrix were calculated as 0.1039×10^6 and 2.1248×10^6 . The two natural frequencies of the structure are the square root values of these eigenvalues, which are 322.3 and 1457.7 rad./sec., respectively. By comparison, one can find that they are almost identical to the results obtained using the MATLAB[®] program.

2.7.2.2.2 Free Vibration of Mid-plane Tapered Composite Beam

A mid-plane tapered composite beam of the same material used in section 2.7.2.1 with the same mechanical properties and the same laminate configuration is considered to

determine its natural frequencies. The number of plies in each element is 12, 10, and 8 respectively (see Figure 2.7 with $l_1 = l_2 = l_3 = 0.12 \text{ m}$ and simply supported type of boundary conditions), and taper angle $\theta = -6^\circ$. The beam is modeled using three elements. The MATLAB[®] program provided the following results for the first three natural frequencies: 1640.48, 6972.14, and 17927.65 rad./sec., respectively.

Validation of the results:

If the taper angle ' θ ' is given a very small value such as 0.4° , the mid-plane tapered composite beam can be considered as an externally tapered composite beam. So in the MATLAB[®] program, the value of ' θ ' was changed to 0.4° , and the values for the number of plies were changed to 8, 6, and 4 respectively, keeping the same values as before for all other parameters. The results for the first three natural frequencies are 87.09, 397.37, and 905.41 rad./sec., respectively. For the externally tapered composite beam with the same number of plies and the same boundary conditions, the results of the MATLAB[®] program are 77.48, 332.32, and 885.64 rad./sec., respectively. As one can see, the two results for each kind of taper are of good match and acceptable. It is believed that the shown difference between the two sets of the results will not underestimate the accuracy of the MATLAB[®] program. This is emphasized by the fact that the stiffness and mass matrices for each kind of taper are based on different formulations.

2.8 Conclusions and Discussion

In this chapter, the concepts of free and forced vibration analysis, and buckling analysis as applied to beams of composite materials are summarized. The formulation employing the conventional finite element modeling and analysis for evaluating the stiffness, geometric stiffness, and mass matrices, is described. This analysis is done for both uniform and externally tapered composite beams, and for mid-plane tapered composite beams. The corresponding computer program is developed in MATLAB[®] software environment. A detailed explanation of the program development is given. Example problems are solved using the developed program to obtain the natural frequencies and the critical buckling load, which demonstrate the developed program. The developed program can also obtain the natural frequencies and the critical buckling load for beams made of isotropic materials. The example problems for the case of metals were also worked out. The program was verified by comparing its results with the results obtained from the exact solution, if it exists, or by another software such as ANSYS[®] 5.4, or by comparing them with another similar problem. The results obtained using the developed program are in excellent agreement with the results obtained using other methods. The formulation will be extended in the next chapter for advanced finite element analysis.

Chapter 3

Dynamic Analysis of Variable Thickness Composite Beams Using Advanced Finite Element Formulation

3.1 Introduction

It was introduced in the last chapter how the approximate methods can be applied for vibration analysis and buckling analysis. The procedure as to how the finite element techniques can be used to solve the Euler-Bernoulli's differential equation (governing equations 2.7 and 2.8) numerically, rather than theoretically has been explained. The technique used was called the conventional finite element formulation.

The limitation of the conventional finite element formulation method is obvious: the beam has to be discretized into many elements to get the desired accuracy as can be verified from problems 2.7.1.1 and 2.7.1.3.1.

It has been shown [31] that the accuracy can be improved by increasing the number of degrees of freedom in the element.

A finite element model that considers both the essential (i.e. geometric) boundary conditions (deflection and slope), and natural (i.e. force) boundary conditions (bending moment and shear force) at each node of the beam element is to be established now. This will require a total of eight degrees of freedom per element (that is, four per each node). Accordingly, a polynomial of the seventh order (an algebraic equation of eight terms) is needed for use as the interpolation function.

In this chapter, a weak formulation based on the Euler-Bernoulli's theory of bending of composite beams is developed first for both uniform and externally tapered composite beams. The formulation is then modified so as to be appropriate and applicable for mid-plane tapered composite beams. The present formulation is performed only for free vibration analysis. Hence equation 2.8 will be the governing equation that will be considered in this chapter.

The resulting formulation, which is based on higher order polynomial, is called herein as the advanced finite element formulation. The analysis considers the coupling of bending and axial deformations due to the axial forces (buckling analysis). Based on the above-mentioned formulation, the stiffness, geometric stiffness, and mass matrices are determined for variable thickness composite beams.

The MATLAB[®] computer program that has been developed in the last chapter is modified further so as to incorporate the new formulation, specifically the two subroutines for the element matrices. The program is demonstrated using many example

problems. These example problems cover both types of materials, metallic and composite.

3.2 Formulation Based on Euler-Bernoulli Theory

The present formulation will follow the same steps used in chapter 2 for the construction of the weak form. The governing equation for forced vibration is the same as in equation 2.7. Accordingly, the basic differential equation is given as:

$$\frac{\partial^2}{\partial x^2} \left(bD_{II} \frac{\partial^2 w}{\partial x^2} \right) + bN_x \frac{\partial^2 w}{\partial x^2} + \rho A \frac{\partial^2 w}{\partial t^2} = q(x, t) \quad (3.1)$$

3.3 Weak Formulation of the Governing Equation

3.3.1 Weak Formulation for Uniform and Externally Tapered Composite Beams

The displacement $w(x, t)$, which is the solution to the differential equation 3.1 can be approximated by developing algebraic relations among the coefficients w_j as follows:

$$w(x, t) \approx \sum_{j=1}^n w_j(t) N_j(x) \quad (3.2)$$

The formulation is achieved through the following steps:

Step 1:

The weight function $v(x, t)$ is used to construct the integral statement for uniform composite beam, and for each uniform segment of an externally tapered composite beam.

Mathematically, this means that bD_{II} is constant, so $\frac{\partial^2}{\partial x^2} \left(bD_{II} \frac{\partial^2 w}{\partial x^2} \right)$ in equation 3.1 can

be expressed as $bD_{II} \frac{\partial^4 w}{\partial x^4}$. So, moving all the expressions of the governing differential equation to one side, multiplying the entire equation with the weight function, and integrating over the domain $\Omega = (0, L)$, one can get:

$$0 = \int_0^L v \left[bD_{II} \frac{\partial^4 w}{\partial x^4} + bN_x \frac{\partial^2 w}{\partial x^2} + \rho A \frac{\partial^2 w}{\partial x^2} - q \right] dx \quad (3.3)$$

The statement 3.3 is called the “weighted-integral” equivalent to the equation 3.1.

Step 2:

i) After integrating by parts the weighted integral statement, and applying the approach of separation of variables as given by equation 3.2, equation 3.1 will become as:

$$0 = \int_0^l \left(\frac{d^2 v}{dx^2} bD_{11} \frac{d^2 W}{dx^2} - bN_x \frac{dv}{dx} \frac{dW}{dx} - \lambda \rho A v W - v q \right) + \left[v \frac{d}{dx} \left(bD_{11} \frac{d^2 W}{dx^2} \right) - \frac{dv}{dx} bD_{11} \frac{d^2 W}{dx^2} + v bN_x \frac{dW}{dx} \right]_0^l \quad (3.4)$$

ii) Boundary conditions:

Examination of the natural boundary conditions (bending moment and shear force) at the boundary points, $x = 0$, and $x = l$ will lead to the following notations (which are the constants of the integrations and can be deduced from equation 3.4):

$$Q_1^e \equiv \left[\frac{d}{dx} \left(bD_{11} \frac{d^2 W}{dx^2} \right) + bN_x \frac{dW}{dx} \right]_{x=0} \quad Q_2^e \equiv \left(bD_{11} \frac{d^2 W}{dx^2} \right)_{x=0} \quad (3.5)$$

$$Q_5^e \equiv - \left[\frac{d}{dx} \left(bD_{11} \frac{d^2 W}{dx^2} \right) + bN_x \frac{dW}{dx} \right]_{x=l} \quad Q_6^e \equiv - \left(bD_{11} \frac{d^2 W}{dx^2} \right)_{x=l} \quad (3.6)$$

iii) Interpolation functions:

In the advanced finite element formulation, eight degrees of freedom are considered for each element. That is to affiliate the shear force and the bending moment at each node in the finite element formulation. Accordingly, this will add four more degrees of freedom to an element. So now, it is no longer needed to make an equivalency for bending moment and shear force, as it used to be done in the conventional

formulation. For example, a distributed load over an element in the conventional finite element formulation is approximated by two concentrated loads at both ends of the beam element (i.e., at the nodes), and two bending moments. Surely, this equivalency is an approximation in itself, which will be of inferior quality in the finite element solution, i.e. less accurate and higher percentages of error. As it appeared in the last chapter, in section 2.7, it was necessary to discretize the beam into many elements to converge the solution of the conventional finite element formulation to the closed form solution. By applying the advanced formulation approach, all the possible degrees of freedom in the structure are implemented in the analysis. Hence, there is no necessity for any equivalency, and further, the accuracy of the solution will improve. As it will be shown in section 3.7 when solving different problems using both formulations, conventional and advanced, the accuracy with the advanced finite element formulation is improved significantly.

The analysis starts by writing a new polynomial function for W that consists of a total of eight terms as follows:

$$W(x) = c_0 + c_1x + c_2x^2 + c_3x^3 + c_4x^4 + c_5x^5 + c_6x^6 + c_7x^7 \quad (3.7)$$

Then, one can show that

$$\theta(x) = \frac{dW(x)}{dx} = c_1 + 2c_2x + 3c_3x^2 + 4c_4x^3 + 5c_5x^4 + 6c_6x^5 + 7c_7x^6 \quad (3.8)$$

$$F(x) = -bD_{II} \frac{d^3W(x)}{dx^3} = -bD_{II} [6c_3 + 24c_4x + 60c_5x^2 + 120c_6x^3 + 210c_7x^4] \quad (3.9)$$

$$M(x) = bD_{11} \frac{d^2 W(x)}{dx^2} = bD_{11} [2c_2 + 6c_3x + 12c_4x^2 + 20c_5x^3 + 30c_6x^4 + 42c_7x^5] \quad (3.10)$$

Applying the notation of '1' for the degrees of freedom at $x = 0$, and '2' for those at $x = l$, one can get the following equations:

$$W(0) = W_1 = c_0 \quad (3.11)$$

$$\theta(0) = \theta_1 = c_1 \quad (3.12)$$

$$F(0) = F_1 = -6bD_{11}c_3 \quad (3.13)$$

$$M(0) = M_1 = 2bD_{11}c_2 \quad (3.14)$$

$$W(l) = W_2 = c_0 + c_1l + c_2l^2 + c_3l^3 + c_4l^4 + c_5l^5 + c_6l^6 + c_7l^7 \quad (3.15)$$

$$\theta(l) = \theta_2 = c_1 + 2c_2l + 3c_3l^2 + 4c_4l^3 + 5c_5l^4 + 6c_6l^5 + 7c_7l^6 \quad (3.16)$$

$$F(l) = F_2 = -[-bD_{11} [6c_3 + 24c_4l + 60c_5l^2 + 120c_6l^3 + 210c_7l^4]] \quad (3.17)$$

$$M(l) = M_2 = -[bD_{11} [2c_2 + 6c_3 + 12c_4l^2 + 20c_5l^3 + 30c_6l^4 + 42c_7l^5]] \quad (3.18)$$

To get the equilibrium of an element, the shear force and the bending moment at $x = l$ have to be equal in magnitude and opposite in direction to the ones at $x = 0$. This is the reason for the negative signs that appear in the right sides of equations 3.17 and 3.18.

In matrix form, the above equations can be written together as:

$$\begin{Bmatrix} W_1 \\ \theta_1 \\ F_1 \\ M_1 \\ W_2 \\ \theta_2 \\ F_2 \\ M_2 \end{Bmatrix} = \begin{bmatrix} 1 & 0 & 0 & 0 & 0 & 0 & 0 & 0 \\ 0 & 1 & 0 & 0 & 0 & 0 & 0 & 0 \\ 0 & 0 & 0 & -6bD_{II} & 0 & 0 & 0 & 0 \\ 0 & 0 & 2bD_{II} & 0 & 0 & 0 & 0 & 0 \\ 1 & l & l^2 & l^3 & l^4 & l^5 & l^6 & l^7 \\ 0 & 1 & 2l & 3l^2 & 4l^3 & 5l^4 & 6l^5 & 7l^6 \\ 0 & 0 & 0 & -6bD_{II} & -24bD_{II}l & -60bD_{II}l^2 & -120bD_{II}l^3 & -210bD_{II}l^4 \\ 0 & 0 & 2bD_{II} & 6bD_{II}l & 12bD_{II}l^2 & 20bD_{II}l^3 & 30bD_{II}l^4 & 42bD_{II}l^5 \end{bmatrix} \begin{Bmatrix} c_0 \\ c_1 \\ c_2 \\ c_3 \\ c_4 \\ c_5 \\ c_6 \\ c_7 \end{Bmatrix} \quad (3.19)$$

To sum up the analysis of finding the interpolation function $[N]$ in matrix form:

Equation 3.7 that defines the new polynomial $W(x)$ (a 1×1 matrix) can be expressed as the multiplication of two matrices, the first one is a 1×8 matrix consisting of the terms in variable x , and the other one is an 8×1 matrix of the constants of the polynomial, c 's. Mathematically, this can be written as:

$$[W(x)]_{1 \times 1} = [x]_{1 \times 8} \times [c]_{8 \times 1}$$

Also, if all the degrees of freedom at both the nodes of the element are put into an 8×1 matrix, which is called $[d]$, and by the definitions obtained using equations 3.11 - 3.18, one can define this matrix $[d]$ as the multiplication of two matrices, one for the constants

$[c]_{8 \times 1}$, and the other matrix is an 8×8 matrix that contains the coefficients associated with the constants, c's, which can be called as matrix $[i]$. Mathematically, this can be written as:

$$[d]_{8 \times 1} = [i]_{8 \times 8} \times [c]_{8 \times 1} \quad (\text{as shown in equation 3.19})$$

But the matrix of $W(x)$ can be expressed as the multiplication of the interpolation function matrix $[N]$ by the nodal matrix $[d]$ as follows:

$$[W(x)]_{1 \times 1} = [N]_{1 \times 8} \times [d]_{8 \times 1} \quad (3.20)$$

Substituting the matrix $[d]$ from equation 3.19 into equation 3.20, then

$$[W(x)]_{1 \times 1} = [N]_{1 \times 8} [i]_{8 \times 8} [c]_{8 \times 1} \quad (3.21)$$

Substituting the matrix $[c]$ from equation 3.7 into equation 3.21, one can get,

$$[W(x)]_{1 \times 1} = [N]_{1 \times 8} [i]_{8 \times 8} [W(x)]_{8 \times 1} [x]^{-1} \quad (3.22)$$

Finally, the matrix of the interpolation function can be expressed as:

$$[N]_{1 \times 8} = [i]_{8 \times 8}^{-1} [x]_{8 \times 1} \quad (3.23)$$

The two matrices $[i]$ and $[x]$ were inputted into the software MAPLE[®] V Release 4, and the resulting matrix of interpolation functions, $[N]$ is obtained as follows:

$$N_1 = 1 - 35\frac{x^4}{l^4} + 84\frac{x^5}{l^5} - 70\frac{x^6}{l^6} + 20\frac{x^7}{l^7} \quad (3.24)$$

$$N_2 = x - 20\frac{x^4}{l^3} + 45\frac{x^5}{l^4} - 36\frac{x^6}{l^5} + 10\frac{x^7}{l^6} \quad (3.25)$$

$$N_3 = -\frac{x^3}{6bD_{11}} + \frac{2x^4}{3bD_{11}l} - \frac{x^5}{bD_{11}l^2} + \frac{2x^6}{3bD_{11}l^3} - \frac{x^7}{6bD_{11}l^4} \quad (3.26)$$

$$N_4 = \frac{x^2}{2bD_{11}} - \frac{5x^4}{bD_{11}l^2} + \frac{10x^5}{bD_{11}l^3} - \frac{15x^6}{2bD_{11}l^4} + \frac{2x^7}{bD_{11}l^5} \quad (3.27)$$

$$N_5 = \frac{35x^4}{l^4} - \frac{84x^5}{l^5} + \frac{70x^6}{l^6} - \frac{20x^7}{l^7} \quad (3.28)$$

$$N_6 = \frac{-15x^4}{l^3} + \frac{39x^5}{l^4} - \frac{34x^6}{l^5} + \frac{10x^7}{l^6} \quad (3.29)$$

$$N_7 = -\frac{x^4}{6bD_{11}l} + \frac{x^5}{2bD_{11}l^2} - \frac{x^6}{2bD_{11}l^3} + \frac{x^7}{6bD_{11}l^4} \quad (3.30)$$

$$N_8 = -\frac{5x^4}{2bD_{11}l^2} + \frac{7x^5}{bD_{11}l^3} - \frac{13x^6}{2bD_{11}l^4} + \frac{2x^7}{bD_{11}l^5} \quad (3.31)$$

These interpolation functions satisfy the following boundary conditions:

$$N_1|_{x=0} = 1 \quad N_i|_{x=0} = 0 \quad (i \neq 1) \quad (3.32)$$

$$N_5|_{x=l} = 1 \quad N_i|_{x=l} = 0 \quad (i \neq 5) \quad (3.33)$$

$$\left. \frac{dN_2}{dx} \right|_{x=0} = 1 \quad \left. \frac{dN_i}{dx} \right|_{x=0} = 0 \quad (i \neq 2) \quad (3.34)$$

$$\left. \frac{dN_6}{dx} \right|_{x=l} = 1 \quad \left. \frac{dN_i}{dx} \right|_{x=l} = 0 \quad (i \neq 6) \quad (3.35)$$

$$bD_{11} \frac{d^2 N_4}{dx^2} \Big|_{x=0} = 1 \qquad bD_{11} \frac{d^2 N_i}{dx^2} \Big|_{x=0} = 0 \quad (i \neq 4) \quad (3.36)$$

$$-bD_{11} \frac{d^2 N_8}{dx^2} \Big|_{x=l} = 1 \qquad -bD_{11} \frac{d^2 N_i}{dx^2} \Big|_{x=l} = 0 \quad (i \neq 8) \quad (3.37)$$

$$-bD_{11} \frac{d^3 N_3}{dx^3} \Big|_{x=0} = 1 \qquad -bD_{11} \frac{d^3 N_i}{dx^3} \Big|_{x=0} = 0 \quad (i \neq 3) \quad (3.38)$$

$$bD_{11} \frac{d^3 N_7}{dx^3} \Big|_{x=l} = 1 \qquad bD_{11} \frac{d^3 N_i}{dx^3} \Big|_{x=l} = 0 \quad (i \neq 7) \quad (3.39)$$

where $i = 1 \dots 8$

The interpolation functions that represent the moments at the two boundaries of the element do not equal to zero, as shown in equations 3.36 and 3.37. The signs in equations 3.36 and 3.37 are opposite to each other to get the equilibrium. Similarly, the same can be noticed on the interpolation functions that represent the shear force, equations 3.38 and 3.39 (check the note right after equation 3.18).

In the following, equations 3.24 – 3.39 are plotted in the Figures 3.1 – 3.7 to demonstrate how the interpolation functions and their derivatives, which represent the bending moment and the shear force, change with respect to x . All these figures are obtained using unit flexural rigidity and unit beam span ($bD_{11} = 1$ and $L = 1$).

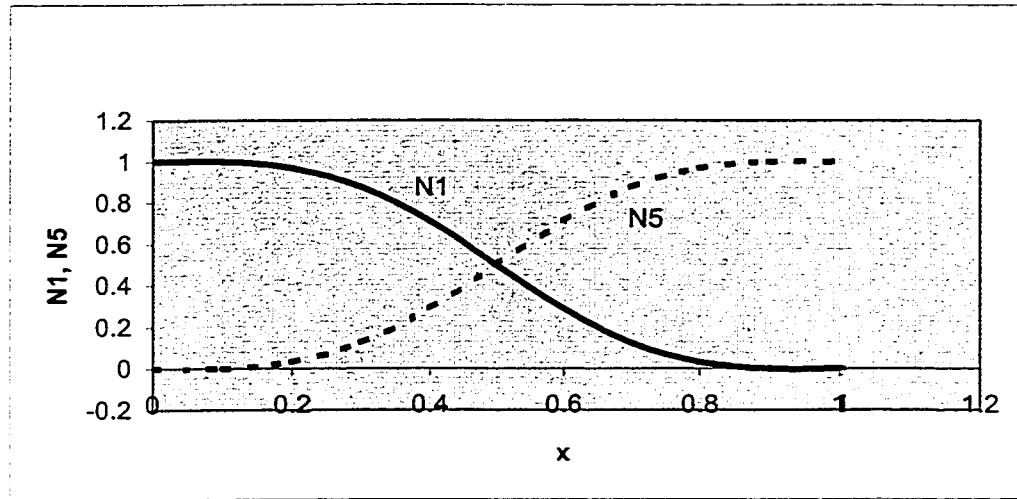
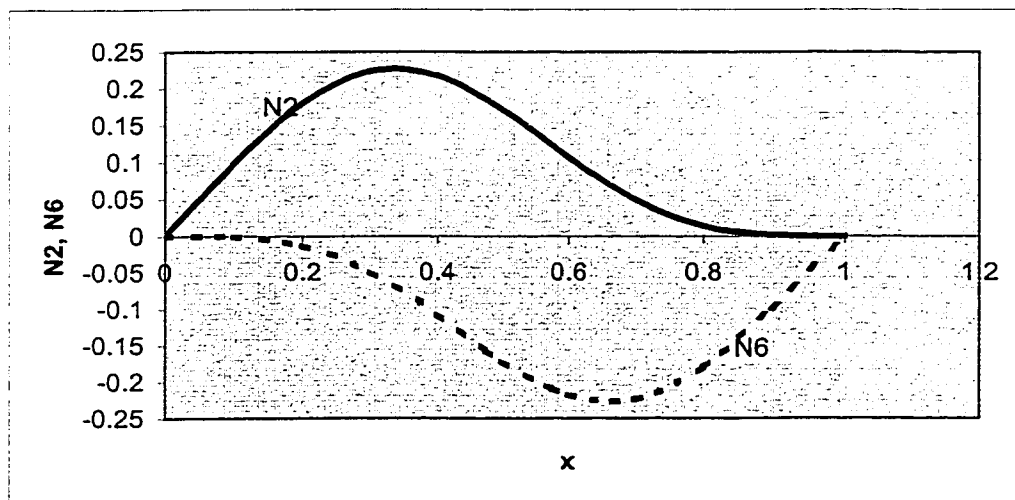


Figure 3.1 Variations of N_1 and N_5 With Respect To x

Both the curves for N_1 and N_5 together are symmetric as shown in Figure 3.1. Also, N_1 is of a negative slope, where N_5 is of a positive slope (N_1 and N_5 are expressed on the graph as $N1$ and $N5$). N_1 and N_5 are grouped together in one figure because they represent the deflection W in the nodal matrix $[d]$.

Figure 3.2 Variations of N_2 and N_6 With Respect To x



It is shown in Figure 3.2 that N_2 is of something like a “sinusoidal” nature in the positive side of the axes, where N_6 is also “sinusoidal”, but shifted from the origin, and is in the negative side of the ordinate (they are shown on the graph as $N2$ and $N6$).

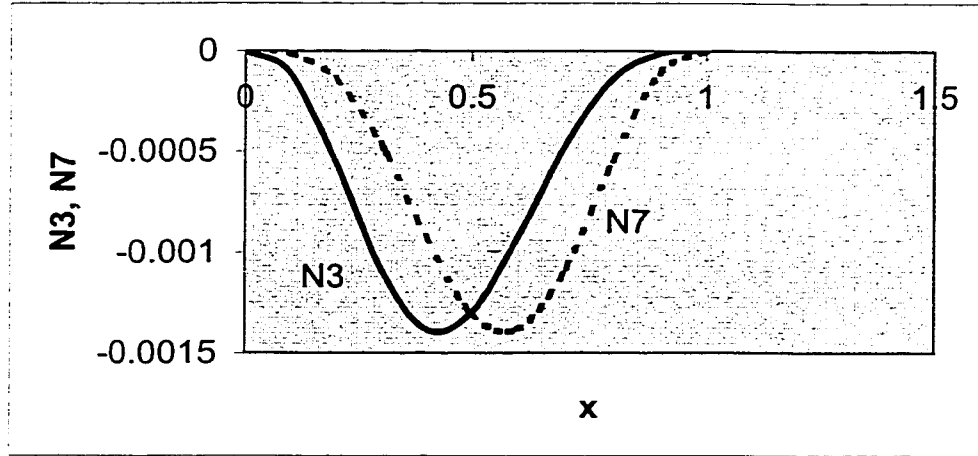


Figure 3.3 Variations of N_3 and N_7 With Respect To x

Figure 3.3 shows that the variations of N_3 and N_7 (appear on the graph as $N3$ and $N7$) are also “sinusoidal-wise”, but in the negative side of the ordinate. The peak of N_3 is more shifted to the left than N_7 .

Figure 3.4 shows that the variations of N_4 and N_8 are of “sinusoidal” nature, where N_4 is in the positive side of the axis, and N_8 is in the negative side.

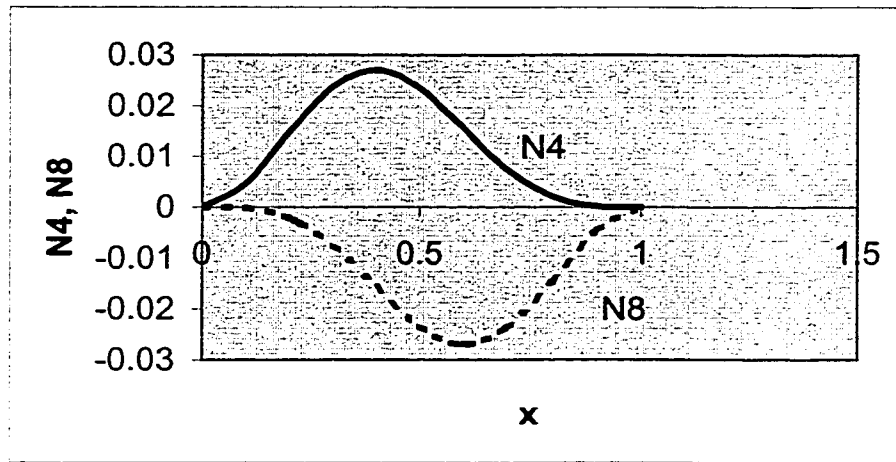


Figure 3.4 Variations of N_4 and N_8 With Respect To x

The following graphs in Figures 3.5 and 3.6 are for the bending moment, recalling that the flexural rigidity is equal to 1.

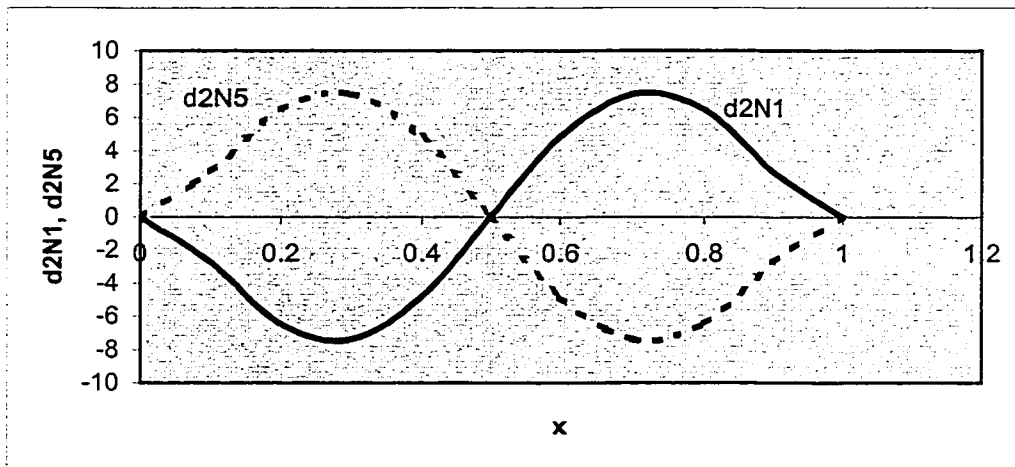


Figure 3.5 Variations of $\frac{d^2 N_1}{dx^2}$ and $\frac{d^2 N_5}{dx^2}$ With Respect To x

Figure 3.5 shows that both the second derivatives of N_I and N_5 are changing “sinusoidally”. The second derivative of N_I (expressed on the graph as d2N1) is of a positive slope, where the second derivative of N_5 (expressed on the graph as d2N5) is of a negative slope.

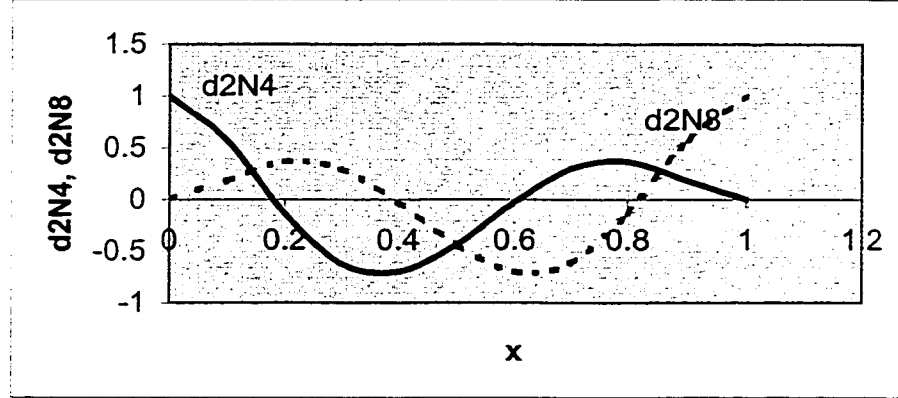


Figure 3.6 Variations of $\frac{d^2 N_4}{dx^2}$ and $\frac{d^2 N_8}{dx^2}$ With Respect To x

The variation of $\frac{d^2 N_4}{dx^2}$ as shown in Figure 3.6 is of a complete cycle of the semi-cosine wave plus another half one, where $\frac{d^2 N_8}{dx^2}$ is as a “sinusoidal” wave plus one-quarter. Each graph has its own frequency.

The following graph (Figure 3.7) shows the variation of the shear force with respect to x (the third derivative of N_3 and N_7 are chosen because they represent both the shear forces in the nodal matrix $[d]$), with the consideration that the flexural rigidity is unity. Also, the negative sign that appears in equations 3.38 and 3.39 is considered.

The rates of change of $\frac{d^3 N_3}{dx^3}$ and $\frac{d^3 N_7}{dx^3}$ with respect to x , as shown in Figure 3.7 below, cannot be described in terms of the known standard curves.

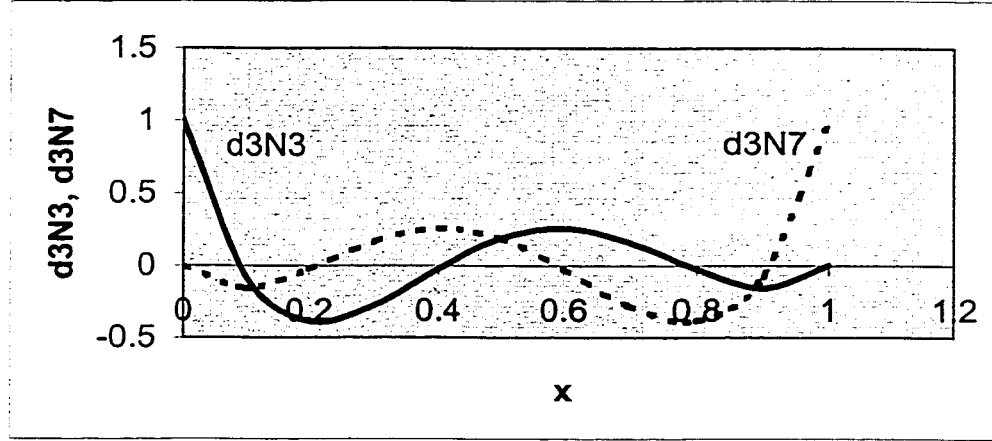


Figure 3.7 Variations of $\frac{d^3 N_3}{dx^3}$ and $\frac{d^3 N_7}{dx^3}$ With Respect To x

To conclude, in steps 1 and 2 an establishment of the interpolation function has been done to be able to set up the element matrices in the coming step, step 3.

Step 3: Finite Element Model

In this step, the element stiffness, element geometric stiffness for both constant and variable axial loads, and element mass matrices can be found out. The Finite Element Model of the governing differential equation 3.1 is obtained by substituting the finite element interpolation functions for W , and the interpolation functions N_i in equations 3.24-3.31 for the weight function v in the weak form given by equation 2.13 as:

$$w(x, t) = W(x)\tau(t) = W(x)e^{i\omega t} \quad (3.40)$$

Since there are eight nodal variables W_i , eight different choices are used for v , that is $v = N_1, \dots, N_8$ to obtain a set of eight algebraic equations. The i -th algebraic equation of the finite element model (for $v = N_i$) is:

$$0 = \sum_{j=1}^8 \left(\int_0^l bD_{11} \frac{d^2 N_i}{dx^2} \frac{d^2 N_j}{dx^2} - bN_x \frac{dN_i}{dx} \frac{dN_j}{dx} - \lambda \rho A v W \right) u_j dx - \int_0^l N_i q dx - Q_i \quad (3.41)$$

$$\text{or, } \sum_{j=1}^8 (K_{ij} - n_{ij} - M_{ij}) u_j - F_i = 0 \quad (3.42)$$

Here u is a common variable for all nodal variables such that,

$$u_1 = W(0) \quad u_2 = \frac{dW}{dx} \Big|_{x=0} \quad (3.43)$$

$$u_5 = W(l) \quad u_6 = \frac{dW}{dx} \Big|_{x=l} \quad (3.44)$$

$$u_3 = F(0) = -bD_{11} \frac{d^3 W(x)}{dx^3} \Big|_{x=0} \quad u_4 = M(0) = bD_{11} \frac{d^2 W(x)}{dx^2} \Big|_{x=0} \quad (3.45)$$

$$u_7 = F(l) = bD_{11} \frac{d^3 W(x)}{dx^3} \Big|_{x=l} \quad u_8 = M(l) = -bD_{11} \frac{d^2 W(x)}{dx^2} \Big|_{x=l} \quad (3.46)$$

Using the equations 2.36, 2.37, and 2.38 from the last chapter, which defined the various element matrices as:

$$K_{ij} = \int_0^l bD_{11} \frac{d^2 N_i}{dx^2} \frac{d^2 N_j}{dx^2} dx \quad (3.47)$$

$$n_{ij} = \int_0^l P \frac{dN_i}{dx} \frac{dN_j}{dx} dx \quad (3.48)$$

$$M_{ij} = \int_0^l \rho A N_i N_j dx \quad (3.49)$$

$$\text{and } F_i = \int_0^l N_i q dx + Q_i \quad (3.50)$$

$$Q_i = \begin{bmatrix} \left[\frac{d}{dx} \left(bD_{11} \frac{d^2 W}{dx^2} \right) + bN_x \frac{dW}{dx} \right]_{x=0} \\ \left[bD_{11} \frac{d^2 W}{dx^2} \right]_{x=0} \\ - \left[\frac{d}{dx} \left(bD_{11} \frac{d^2 W}{dx^2} \right) + bN_x \frac{dW}{dx} \right]_{x=l} \\ - \left[bD_{11} \frac{d^2 W}{dx^2} \right]_{x=l} \end{bmatrix} \quad (3.51)$$

The element matrices obtained are consistent to the new interpolation functions given by equations 3.22-3.29.

The above-mentioned integrations were evaluated with the new interpolation functions using MAPLE[®] V Release 4, and the results are given in the following:

The element stiffness matrix is:

$$[K] = \frac{bD_{11}}{l^3} \begin{bmatrix} \frac{280}{11} & \frac{140}{11}l & \frac{1}{22} \frac{l^3}{bD_{11}} & \frac{40}{33} \frac{l^2}{bD_{11}} & -\frac{280}{11} & \frac{1}{22} \frac{l^3}{bD_{11}} & -\frac{40}{33} \frac{l^2}{bD_{11}} \\ \frac{140}{11}l & \frac{600}{77}l^2 & \frac{8}{231} \frac{l^4}{bD_{11}} & \frac{379}{462} \frac{l^3}{bD_{11}} & -\frac{140}{11}l & \frac{5}{462} \frac{l^4}{bD_{11}} & -\frac{181}{462} \frac{l^3}{bD_{11}} \\ \frac{1}{22} \frac{l^3}{bD_{11}} & \frac{8}{231} \frac{l^4}{bD_{11}} & \frac{2}{3465} \frac{(bD_{11})^2}{bD_{11}} & \frac{1}{99} \frac{l^5}{bD_{11}} & -\frac{1}{22} \frac{l^3}{bD_{11}} & \frac{1}{4620} \frac{(bD_{11})^2}{bD_{11}} & -\frac{5}{2772} \frac{(bD_{11})^2}{bD_{11}} \\ \frac{40}{33} \frac{l^2}{bD_{11}} & \frac{379}{462} \frac{l^3}{bD_{11}} & \frac{1}{99} \frac{l^5}{bD_{11}} & \frac{50}{231} \frac{l^5}{(bD_{11})^2} & -\frac{40}{33} \frac{l^2}{bD_{11}} & \frac{5}{2772} \frac{(bD_{11})^2}{bD_{11}} & -\frac{1}{462} \frac{l^5}{(bD_{11})^2} \\ -\frac{280}{11} & -\frac{140}{11}l & -\frac{1}{22} \frac{l^3}{bD_{11}} & \frac{40}{33} \frac{l^2}{bD_{11}} & \frac{280}{11} & -\frac{1}{22} \frac{l^3}{bD_{11}} & \frac{40}{33} \frac{l^2}{bD_{11}} \\ \frac{140}{11}l & \frac{380}{77}l^2 & \frac{5}{462} \frac{l^4}{bD_{11}} & \frac{181}{462} \frac{l^3}{bD_{11}} & -\frac{140}{11}l & \frac{8}{231} \frac{l^4}{bD_{11}} & -\frac{379}{462} \frac{l^3}{bD_{11}} \\ \frac{1}{22} \frac{l^3}{bD_{11}} & \frac{5}{462} \frac{l^4}{bD_{11}} & -\frac{1}{22} \frac{l^3}{bD_{11}} & \frac{5}{2772} \frac{(bD_{11})^2}{bD_{11}} & \frac{1}{22} \frac{l^3}{bD_{11}} & \frac{2}{3465} \frac{(bD_{11})^2}{bD_{11}} & -\frac{1}{99} \frac{l^5}{(bD_{11})^2} \\ \frac{40}{33} \frac{l^2}{bD_{11}} & -\frac{181}{462} \frac{l^3}{bD_{11}} & \frac{5}{2772} \frac{(bD_{11})^2}{bD_{11}} & \frac{1}{462} \frac{l^4}{bD_{11}} & -\frac{40}{33} \frac{l^2}{bD_{11}} & \frac{1}{99} \frac{l^5}{(bD_{11})^2} & -\frac{50}{231} \frac{l^4}{(bD_{11})^2} \end{bmatrix} \quad (3.52)$$

The mass matrix is given as:

$$[M] = \frac{\rho A l}{420} \begin{bmatrix} \frac{72940}{429} & \frac{4530}{143} l & \frac{383}{2574} l^2 & \frac{1370}{429} l^2 & \frac{17150}{429} & \frac{1905}{143} l & \frac{521}{5148} l^3 & \frac{775}{429} l^2 \\ \frac{4530}{143} l & \frac{100}{13} l^2 & \frac{6}{143} l^4 & \frac{245}{286} l^3 & \frac{1905}{143} l & \frac{1865}{429} l^2 & \frac{5}{156} l^4 & \frac{995}{1716} l^3 \\ \frac{383}{2574} l^2 & \frac{6}{143} l^4 & \frac{1}{3861} (bD_{11})^2 & \frac{1}{198} (bD_{11})^2 & \frac{521}{5148} l^3 & \frac{5}{156} l^4 & \frac{7}{30888} (bD_{11})^2 & \frac{43}{10296} l^5 \\ \frac{1370}{429} l^2 & \frac{245}{286} l^3 & \frac{1}{198} (bD_{11})^2 & \frac{43}{429} l^4 & \frac{775}{429} l^2 & \frac{995}{1716} l^3 & \frac{43}{10296} (bD_{11})^2 & \frac{131}{1716} l^4 \\ \frac{17150}{429} & \frac{1905}{143} l & \frac{521}{5148} l^3 & \frac{72940}{429} & \frac{1905}{143} l & \frac{4530}{143} l & \frac{383}{2574} l^3 & \frac{1370}{429} l^2 \\ \frac{1905}{143} l & \frac{1865}{429} l^2 & \frac{5}{156} l^4 & \frac{995}{1716} l^3 & \frac{4530}{143} l & \frac{100}{13} l^2 & \frac{6}{143} l^4 & \frac{245}{286} l^3 \\ \frac{521}{5148} l^3 & \frac{5}{156} l^4 & \frac{7}{30888} (bD_{11})^2 & \frac{43}{10296} (bD_{11})^2 & \frac{383}{2574} l^3 & \frac{6}{143} l^4 & \frac{1}{3861} (bD_{11})^2 & \frac{1}{198} (bD_{11})^2 \\ \frac{775}{429} l^2 & \frac{995}{1716} l^3 & \frac{43}{10296} (bD_{11})^2 & \frac{131}{1716} l^4 & \frac{1370}{429} l^2 & \frac{245}{286} l^3 & \frac{1}{198} (bD_{11})^2 & \frac{43}{429} l^4 \end{bmatrix} \quad (3.53)$$

The geometric stiffness matrix for constant axial loads (n_c) is given below:

$$[n_c] = bN_x \begin{bmatrix} \frac{700}{429} \frac{1}{l} & \frac{271}{858} & -\frac{5}{5148} \frac{l^2}{bD_{11}} & \frac{23}{858} \frac{1}{l} & -\frac{700}{429} \frac{1}{l} & \frac{5}{5148} \frac{l^2}{bD_{11}} & \frac{23}{858} \frac{1}{l} \\ \frac{271}{858} & \frac{300}{1001} \frac{1}{l} & -\frac{25}{18018} \frac{l^3}{bD_{11}} & \frac{123}{4004} \frac{l^2}{bD_{11}} & -\frac{271}{858} & \frac{97}{6006} \frac{1}{l} & -\frac{47}{12012} \frac{l^2}{bD_{11}} \\ \frac{5}{5148} \frac{l^2}{bD_{11}} & \frac{25}{18018} \frac{l^3}{bD_{11}} & \frac{1}{90090} (bD_{11})^2 & \frac{37}{18018} \frac{l^4}{bD_{11}} & -\frac{5}{5148} \frac{l^2}{bD_{11}} & \frac{1}{144144} (bD_{11})^2 & \frac{73}{720720} (bD_{11})^2 \\ \frac{23}{858} \frac{1}{l} & \frac{123}{4004} \frac{l^2}{bD_{11}} & \frac{37}{18018} \frac{l^4}{bD_{11}} & \frac{73}{18018} \frac{l^3}{bD_{11}} & -\frac{23}{858} \frac{1}{l} & \frac{47}{12012} \frac{l^2}{bD_{11}} & -\frac{7}{5148} \frac{l^3}{bD_{11}} \\ \frac{700}{429} \frac{1}{l} & \frac{271}{858} & -\frac{5}{5148} \frac{l^2}{bD_{11}} & \frac{23}{858} \frac{1}{l} & -\frac{700}{429} \frac{1}{l} & \frac{5}{5148} \frac{l^2}{bD_{11}} & \frac{23}{858} \frac{1}{l} \\ \frac{271}{858} \frac{1}{l} & \frac{300}{1001} \frac{1}{l} & -\frac{25}{18018} \frac{l^3}{bD_{11}} & \frac{123}{4004} \frac{l^2}{bD_{11}} & -\frac{271}{858} & \frac{97}{6006} \frac{1}{l} & -\frac{123}{4004} \frac{l^2}{bD_{11}} \\ \frac{5}{5148} \frac{l^2}{bD_{11}} & \frac{25}{18018} \frac{l^3}{bD_{11}} & \frac{1}{90090} (bD_{11})^2 & \frac{37}{18018} \frac{l^4}{bD_{11}} & -\frac{5}{5148} \frac{l^2}{bD_{11}} & \frac{1}{90090} (bD_{11})^2 & \frac{37}{18018} \frac{l^4}{bD_{11}} \\ \frac{23}{858} \frac{1}{l} & \frac{123}{4004} \frac{l^2}{bD_{11}} & \frac{37}{18018} \frac{l^4}{bD_{11}} & \frac{73}{18018} \frac{l^3}{bD_{11}} & -\frac{23}{858} \frac{1}{l} & \frac{47}{12012} \frac{l^2}{bD_{11}} & -\frac{7}{5148} \frac{l^3}{bD_{11}} \end{bmatrix} \quad (3.54)$$

For evaluating the geometric stiffness matrix corresponding to the variable axial load, the axial load ' P ' is now written as a function of ' x '. Its equation is stated in chapter 2 as:

$$P(x) = P_o + P_d(x) \quad (3.55)$$

$$\text{in which } P_d(x) = p_o l \left\{ 1 - \frac{x}{l} + \frac{r}{l + \alpha} \left[1 - \left(\frac{x}{l} \right)^{\alpha + 1} \right] \right\} \quad (3.56)$$

Substituting this value of $P(x)$ with the new interpolation functions into the integration of equation 3.48, one can obtain the matrix of geometric stiffness coefficients (nd) using the software MAPLE® V Release 4. There are repeated terms throughout the coefficients of the matrix (nd) such as, A...O, which are given right after the coefficients. The results are as follows:

$$nd_{11} = \frac{700}{429} \frac{P}{l} + \frac{350}{429} P + \frac{700}{429} ps - 14112000A \quad (3.57)$$

$$nd_{12} = \frac{271}{858} P + \frac{49}{429} pl + \frac{271}{858} pls - 302400B \quad (3.58)$$

$$nd_{13} = -\frac{5}{5148} \frac{Pl^2}{bD_{11}} - \frac{5}{5148} \frac{Pl^3s}{bD_{11}} + 16800C \quad (3.59)$$

$$nd_{14} = \frac{23}{858} \frac{lP}{bD_{11}} + \frac{1}{2574} \frac{pl^2(14 + 69s)}{bD_{11}} - 100800F \quad (3.60)$$

$$nd_{15} = -\frac{700}{429} \frac{P}{l} - \frac{350}{429} P - \frac{700}{429} ps + 14112000A \quad (3.61)$$

$$nd_{16} = \frac{271}{858} P + \frac{173}{858} pl + \frac{271}{858} pls + 840G \quad (3.62)$$

$$nd_{17} = -\frac{5}{5148} \frac{Pl^2}{bD_{11}} - \frac{5}{5148} \frac{Pl^3(1+s)}{bD_{11}} + 8400H \quad (3.63)$$

$$nd_{18} = -\frac{23}{858} \frac{lP}{bD_{11}} - \frac{1}{2574} \frac{pl^2(55+69s)}{bD_{11}} + 3360J \quad (3.64)$$

$$nd_{22} = \frac{300}{1001} lP + \frac{61}{286} pl^2 + \frac{300}{1001} pl^2s - \frac{259200l^2psO}{(1+f)(4+f)(5+f)(6+f)(7+f)(8+f)(9+f)(10+f)(11+f)(12+f)(13+f)} \quad (3.65)$$

$$nd_{23} = -\frac{25}{18018} \frac{l^3P}{bD_{11}} - \frac{1}{360360} \frac{pl^4(301+500s)}{bD_{11}} + \frac{2880l^4(399f^2+110f^3+10f^4+1500+767f)ps}{(bD_{11})(3+f)(4+f)(5+f)(6+f)(7+f)(8+f)(9+f)(10+f)(11+f)(12+f)(13+f)} \quad (3.66)$$

$$nd_{24} = \frac{123}{4004} \frac{l^2P}{bD_{11}} + \frac{1}{12012} \frac{pl^3(238+369)}{bD_{11}} - \frac{21600l^3(2952+20f^4+1454f+841f^2+235f^3)ps}{bD_{11}(2+f)(4+f)(5+f)(6+f)(7+f)(8+f)(9+f)(10+f)(11+f)(12+f)(13+f)} \quad (3.67)$$

$$nd_{25} = -\frac{271}{858} P - \frac{49}{429} pl - \frac{271}{858} pls + 302400B \quad (3.68)$$

$$nd_{26} = \frac{97}{6006} lP + \frac{97}{12012} pl^2 + \frac{97}{6006} pl^2s + \frac{360l^2(-63720f + 15552f^2 - 46560 + 1583f^4 + 11602f^3 + 62f^5 + f^6)ps}{T} \quad (3.69)$$

$$nd_{27} = \frac{5}{12012} \frac{l^3P}{bD_{11}} + \frac{1}{720720} \frac{pl^4(127 + 300s)}{bD_{11}} - \frac{360l^4psO}{bD_{11}T} \quad (3.70)$$

$$nd_{28} = \frac{47}{12012} \frac{l^2P}{bD_{11}} + \frac{1}{36036} \frac{pl^3(52 + 141s)}{bD_{11}} - \frac{360l^3(4752f + 6521f^2 + 11280 + 215f^4 + 2148f^3 + 4f^5)ps}{bD_{11}T} \quad (3.71)$$

$$nd_{33} = \frac{1}{90090} \frac{l^5P}{(bD_{11})^2} + \frac{1}{1081080} \frac{pl^6(7 + 12s)}{(bD_{11})^2} - \frac{160(4 + f)(f + 18 + 2f^2)f^6ps}{(bD_{11})^2T} \quad (3.72)$$

$$nd_{34} = -\frac{37}{180180} \frac{l^4P}{(bD_{11})^2} - \frac{1}{1081080} \frac{pl^5(133 + 222s)}{(bD_{11})^2} + \frac{240l^5(213f + 125f^2 + 888 + 20f^3)ps}{(bD_{11})^2T} \quad (3.73)$$

$$nd_{35} = \frac{5}{5148} \frac{l^2P}{bD_{11}} + \frac{5}{5148} \frac{l^3sp}{bD_{11}} - 16800C \quad (3.74)$$

$$nd_{36} = \frac{5}{12012} \frac{l^3P}{bD_{11}} + \frac{1}{720720} \frac{pl^4(173 + 300s)}{bD_{11}} -$$

$$\frac{4l^4(4+f)(5+f)(5400-1104f+f^4+986f^2+51f^3)ps}{(bD_{II})T} \quad (3.75)$$

$$nd_{37} = -\frac{l}{144144} \frac{l^5 P}{(bD_{II})^2} - \frac{l}{288288} \frac{pl^6(1+2s)}{(bD_{II})^2} +$$

$$\frac{20l^6(f+18+2f^2)(4+f)(5+f)ps}{(bD_{II})^2 T} \quad (3.76)$$

$$nd_{38} = -\frac{73}{720720} \frac{l^4 P}{(bD_{II})^2} - \frac{l}{2162160} \frac{pl^5(110+219s)}{(bD_{II})^2} +$$

$$\frac{4l^5(1314+39f+169f^2+4f^3)(4+f)(5+f)ps}{(bD_{II})^2 T} \quad (3.77)$$

$$nd_{44} = \frac{73}{18018} \frac{l^3 P}{(bD_{II})^2} + \frac{l}{36036} \frac{pl^4(91+146s)}{(bD_{II})^2} -$$

$$\frac{14400l^4(35f^2+5f^3+219+49f)(4+f)ps}{(bD_{II})^2(3+f)T} \quad (3.78)$$

$$nd_{45} = -\frac{23}{858} \frac{lP}{(bD_{II})} - \frac{l}{2574} \frac{pl^2(14+69s)}{(bD_{II})} + 100800F \quad (3.79)$$

$$nd_{46} = -\frac{47}{12012} \frac{l^2 P}{(bD_{II})} - \frac{l}{36036} \frac{pl^3(89+141s)}{(bD_{II})} +$$

$$\frac{60l^3(57f^4+1295f^3-5760f+16920+4959f^2+f^5)(4+f)ps}{(bD_{II})T} \quad (3.80)$$

$$nd_{47} = \frac{73}{720720} \frac{l^4 P}{(bD_{II})^2} + \frac{1}{2162160} \frac{pl^5(109 + 219s)}{(bD_{II})^2} - \frac{120l^5(2f^2 + 97f^3 + 521f + 2940 + 556f^2)(4 + f)ps}{(bD_{II})^2 T} \quad (3.81)$$

$$nd_{48} = \frac{7}{5148} \frac{l^3 P}{(bD_{II})^2} + \frac{7}{10296} \frac{pl^4(1 + 2s)}{(bD_{II})^2} - \frac{120l^4(2f^4 + 97f^3 + 521f + 2940 + 556f^2)(4 + f)ps}{(bD_{II})^2 T} \quad (3.82)$$

$$nd_{55} = \frac{700}{429} \frac{P}{l} + \frac{350}{429} p + \frac{700}{429} ps - 14112000 A \quad (3.83)$$

$$nd_{56} = -\frac{271}{858} P - \frac{173}{858} pl - \frac{271}{858} pls - 840 G \quad (3.84)$$

$$nd_{57} = \frac{5}{5148} \frac{l^2 P}{bD_{II}} + \frac{5}{5148} \frac{pl^3(1 + s)}{bD_{II}} + 8400 H \quad (3.85)$$

$$nd_{58} = \frac{23}{858} \frac{lP}{bD_{II}} + \frac{1}{2574} \frac{pl^2(55 + 69s)}{bD_{II}} + 3360 J \quad (3.86)$$

$$nd_{66} = \frac{300}{1001} lP + \frac{173}{2002} pl^2 + \frac{300}{1001} pl^2 s - \frac{l^2(2592000 + 256966f^2 + 31323f^3 + 2017f^4 + 69f^5f^6 + 806904f)ps}{(7 + f)(8 + f)(9 + f)(10 + f)(11 + f)(12 + f)(13 + f)} \quad (3.87)$$

$$nd_{67} = -\frac{25}{18018} \frac{l^3 P}{bD_{II}} - \frac{1}{360360} \frac{pl^4(199 + 500s)}{bD_{II}} + \frac{l^4(12000 + 851f^2 + 48f^3 + f^4 + 1548f)ps}{bD_{II}(7 + f)(8 + f)(9 + f)(10 + f)(11 + f)(12 + f)(13 + f)} \quad (3.88)$$

$$nd_{68} = -\frac{123}{4004} \frac{l^2 P}{bD_{11}} - \frac{1}{12012} \frac{pl^3(131+369s)}{bD_{11}} +$$

$$\frac{l^3(265680 + 20597f^2 + 1763f^3 + 67f^4 + 54612f + f^5)ps}{bD_{11}(7+f)(8+f)(9+f)(10+f)(11+f)(12+f)(13+f)} \quad (3.89)$$

$$nd_{77} = \frac{1}{90090} \frac{l^5 P}{(bD_{11})^2} + \frac{1}{1081080} \frac{pl^6(5+12s)}{(bD_{11})^2} -$$

$$\frac{2l^6(48+3f^2+5f)ps}{(bD_{11})^2(7+f)(8+f)(9+f)(10+f)(11+f)(12+f)(13+f)} \quad (3.90)$$

$$nd_{78} = \frac{37}{180180} \frac{l^4 P}{(bD_{11})^2} + \frac{1}{1081080} \frac{pl^5(89+222s)}{(bD_{11})^2} -$$

$$\frac{l^5(1776+116f^2+3f^3+233f)ps}{(bD_{11})^2(7+f)(8+f)(9+f)(10+f)(11+f)(12+f)(13+f)} \quad (3.91)$$

$$nd_{88} = \frac{73}{18018} \frac{l^3 P}{(bD_{11})^2} + \frac{1}{36036} \frac{pl^4(55+146s)}{(bD_{11})^2} -$$

$$\frac{2l^4(17520+1211f^2+3044f+f^4+64f^3)ps}{(bD_{11})^2(7+f)(8+f)(9+f)(10+f)(11+f)(12+f)(13+f)} \quad (3.92)$$

$$T = (4+f)(5+f)(6+f)(7+f)(8+f)(9+f)(10+f)(11+f)(12+f)(13+f) \quad (3.93)$$

$$A = \frac{ps}{(7+f)(8+f)(9+f)(10+f)(11+f)(12+f)(13+f)} \quad (3.94)$$

$$B = \frac{l(1053f + 265f^2 + 1084 + 20f^3)ps}{T} \quad (3.95)$$

$$C = \frac{l^3(3+4f)(4+f)(5+f)ps}{bD_{II}T} \quad (3.96)$$

$$F = \frac{l^2(4+f)(75f + 69 + 10f^2)}{(bD_{II})T} \quad (3.98)$$

$$G = \frac{l(-3252 + 48f^2 + f^3 851f)ps}{(7+f)(8+f)(9+f)(10+f)(11+f)(12+f)(13+f)} \quad (3.99)$$

$$H = \frac{l(f-1)ps}{(bD_{II})(7+f)(8+f)(8+f)(9+f)(10+f)(11+f)(12+f)(13+f)} \quad (3.100)$$

$$J = \frac{l^2(f^2 + 40f - 69)ps}{(bD_{II})(7+f)(8+f)(8+f)(9+f)(10+f)(11+f)(12+f)(13+f)} \quad (3.101)$$

$$O = 1200 + 463f^2 624f + 125f^3 + 10f^4 \quad (3.102)$$

$$s = l + \alpha \quad (3.103)$$

The other coefficients of this matrix can be deduced from the above-described coefficients since the matrix is symmetric.

For the case of constant 'q' over an element, the element matrix of generalized forces F_i will be:

$$F = q \begin{bmatrix} \frac{l}{2} \\ \frac{3l^2}{28} \\ -\frac{l^4}{1680bD_{II}} \\ \frac{l^3}{84bD_{II}} \\ \frac{l}{2} \\ -\frac{3l^2}{28} \\ \frac{l^4}{1680bD_{II}} \\ -\frac{l^3}{84bD_{II}} \end{bmatrix} + \begin{bmatrix} Q_1 \\ Q_2 \\ 0 \\ 0 \\ Q_3 \\ Q_4 \\ 0 \\ 0 \end{bmatrix} \quad (3.104)$$

It can easily be verified that the first part of the right side of equation 3.104 (let us give it symbol as F_N , since it is coming from the interpolation functions N_i) represents the “work equivalent” forces and moments at nodes 1 and 2 due to the uniformly distributed load over the element in the advanced formulation. When q is an algebraically complicated function of x , equation 3.50 provides a straightforward approach of computing the generalized “work equivalent” force and moment components.

By examining F_N , one can see that not all the coefficients of it represent forces or moments. The coefficients $F_N(3,1)$, and $F_N(7,1)$ represent deflection (this can be verified by checking the units), and $F_N(4,1)$, and $F_N(8,1)$ represent slope. This means that this part of the force matrix is not purely force matrix. It also means that in the

advanced formulation, as the shear force and bending moment are becoming degrees of freedom the same as deflection and slope in the nodal matrix $[d]$, the deflection and slope convert to forces, in a sense, in the force matrix $[F]$. This is exactly what creates confusion in the processing the problem in MATLAB software, while adding the shear force in the nodal matrix $[d]$ (it will be discussed in detail in section 3.7.1.1. This becomes more evident by checking the units of the results of product of the coefficients of the stiffness matrix $[k]$ by the nodal matrix $[d]$, they all the units of force. This makes sense, because the basic rule is: $kx = F$.

3.3.2 Weak Formulation for Mid-Plane Tapered Composite Beams

The classical lamination theory states that [57]:

$$D_{II} = \sum_{p=1}^n \left[t_p \bar{Z}_p^2 + \frac{t_p^3}{12} \right] (\bar{Q}_{II})_p \quad (3.105)$$

where D_{II} is the bending or flexural laminate stiffness relating the bending moment M_x to curvature κ_x , $(\bar{Q}_{II})_p$ is the transformed stiffness coefficient of a ply, t_p is the ply thickness, \bar{Z}_p is the distance between the centreline of the ply and the centreline of the whole laminate, and n is the total number of plies.

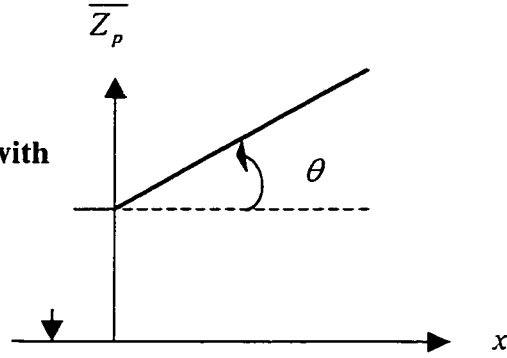
For tapered composite beams the height of the centreline of each ply (\overline{Z}_p) is a function of x (as shown in Figure 3.8). The equation for \overline{Z}_p is:

$$\overline{Z}_p = mx + g \quad (3.106)$$

In equation 3.106 ' m ' is the slope of the straight line ($= \tan \theta$), and ' g ' is its intercept at $x = 0$. Then equation 3.105 can be written as:

$$D_{II} = \sum_{p=1}^n \left[t_p (\overline{mx + g})_p^2 + \frac{t_p^3}{12} \right] (\overline{Q}_{II})_p \quad (3.107)$$

Figure 3.8 Variation of \overline{Z}_p with x -axis



Hence, the ply stiffness coefficient D_{II} will be a function of x too. In the previous section the three matrices, $[K]$, $[n]$, and $[M]$ required for the dynamic analysis of composite beams were established (equations 3.52-3.104). By examining them one can find that the element matrices will be affected by this change because they are functions of bD_{II} . Mathematically, this involves the calculation of the integrations (equations 3.47-3.49) after replacing D_{II} in the integration by the equation 3.107. This integration is performed using the software Maple[®] V Release 4, and the stiffness matrix for the mid-plane tapered composite beam has been obtained as:

$$k_{II} = \frac{70}{429} AI \quad (3.108)$$

$$k_{21} = \frac{5}{429} A2 \quad (3.109)$$

where

$$A1 = \sum_{p=1}^n \frac{b(\overline{Q_{11}})_p t_p (13tp^2 + 48l^2 m^2 + 156lgm + 156g^2)}{l^3} \quad (3.110)$$

$$A2 = \sum_{p=1}^n \frac{b(\overline{Q_{11}})_p t_p (91tp^2 + 258l^2 m^2 + 936lgm + 1092g^2)}{l^2} \quad (3.111)$$

It may be noted that the coefficients are evaluated using symbolic manipulation. As a result, long equations are obtained in Maple for each coefficient. For instance, the coefficient k_{23} alone took two pages in the printout, and the whole matrix was printed out on 90 pages. Accordingly, the stiffness matrix is difficult to be provided here within this text. Therefore, the stiffness matrix will be given as an attachment to this thesis in a floppy disc.

In a similar manner, the mass matrix should also be changed. As in the advanced formulation the mass matrix is a function of flexural rigidity (bD_{11}), it will be a function of x too. The mass matrix was determined using Maple[®] V Release 4. The coefficients M_{11} and M_{12} are given below as:

$$M_{11} = \frac{521}{1287} l \rho A \quad (3.112)$$

$$M_{12} = \frac{151}{2002} l^2 \rho A \quad (3.113)$$

Again the entry M_{13} alone took 8 pages, and the whole matrix was printed out on 122 pages. As it was done for the stiffness matrix, the mass matrix will also be provided as an attachment to the thesis in a floppy disc.

3.4 Assembly of Element Equations and Imposing the Boundary Conditions

3.4.1 Assembly of Element Equations

The assembly of elements is based on: a) interelement continuity of the primary variables (deflection and slope) and (b) interelement equilibrium of the secondary variables (shear force and bending moment) at the nodes common to the elements. To demonstrate the assembly procedure, a two-element model is selected (see Figure 3.9).

There are three global nodes and a total of twelve global generalized displacements and forces. The continuity of the primary variables implies the following relations between the element degrees of freedom u_i^e and the global degrees of freedom U_i^e as follows:

$${}^1u_1 = U_1, \quad {}^1u_2 = U_2, \quad {}^1u_3 = U_3, \quad {}^1u_4 = U_4 \quad (3.114)$$

$${}^1u_5 = {}^2u_1 = U_5, \quad {}^1u_6 = {}^2u_2 = U_6, \quad {}^1u_7 = {}^2u_3 = U_7, \quad (3.115)$$

$${}^1u_8 = {}^2u_4 = U_8, \quad {}^2u_5 = U_9 \quad (3.116)$$

$${}^2u_6 = U_{10}, \quad {}^2u_7 = U_{11}, \quad {}^2u_8 = U_{12} \quad (3.117)$$

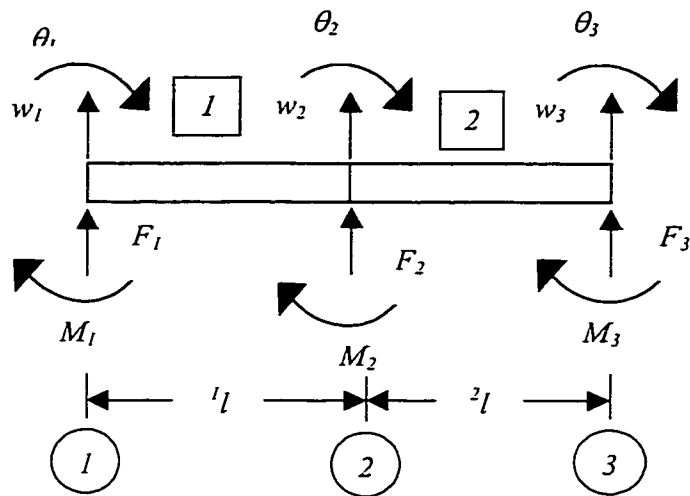


Figure 3.9 Assembling Two Elements in Advanced Finite Element Formulation

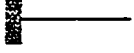






Since there are four degrees of freedom per node, and node 2 is repeated in elements 1 and 2, the associated degrees of freedom will add up. Then in the global stiffness matrix, the entries that correspond to whatever common nodes between the elements will add up.

In general, the assembled stiffness matrix for the assembly of beam elements has the form shown in the following equation 3.118.

$$K = \begin{bmatrix} {}^1W_1 & {}^1\theta_1 & {}^1F_1 & {}^1M_1 & {}^1W_2({}^2W_1) & {}^1\theta_2({}^2\theta_1) & {}^1F_2({}^2F_1) & {}^1M_2({}^2M_1) & {}^2W_2 & {}^2\theta_2 & {}^2F_2 & {}^2M_2 \\ {}^1k_{11} & {}^1k_{12} & {}^1k_{13} & {}^1k_{14} & {}^1k_{15} & {}^1k_{16} & {}^1k_{17} & {}^1k_{18} & 0 & 0 & 0 & 0 \\ {}^1k_{21} & {}^1k_{22} & {}^1k_{23} & {}^1k_{24} & {}^1k_{25} & {}^1k_{26} & {}^1k_{27} & {}^1k_{28} & 0 & 0 & 0 & 0 \\ {}^1k_{31} & {}^1k_{32} & {}^1k_{33} & {}^1k_{34} & {}^1k_{35} & {}^1k_{36} & {}^1k_{37} & {}^1k_{38} & 0 & 0 & 0 & 0 \\ {}^1k_{41} & {}^1k_{42} & {}^1k_{43} & {}^1k_{44} & {}^1k_{45} & {}^1k_{46} & {}^1k_{47} & {}^1k_{48} & 0 & 0 & 0 & 0 \\ {}^1k_{51} & {}^1k_{52} & {}^1k_{53} & {}^1k_{54} & {}^1k_{55} + {}^2k_{11} & {}^1k_{56} + {}^2k_{12} & {}^1k_{57} + {}^2k_{13} & {}^1k_{58} + {}^2k_{14} & {}^2k_{15} & {}^2k_{16} & {}^2k_{17} & {}^2k_{18} \\ {}^1k_{61} & {}^1k_{62} & {}^1k_{63} & {}^1k_{64} & {}^1k_{65} + {}^2k_{21} & {}^1k_{66} + {}^2k_{22} & {}^1k_{67} + {}^2k_{23} & {}^1k_{68} + {}^2k_{24} & {}^2k_{25} & {}^2k_{26} & {}^2k_{27} & {}^2k_{28} \\ {}^1k_{71} & {}^1k_{72} & {}^1k_{73} & {}^1k_{74} & {}^1k_{75} + {}^2k_{31} & {}^1k_{76} + {}^2k_{32} & {}^1k_{77} + {}^2k_{33} & {}^1k_{78} + {}^2k_{34} & {}^2k_{35} & {}^2k_{36} & {}^2k_{37} & {}^2k_{38} \\ {}^1k_{81} & {}^1k_{82} & {}^1k_{83} & {}^1k_{84} & {}^1k_{85} + {}^2k_{41} & {}^1k_{86} + {}^2k_{42} & {}^1k_{87} + {}^2k_{43} & {}^1k_{88} + {}^2k_{44} & {}^2k_{45} & {}^2k_{46} & {}^2k_{47} & {}^2k_{48} \\ 0 & 0 & 0 & 0 & {}^2k_{51} & {}^2k_{52} & {}^2k_{53} & {}^2k_{54} & {}^2k_{55} & {}^2k_{56} & {}^2k_{57} & {}^2k_{58} \\ 0 & 0 & 0 & 0 & {}^2k_{61} & {}^2k_{62} & {}^2k_{63} & {}^2k_{64} & {}^2k_{65} & {}^2k_{66} & {}^2k_{67} & {}^2k_{68} \\ 0 & 0 & 0 & 0 & {}^2k_{71} & {}^2k_{72} & {}^2k_{73} & {}^2k_{74} & {}^2k_{75} & {}^2k_{76} & {}^2k_{77} & {}^2k_{78} \\ 0 & 0 & 0 & 0 & {}^2k_{81} & {}^2k_{82} & {}^2k_{83} & {}^2k_{84} & {}^2k_{85} & {}^2k_{86} & {}^2k_{87} & {}^2k_{88} \end{bmatrix} \begin{matrix} {}^1W_1 \\ {}^1\theta_1 \\ {}^1F_1 \\ {}^1M_1 \\ {}^1W_2({}^2W_1) \\ {}^1\theta_2({}^2\theta_1) \\ {}^1F_2({}^2F_1) \\ {}^1M_2({}^2M_1) \\ {}^2W_2 \\ {}^2\theta_2 \\ {}^2F_2 \\ {}^2M_2 \end{matrix} \quad (3.118)$$

3.4.2 Imposition of Boundary Conditions

Table 3.1 Geometric and Natural Boundary Conditions For Different Supports

Type of Support		Geometric Boundary Conditions	Natural Boundary Conditions ¹
Clamped		$W(0) = 0$, $\frac{\partial W}{\partial x}(0) = 0$	$\frac{\partial^2 W}{\partial x^2}(l) = 0$, $\frac{\partial^3 W}{\partial x^3}(l) = 0$
Pinned		$W(0) = 0$	$\frac{\partial^2 W}{\partial x^2}(0) = 0$, $\frac{\partial^2 W}{\partial x^2}(l) = 0$
Roller		$W(0) = 0$	$\frac{\partial^2 W}{\partial x^2}(0) = 0$, $\frac{\partial^2 W}{\partial x^2}(l) = 0$
Free			$\frac{\partial^2 W}{\partial x^2}(0) = 0$, $\frac{\partial^2 W}{\partial x^2}(l) = 0$
			$\frac{\partial^3 W}{\partial x^3}(0) = 0$, $\frac{\partial^3 W}{\partial x^3}(l) = 0$
Sliding			$\frac{\partial^3 W}{\partial x^3}(0) = 0$, $\frac{\partial W}{\partial x}(0) = 0$

At this step of analysis, a specification of the particular boundary conditions must be executed, i.e. geometric constraints and forces applied on the particular structure have to be specified. The type of essential (also known as geometric) boundary conditions for a specific beam problem depends on the nature of the geometry. The natural (also called force) boundary conditions involve the specification of the generalized forces when the

¹ 'x' is measured zero at the left end, and is equal to 'l' at the right end of any type of support

corresponding primary variables are not constrained. Table 3.1 given above, contains a list of commonly used geometric and natural boundary conditions.

3.5 Modeling Variable Thickness Composite Beams

3.5.1 Modeling Externally Tapered Composite Beams

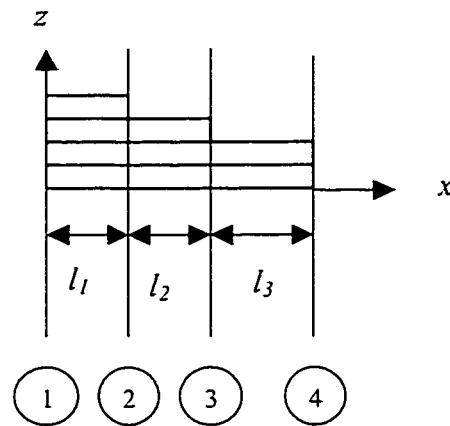


Figure 3.10 Modeling of Externally Tapered Composite Beam

This type of beams is modeled using uniform one-dimensional finite elements. In the present case, the geometry requires selecting the locations of nodes, and consequently the elements where the thickness changes. Therefore, the beam shown in Figure 3.10 is divided into three elements with a total of four nodes, and sixteen global degrees of freedom (before imposing the boundary conditions). The numbering of plies starts from the bottom, so the common ply in all elements will have the same number. To simplify

the analysis the coordinates are taken at the first node, so the x-coordinate of node 1 is zero.

The present configuration is merely an example, but the number of plies for each element, the number of elements, and the length of each element can be modified according to the structures used in industry.

One should note that the finite element solution of a similar problem for metals is also defined element-wise (because of the discontinuity in the flexural rigidity). In other words, this way of modeling is not far from the solution employed for similar metallic beams of variable thickness.

3.5.2 Modeling Mid-plane Tapered Composite Beams

This type of beams is modeled using non-uniform one-dimensional finite elements that are made of symmetric type of laminate. Again, the geometry of the present case requires selecting the locations of nodes, and consequently the elements where the plies are terminated (see Figure 3.11). Therefore, the beam shown in Figure 3.11 is divided into three elements with a total of four nodes, and eight global degrees of freedom (before imposing the boundary conditions). The numbering of plies starts from the top ply, so that the common ply in all elements will have the same number. The origin of the coordinates is located at the first node, and so the x-coordinate of node 1 is zero.

The present configuration is merely an example, but the number of plies for each element, the number of elements, and the length of each element can be modified according to the structures used in the industry.

There are two approximations that are involved in the modeling. First, by examining the configuration shown in Figure 3.11, one can notice that the terminated plies (plies 4, 5, 6, 7, 8, and 9) have larger cross-sectional areas at the axis of symmetry. The effect of this on the bending and shear response is ignored. Secondly, the cross-sectional area of each drop-off ply (plies 6 & 7) is approximated by the cross-sectional area of a ply that is common to all elements.

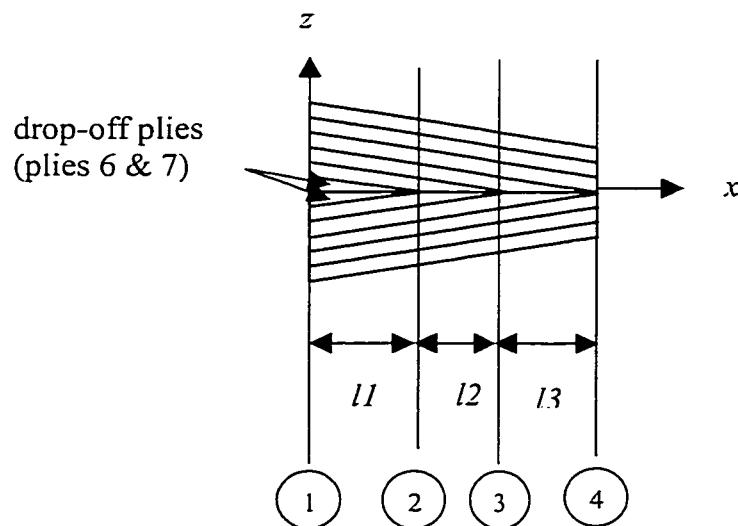


Figure 3.11 Modeling of Mid-plane Tapered Composite Beam

It is believed that these two approximations in the modeling do not violate any of the basics of the governing differential equation or its weak form for the following

reason. The slight change in thickness is very small. It is of the order of 10^{-5} m; hence its effect on the calculations will be of minor significance.

3.6 Program Development For Advanced Formulation

The developed program explained in chapter 2, in section 6 is used here for vibration and buckling analyses. One can conclude from the analysis in the previous sections that the stiffness and mass matrices are modified. Hence, the two subroutines ELESTF and ELEMAS in the last chapter are going to change to ELESTF8 and ELEMAS8. Here is the explanation of both of them.

3.6.1 Subroutine ELESTF8

The function of this subroutine is to calculate the entries of the element stiffness matrix for advanced finite element formulation (it is a 8×8 matrix) (coefficients are calculated using local coordinates). It will be given in Appendix I.

3.6.2 Subroutine ELEMAS8

This subroutine is to compute the consistent element mass matrix (it is a 8×8 matrix) (coefficients are calculated using local coordinates) for the advanced formulation, and it will be described in Appendix I.

3.7 Example Problem and Validation

The problems solved using the conventional finite element formulation in the last chapter are worked out here using the advanced finite element formulation to highlight the improvement of the results. There are tables provided to compare the results obtained using both the formulations, and how the finite element analyst can obtain more accurate results by employing the advanced finite element formulation.

3.7.1 Example Problems Involving Metallic Material and Validation

3.7.1.1 Free Vibration of Simply Supported Beam

Consider the beam described in section 2.7.1.1 with the same data and the same method of modeling as depicted in Figure 2.10. First, the shear force is considered as a degree of freedom, and for a three-element modeling the values of percentage of errors in natural frequencies are obtained to be -6.8 , -14.25 , -25.88 %, which are very high. The calculation of the error is based on the following definition:

$$error = \left(\frac{\omega - \omega_{exact}}{\omega_{exact}} \right) \times 100 \quad (3.119)$$

where ω is the natural frequency calculated using the MATLAB[®] program, and ω_{exact} is the natural frequency calculated using the exact solution given in Ref. [43] as:

$$\omega_i = \left(\frac{i\pi}{L} \right) \sqrt{\frac{EI}{\rho A}} \quad (3.120)$$

in which $i = 1, 2, 3, \dots$ is the mode number, and L is the beam span.

With excluding the shear force as a degree of freedom, the resulting values of the lowest three natural frequencies obtained from the MATLAB[®] program are: 74.48, 298.45, and 677.89 rad./sec., respectively. The values of the percentage of error were significantly reduced to 0.03, 0.20, and 1.15 %.

Shearing force is repeated twice throughout the analysis, once in the matrix of external forces 'Q' as in equations 3.3 and 3.4, and again in the interpolation functions as a degree of freedom. This repetition affects the calculation of the natural frequencies. Hence, all the forthcoming problems of uniform beams (both metallic and composite) will be solved with dropping the shearing force as a degree of freedom.

Table 3.2 given below shows a comparison between the values of the percentage of error in the natural frequencies obtained using the advanced formulation and that obtained using the conventional formulation.

One can now see how the advanced formulation remarkably reduces the percentage of error. In other words, the analyst can use a two-element model with the advanced formulation to get the natural frequencies with much higher accuracy (1.15 % as a percentage of error in the third mode) than the conventional formulation (the percentage of error is 24 % in the third mode).

Table 3.2 Comparison Between the Percentage of Error in the Natural frequencies Obtained Using the Advanced Formulation and the Conventional Formulation

No. of Elements	Formulation Method					
	Advanced Formulation			Conventional Formulation		
2	0.09	0.66	1.15	0.39	10.99	23.99
3	0.03	0.20	1.15	0.08	1.18	10.99
4	0.01	0.09	0.28	0.03	0.39	1.83
5	0.01	0.05	0.15	0.01	0.17	0.79
6	0.01	0.03	0.09	0.01	0.08	0.40
7	0.00	0.02	0.06	0.00	0.04	0.22
8	0.00	0.01	0.04	0.00	0.03	0.13
9	0.00	0.01	0.03	0.00	0.16	0.08
10	0.00	0.01	0.02	0.00	0.01	0.05

3.7.2 Example Problems and Validation For Composite Beams

3.7.2.1 Example Problems and Validation For Uniform Composite Beams

3.7.2.1.1 Free Vibration of Fixed-Fixed [0/90]_s Composite Beam

The same problem solved in section 2.7.2.1.2 is solved here using the advanced formulation to see its contribution to the accuracy of the results.

Table 3.3 given below shows the comparison between the two types of modeling. Apparently, the analyst can get results with higher accuracy using lesser number of elements that are based on advanced formulation.

In Table 3.3 the percentage of error is calculated using equation 3.105, where ω_{exact} can be deduced from the following equation given in Ref. [45] as:

$$\omega_i = \left(\frac{k_i}{L} \right) \sqrt{\frac{bD_{II}}{\rho A}} \quad (3.121)$$

in which $k_1 = 4.730041$, $k_2 = 5.853205$, and $k_3 = 10.995607$.

By checking the table above, one can find that the percentage of error in the third mode using the conventional formulation is 21.0 %, whereas using the advanced formulation it is reduced to 1.1 % (for three-element modeling). Such results urge the use of the advanced finite element formulation.

Table 3.3 Comparison of the Percentages of Error in Lowest Three Natural Frequencies Obtained Using Conventional and Advanced Formulations

No. of Elements	Formulation Method					
	Advanced Formulation			Conventional Formulation		
1	0.91	0.516	- ¹	-	-	- ²
2	0.10	0.31	1.13	1.62	32.92	-
3	0.10	0.12	1.10	0.41	2.0	21.01
4	0.05	0.14	0.13	0.13	0.93	2.14
5	0.04	0.09	0.19	0.06	0.40	1.39
6	0.025	0.06	0.13	0.03	0.20	0.72
7	0.018	0.04	0.09	0.01	0.11	0.40
8	0.014	0.03	0.067	0.01	0.06	0.24
9	0.01	0.03	0.05	0.01	0.04	0.15
10	0.01	0.02	0.04	0.00	0.03	0.10

¹ For the case of fixed-fixed beam modeled by one element in the advanced formulation, there will be two degrees of freedom. Hence, there will be only two modes (two values of natural frequencies).

² In the conventional formulation for this case, a one-element model will lead to no degrees of freedom. Hence, there are no values for the natural frequencies.

3.7.2.1.2 Buckling of Simply Supported [0/90] s Composite Beam

With the same input of the problem given in section 2.7.2.1.3, and using the model with the advanced formulation, the critical buckling load and the associated percentage of error are determined.

The closed-form solution for the critical buckling load is [50]:

$$P_{cr} = \frac{n^2 \pi^2}{L^2} b D_{11} \quad (3.122)$$

The critical buckling load calculated using equation 3.122 is 8789.9 N, and the resulting percentage of error (calculated as stated in equation 3.119) is – 0.012 %. The percentage of error associated with the buckling load calculated using the conventional formulation has been – 0.010 %, as can be seen from the last chapter, section 2.7.2.2. It may be noted that the difference in the percentage of error values is not much and is in the third decimal place.

3.7.2.2 Example Problems and Validation For Tapered Composite Beams

As it might be expected, still the insertion of the shear force into the MATLAB program does not give favorable results with the tapered composite beams.

3.7.2.2.1 Free Vibration of Simply Supported [0/90]_s Externally Tapered Composite Beam

An externally tapered composite beam made up of the same material described in section 2.7.2.1.1 and with the same mechanical properties and the laminate configuration is considered to determine its natural frequencies. The beam is modeled using three elements, and the number of plies in each element is 12, 10, and 8 respectively.

The MATLAB[®] program provides the following results for the lowest three natural frequencies: 137.74, 527.87, 1072.96 rad./ sec., respectively.

Validation of the results:

The same problem was solved using the conventional formulation, and the results for the natural frequencies are: 141.20, 578.74, 1479.38 rad./sec., respectively. Notably, the natural frequencies obtained using the advanced formulation are lower in magnitude than that obtained using the conventional formulation. This observation emphasizes the conclusion about the higher accuracy one can get by using the advanced formulation.

As it might be recalled from the problems solved in the last sections, where there were exact solutions for them, always the results of the percentage of error obtained using

the advanced formulation were lower than the results of the percentage of error obtained using the conventional formulation. This means that the output of the advanced formulation is closer to the exact solution than the output of the conventional formulation.

3.7.2.2.2 Free Vibration of Fixed-Fixed $[0/90]_s$ Mid-Plane Tapered Composite Beam

A mid-plane tapered composite beam made up of the same material described in section 2.7.2.2.2 and with the same mechanical properties and the same laminate configuration is considered to determine its natural frequencies. The only difference here is that the taper angle $\theta = -2^\circ$.

Because of the very big size of the mass and stiffness matrices, as it was mentioned before, these matrices were not provided into the MATLAB[®] program symbolically. Hence, the problem was solved for this specific input data of this problem.

The MATLAB[®] program provides the following results for the lowest three natural frequencies: 1089.15, 2710.46, 5899.42 rad./ sec., respectively.

Validation of the results:

The same problem was solved using the conventional formulation, and the results for the natural frequencies are: 1060.24, 4856.23, 13988.63 rad./sec., respectively.

As one can see, the values of the natural frequency corresponding to the first mode obtained using both the formulations are close to each other, and they start to deviate from the second mode. This should not underestimate the efficiency of the advanced formulation for mid-plane tapered composite beam, rather confirm it. This is due to the fact that the problem was solved numerically, i.e. the entries of the stiffness and mass matrices were inputted numerically and not symbolically.

3.8 Conclusions and Discussion

In this chapter, an advanced finite element formulation has been developed and described. Eight degrees of freedom are employed into the interpolation functions (four degrees of freedom per each node for a two-node element modeling). Mathematically, the interpolation function is an algebraic equation consisting of eight terms. The evaluation of the element matrices that are the stiffness, geometric stiffness and mass matrices has been performed. The analysis is done for both uniform and externally tapered composite beams, and also for mid-plane tapered composite beams.

The computer program developed in MATLAB[®] software environment provided in the last chapter has been further modified so as to adapt to the advanced formulation.

The applications of the advanced formulation to the free vibration analysis, and buckling analysis have been carried out. Example problems are solved using the developed program to obtain the natural frequencies and the critical buckling load, for demonstration purposes. The developed program can also perform the same analyses for beams made of isotropic materials. The example problems for the case of metals were also worked out.

The program was verified by comparing its results with the results obtained from the exact solution, if it exists, or by comparing them with the problems solved using the conventional formulation. The results obtained using the advanced formulation show superiority over the results obtained using the conventional formulation.

CHAPTER 4

Parametric Study on Variable Thickness Composite Beams

4.1 Introduction

In the previous two chapters, the finite element modeling procedures for external and mid-plane tapered composite beams were established. First, in chapter 2 the conventional finite element formulation was used, that is to consider the geometric (associated with essential boundary conditions) degrees of freedom in the interpolation functions. Second, in chapter 3 the advanced finite element formulation was established, which considers not only the geometric degrees of freedom, but also the generalized force (associated with natural boundary conditions) degrees of freedom. Then the element stiffness and mass matrices were set up. The analysis is now completed with a comprehensive parametric study that employs the developed formulations.

In this chapter, in section 4.2 a parametric study on the externally tapered composite beams is provided. The material chosen is NCT-301 graphite/epoxy, which is currently available in our lab. The specifications of the composite laminate, regarding the mechanical properties and geometric characteristics were first given. All the

problems are solved using both the finite element formulations, conventional and advanced.

The external type of taper is examined for all possible variations: variations in the boundary conditions, variations in the stacking sequences, and variations of the beam discretization. For each variation, the results for the lowest three natural frequencies are plotted in figures to elaborate on the interpretations. These figures are plotted once for the results obtained using conventional formulation, and again for the results obtained using the advanced formulation. Right after each figure, concise and elaborating interpretations are provided to explain how and why these variations affect the natural frequencies of the composite beams. For example, how the variations in the boundary conditions are related to the global degrees of freedom, and how this will affect the natural frequencies, how the variations in the inclination angles affects the natural frequencies through changes in the flexural rigidity of the laminate, and so on are detailed. Also, a comparison between the results obtained using both the methods of formulation is done with the help of the figures. Each sub-section ends by a table that summarizes the results mentioned in it.

In section 4.3 the variations in the boundary conditions, variations in the stacking sequences, and the variations in the taper angle were considered for the mid-plane tapered composite beams.

In section 4.4 a parametric study on the buckling of the externally tapered composite beams is performed considering various changes in the fiber orientations using conventional and advanced formulations.

In the last section, section 4.5 overall conclusions that relates between the two types of tapers and the different changes within the same kind of taper are provided that serve as the design aspects. These conclusions can guide the designer on the choice of the type of taper, and other parameters involved in the problem such as the boundary conditions.

4.2 Parametric Study on Dynamic Analysis for Externally Tapered Composite Beams

Problem Description:

A composite beam (see Figure 2.6) made up of NCT-301 graphite/epoxy material with the following ply material properties is considered for the present parametric study: $E_{11} = 113.9 \text{ GPa}$, $E_{22} = 7.985 \text{ GPa}$, $\nu_{12} = 0.288$, $\nu_{21} = 0.018$, and $\rho = 1480 \text{ kg/m}^3$. The number of plies for each portion is 100, 80, and 60 respectively. The beam span is taken to be 1.08 m, and the ply thickness is taken to be 0.5 mm (for analysis purposes). The laminate is cross-ply, and the element length is 0.36 m. The beam is modeled using three elements. This fully matches with the geometric nature of the beam, where the ply

thickness changes due to the change in the number of plies. The lowest three natural frequencies are to be determined for all possible changes that can be performed on the composite beam such as, the change in the boundary conditions, the change in the inclination angle, and the change in the element discretization. The results of the natural frequencies are obtained using both the methods of formulations, conventional and advanced as described in chapters 2 and 3. There will be tables and figures provided for comparison and commenting purposes.

4.2.1 The Effect of Boundary Conditions on the Natural Frequencies

First, the conventional formulation is considered. The data of the problem were inputted into the MATLAB[®] program. The results for the lowest three natural frequencies for the fixed-fixed type of support are obtained as: 2830.97, 7713.23, and 19075.25 rad./sec., respectively. For hinged-roller support the results are: 1183.83, 4906.63, and 12739.89 rad./sec., respectively. For fixed-free support the results are: 648.37, 2991.39, and 7627.84 rad./sec., respectively, and for free-fixed support the results are: 284.34, 2490.48, and 7568.24 rad./sec. respectively. These results are plotted in Figure 4.1.

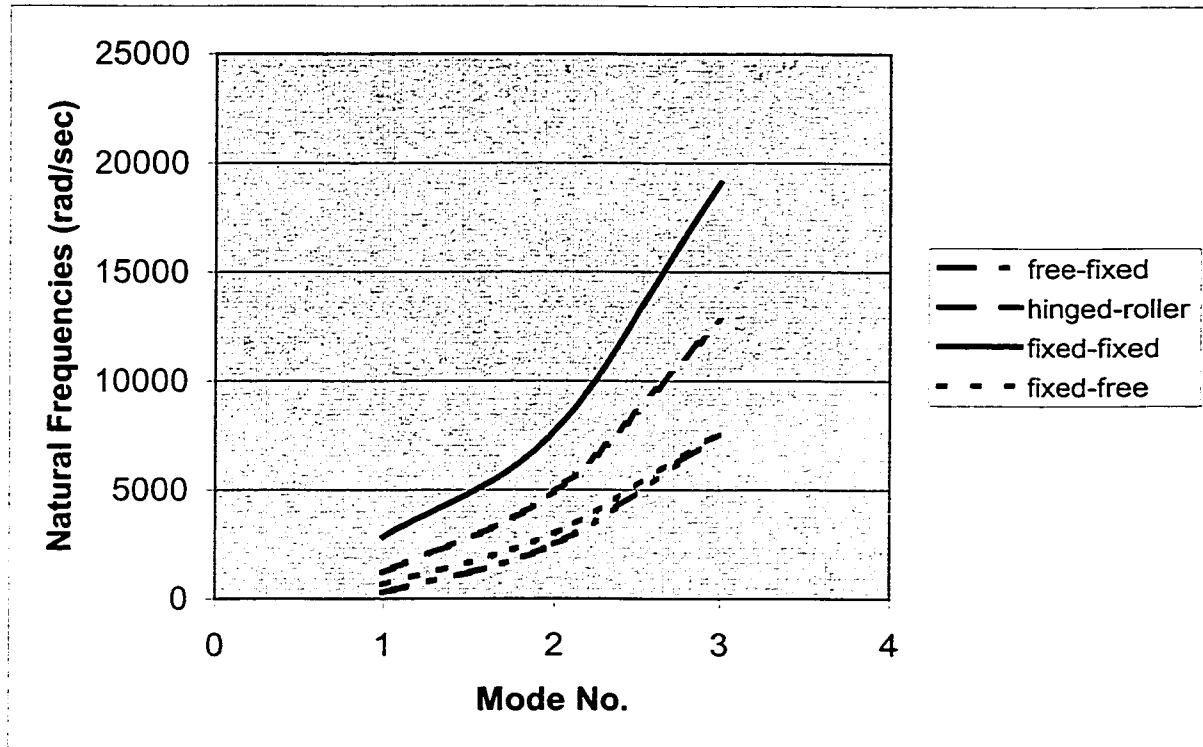


Figure 4.1 The Variations of the Natural Frequencies with Different Boundary Conditions Obtained Using Conventional Formulation

One can conclude from Figure 4.1 that the boundary conditions have their remarkable influence on the natural frequencies. The fixed-fixed type of support gives the highest values of the natural frequencies, whereas the free-fixed type gives the lowest values (in the first mode its value is 10 % of that of the first mode in the fixed-fixed support). Hinged-roller type of support comes as the second highest, and the fixed-free is the third. It is worth noting that changing the location of the fixity from the end of the beam where the origin is located to the other end of the beam (i.e., making the fixed-free support as free-fixed) will reduce the natural frequencies significantly (the drop in the first mode is more than 50%).

It is very obvious here that the number of degrees of freedom and their locations, i.e., how many of them and at what node, have their contributions to the values of the natural frequencies, large or small. In the fixed-fixed type of support, the number of degrees of freedom is four, and they are located at the two nodes in the middle (nodes 2 and 3), whereas there are six degrees of freedom for the other three types of support. So first, it can be concluded that more degrees of freedom reduces the values of the natural frequencies, which is confirmed also in the study using the advanced formulation. Second, the location of these degrees of freedom has its significance also. As each one of the other three types of support has six degrees of freedom, but they differ in the way they are distributed on the nodes. At any case, there are four degrees of freedom at the two nodes in the middle (two per node). In hinged-roller support, the other two are distributed one at each support, where in the case of fixed-free, they are located together at the free end. It is the same for the free-fixed case, but this free end is at node 1, not at node 4 as in the case of fixed-free support.

It is evident that the continuity of the degrees of freedom from one node to another, starting from the first node participates extraordinarily in reducing the values of the natural frequencies. It is seen from above that for specific input data, one can get the lowest values of the natural frequencies if the degrees of freedom are distributed through the nodes as two, two, two, and zero, which is the case of free-fixed support. Any violation of this distribution of the degrees of freedom will increase the values of the natural frequencies, and in some cases by ten times.

The problem is now to be worked out using the advanced formulation to look up the contribution of this method of formulation on the determination of the natural frequencies, while keeping all other parameters of the problem as they are.

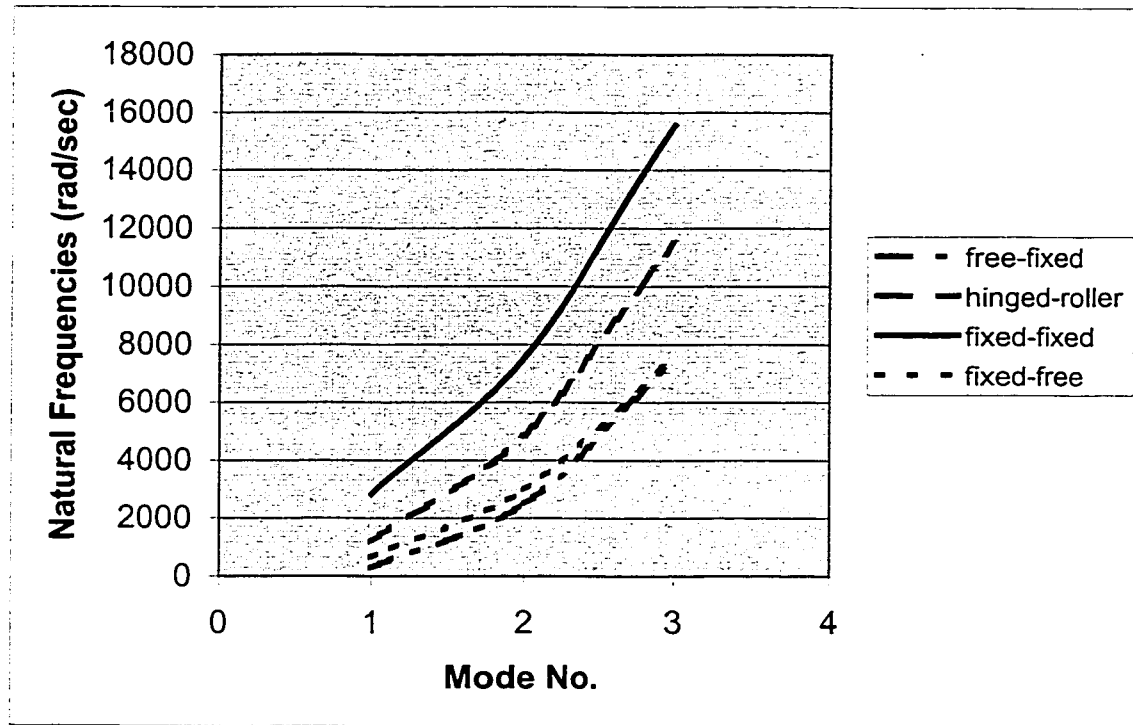


Figure 4.2 The Variations of the Natural Frequencies with Different Boundary Conditions Obtained Using the Advanced Formulation

The results for the lowest three natural frequencies for the fixed-fixed type of support *using the advanced formulation* are obtained as: 2821.75, 7533.17, and 15553.41 rad./sec., respectively. For hinged-roller support the results are: 1183.32, 4847.44, and 11481.92 rad./sec., respectively. For fixed-free support the results are: 648.25, 2982.95, and 7540.69 rad./sec., respectively, and for free-fixed support the results are: 284.35, 2485.47, and 7420.20 rad./sec. respectively. These results are plotted in Figure 4.2.

The observation about the order of the values of the natural frequencies is still valid as can be seen from the results obtained using the advanced formulation. Still the fixed-fixed type of support gives the highest values, and the hinged-roller, fixed-free, and free-fixed support cases give the successively lower values, as shown in Figure 4.2.

The reasons for these variations in the natural frequencies are as before, the number and location of the degrees of freedom. The fixed-fixed and hinged-roller types of support are leading to eight degrees of freedom, and the fixed-free and free-fixed cases are leading to nine degrees of freedom. Hence, in the advanced formulation, the number of the degrees of freedom, their distributions, the continuity of these distributions, and the type of them (geometric or natural) play their major role in the values of the natural frequencies. For example, with the fixed-fixed support, which gives the highest values of the natural frequencies, the distribution of the degrees of freedom goes as: one (bending moment), three, three, and one (bending moment); where in free-fixed case, which gives the lowest values of the natural frequencies, it goes as: two (deflection and slope), three, three, and one (bending moment). Here comes a new aspect about the relation between the values of the natural frequencies and the type of support if the advanced formulation is used for solving the problem. It is not only the distribution of the degrees of freedom, nor only the continuity of them, rather, the type of them, i.e. whether they are geometric or natural.

The next step is to compare between the two methods of formulation to see how the method of formulation can affect the results of the natural frequencies for the

specified boundary condition. The fixed-fixed support and the free-fixed support are chosen for comparison, because the former gives the highest values, and the latter gives the lowest.

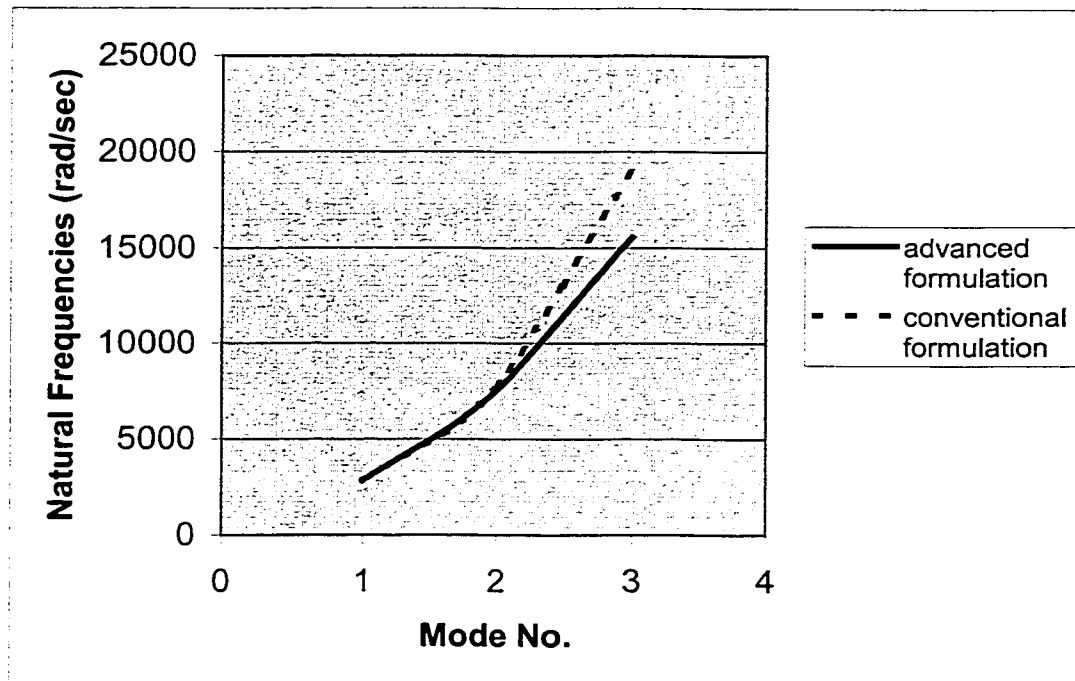


Figure 4.3 The Natural Frequencies Obtained Using Conventional Formulation and Advanced Formulation for the Fixed-Fixed Support

Figure 4.3 shows the comparison for the fixed-fixed support. As it was mentioned before in chapter 3 on how the advanced formulation reduces the values of the natural frequencies. It was mentioned also that this leads to the higher accuracy attainable by using it. This comes from a remark on the output of the MATLAB[®] program, where its output is always higher than the exact solution. Mathematically, this was expressed in the form of lower percentage of error obtained using the advanced formulation, even with less discretization than the discretization used with the

conventional formulation (one may check the sections, for example, problems in chapters 2 and 3, section 2.7 and section 3.7). It is also noted from Figure 4.3 that the values of the natural frequencies corresponding to the first two modes obtained using the advanced formulation are almost identical to the results of the conventional formulation. The improvement in the results starts to appear in the third mode, which provides a smooth transition in the natural frequencies from one mode to another. This reflects on the advantage of choosing more degrees of freedom, which happens in the advanced formulation.

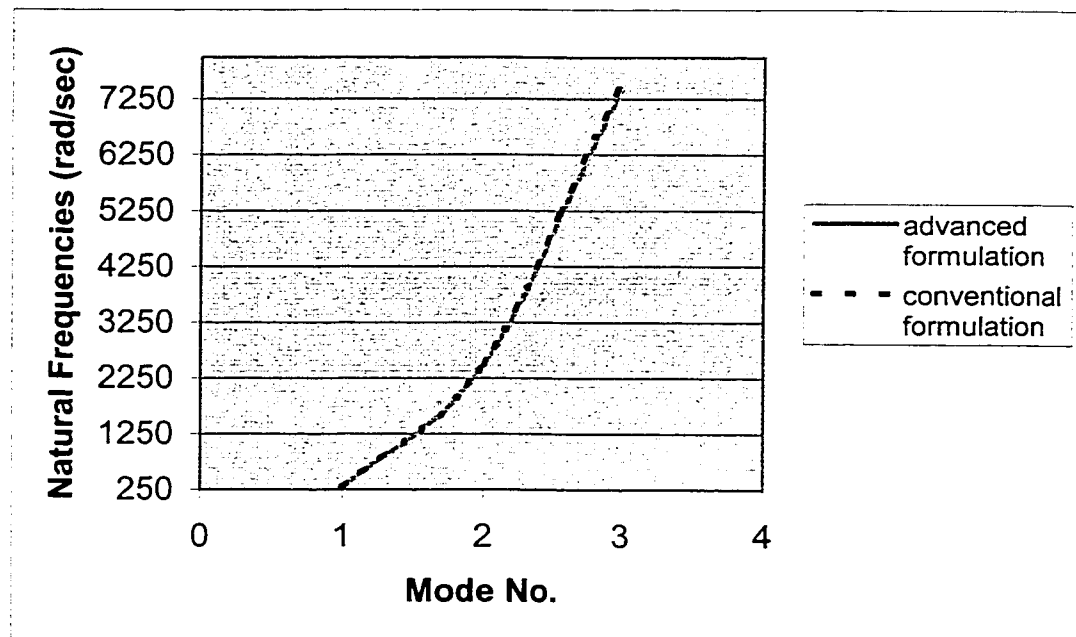


Figure 4.4 A Comparison Between the Natural Frequencies Obtained Using Conventional Formulation and Advanced Formulation for Free-Fixed Support

The comparison done for fixed-fixed case is repeated now for free-fixed case, as shown in Figure 4.4. Most of the observations resulting from the fixed-fixed support case

can be said here. The only difference is that the jump in the values of the natural frequencies in the case of free-fixed support is not as sharp as it was before in the case of fixed-fixed case.

Basically, one can say that having more degrees of freedom improves the results of the natural frequencies. This improvement appears in the lower values of the natural frequencies in the advanced formulation in the second and third modes. The addition of the shear force in the formulation as mentioned in section 3.7 will improve these results, especially in the first mode.

Table 4.1 Comparison of the Natural Frequencies Obtained Using Conventional and Advanced Formulations for Different Boundary Conditions

Type of Support	Formulation Method					
	Conventional Formulation			Advanced Formulation		
	Mode No.			Mode No.		
	1	2	3	1	2	3
Fixed-Fixed	2830.97	7713.23	19075.25	2821.75	7533.17	15553.41
Hinged-Roller	1183.83	4906.63	12739.89	1183.32	4847.44	11481.92
Fixed-Free	648.37	2991.39	7627.84	648.25	2982.95	7540.69
Free-Fixed	284.34	2490.48	7568.24	284.35	2485.47	7420.20

To summarize all the above-mentioned results, all the values of the natural frequencies (in rad./sec.) for different boundary conditions obtained using conventional and advanced formulations are provided in Table 4.1.

4.2.2 The Effect of Fiber Orientations on the Natural Frequencies

The same input data used in the last sub-section are again used, except that the type of support here is set to be fixed-free. The lowest three natural frequencies are to be determined for the laminates with the following ply groups: $[0/90]_s$, $[\pm 45]_s$, and $[\pm 15]_s$, and using both the methods of formulation, conventional and advanced.

First, *using the conventional formulation*, the lowest three natural frequencies for the laminate configuration with $[0/90]_s$ ply groups are obtained as: 648.37, 2991.39, and 7627.84 rad./sec., respectively. For the laminate configuration with $[\pm 45]_s$ ply groups, they are: 485.23, 2235.84, and 5698.55 rad./sec., respectively. For the laminate configuration with $[\pm 15]_s$ ply groups they are: 825.64, 3804.35, and 9696.25 rad./sec., respectively. These results are shown in Figure 4.5 (the laminate configurations with $[\pm 45]_s$ and $[\pm 15]_s$ ply groups are shown on the graph as 45 and 15).

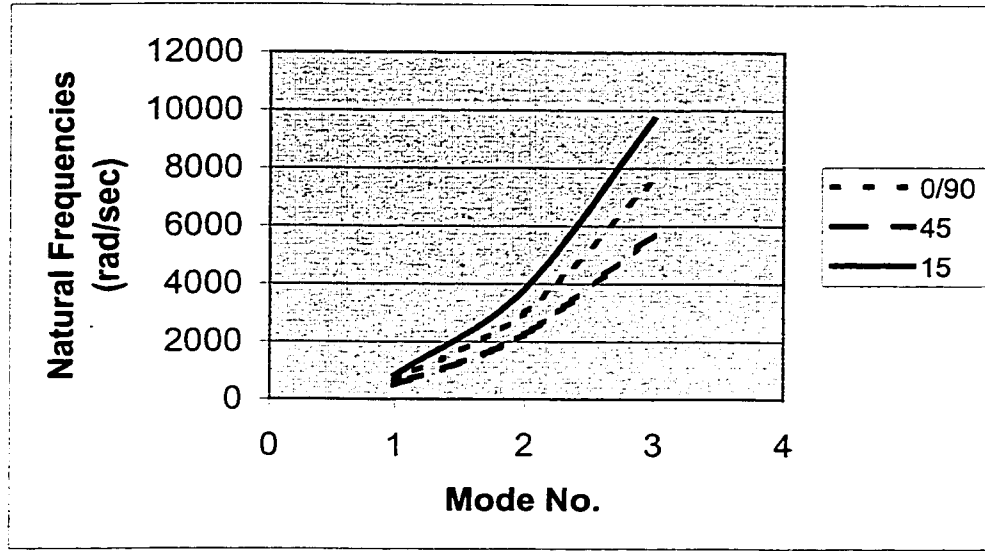


Figure 4.5 The Lowest Three Natural Frequencies for Different Laminate Configurations of an Externally Tapered Composite Beam Based on Conventional Formulation

As shown in Figure 4.5, the laminate configuration with $[\pm 45]_s$ ply groups gives the lowest values of the natural frequencies among the three laminate configurations. The $[0/90]_s$ type comes in the second place, and the $[\pm 15]_s$ configuration gives the highest values. The natural frequency for the third mode of the laminate with $[\pm 15]_s$ ply groups is 1.7 times higher than the corresponding value in $[\pm 45]_s$ configuration.

The change in the fiber orientation has its direct effect on the flexural rigidity of the laminate, bD_{II} . It is recalled from chapter 2, equation 2.46 that states:

$$D_{II} = \sum_{p=1}^n \left[t_p \bar{Z}_p^2 + \frac{t_p^3}{12} \right] (\bar{Q}_{II})_p \quad (4.1)$$

where D_{11} is the bending or flexural laminate stiffness relating the bending moment M_x to curvature κ_x . $(\overline{Q_{11}})_p$ is the transformed stiffness coefficient of a ply, which can be defined as:

$$(\overline{Q_{11}})_p = \cos^4(\theta)Q_{11} + \sin^4(\theta)Q_{22} + 2\cos^2(\theta)\sin^2(\theta)Q_{12} + 4\cos^2(\theta)\sin^2(\theta)Q_{33} \quad (4.2)$$

where Q_{11} , Q_{12} , Q_{22} , and Q_{33} are coefficients of the ply stiffness matrix, and they are merely functions of the ply mechanical properties.

It is obvious from equations 4.1 and 4.2 that, eventually, the flexural rigidity of a ply, and hence, the laminate flexural rigidity is a function of the ply orientations (because the calculations done in equation 4.2 will be repeated considering the number of plies). This is also clear from the output results of the flexural rigidities calculated using the MATLAB[®] program.

The values of the flexural rigidity of each finite element in each type of laminate configuration (they differ in their values because the number of plies is different from one element to another) are now given. For $[0/90]_s$ configuration, the flexural rigidities of the three finite elements are: 2.59, 1.33, and 0.563 MPa, respectively. For $[\pm 45]_s$ they are: 1.45, 0.742, and 0.313 MPa, respectively. For $[\pm 15]_s$ they are: 4.20, 2.15, and 0.907 MPa, respectively. These results are shown in Figure 4.6.

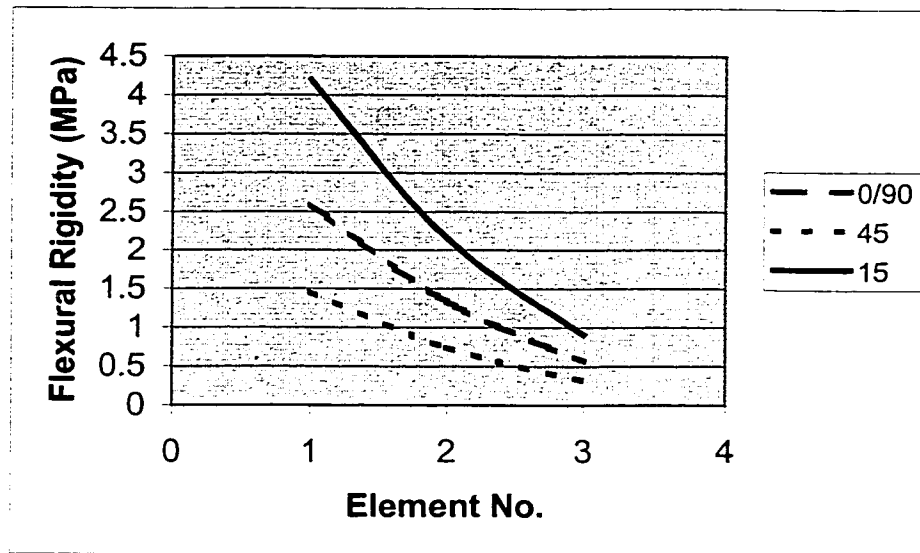


Figure 4.6 The Variation of the Flexural Rigidity in the Finite Element Mesh of an Externally Tapered Composite Beam for Different Ply Orientations

It is observed from Figure 4.6 that the $[\pm 15]_s$ type of configuration raises the flexural rigidity of the laminate significantly over the other two types of configurations, whereas the $[0/90]_s$ configuration comes in the second place, and the lowest values correspond to the $[\pm 45]_s$ configuration.

Higher flexural rigidity will lead to a stiffer laminate, and accordingly, higher natural frequencies are obtained, and that is what was noticed from Figure 4.5. So from the stress point of view, the $[\pm 15]_s$ configuration is the best for designing, whereas the $[\pm 45]_s$ configuration is the best from the dynamic analysis point of view. Accordingly, the designer has to compromise between both the points of view. The suggestion here is to choose the cross-ply type of configuration, since it gives moderate values for both points of view among all the types of configurations.

Using the advanced formulation, the lowest three natural frequencies for cross-ply laminate are calculated to be: 648.25, 2982.95, and 7540.69 rad./sec., respectively. For $[\pm 45]_s$ configuration they are: 485.14, 2229.53, and 5633.21 rad./sec., respectively, and for $[\pm 15]_s$ configuration they are: 825.48, 3793.61, and 9585.08 rad./sec., respectively. These results are plotted in Figure 4.7.

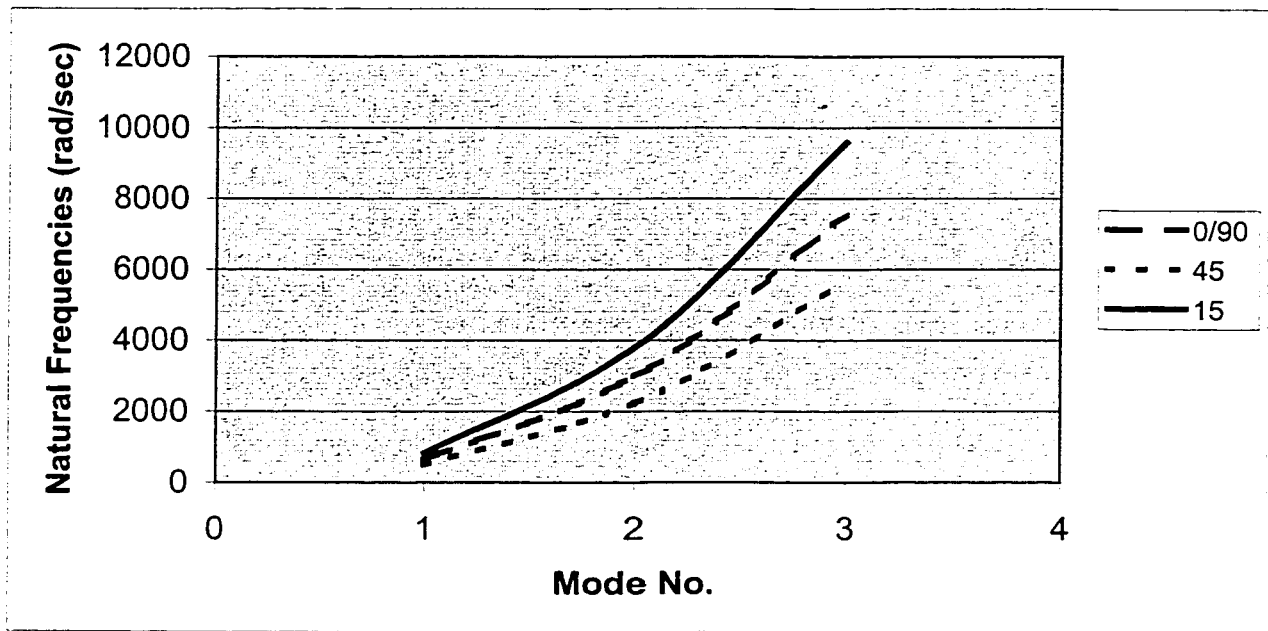


Figure 4.7 The Lowest Three Natural Frequencies for Different Laminate Configurations of an Externally Tapered Composite Beam Obtained Using Advanced Formulation

It is observed from Figure 4.7 that still the $[\pm 45]_s$ type of configuration gives the lowest values of the natural frequencies, then comes the cross-ply configuration, and the highest values are reserved for the $[\pm 15]_s$ configuration. The conclusions observed

before while using the conventional formulation regarding the relatively low values of the natural frequencies in the case of the $[\pm 45]_s$ configuration are still applicable here with the advanced formulation, and for the same reasons.

To conclude on what is already said about the differences in the results of either formulation used, a comparison should be provided. The lowest three natural frequencies obtained using both the conventional and advanced formulation for cross-ply configuration are plotted in Figure 4.8.

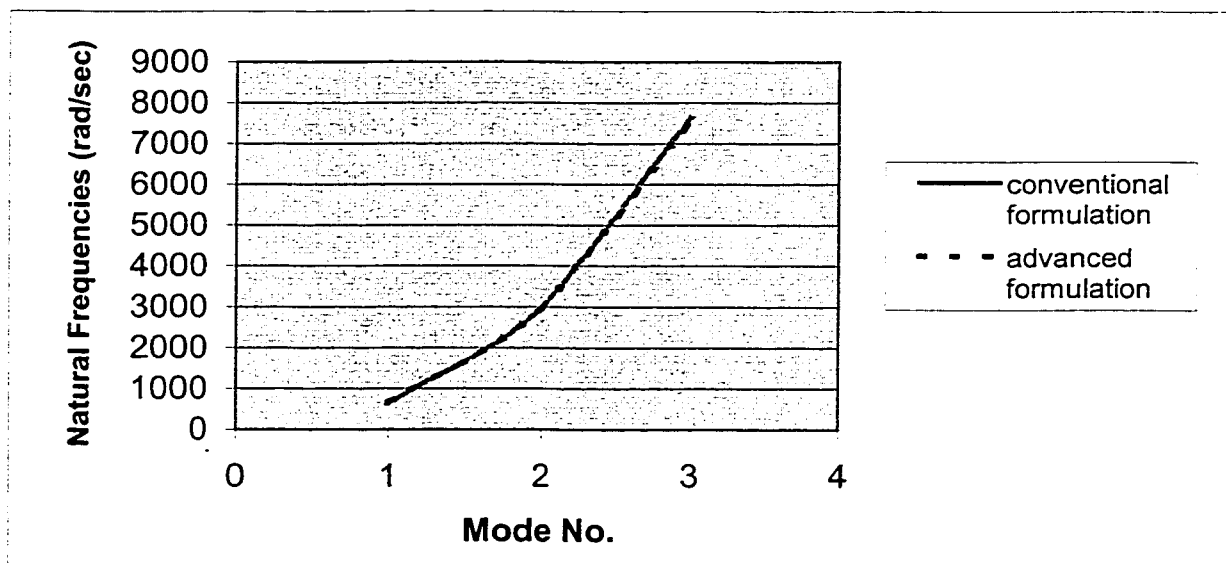


Figure 4.8 A Comparison Between the Natural Frequencies Obtained Using Conventional Formulation and Advanced Formulation for Cross-Ply Laminate

The upper hand of the advanced formulation is not very clear in Figure 4.8, as the differences are in the range of hundreds.

Table 4.2 below encapsulates all the results mentioned before about the effect of the changes in the fiber orientations on the natural frequencies that are obtained using both the methods of formulation, conventional and advanced. The type of support for the beam is fixed-free.

Table 4.2 Comparison of the Natural Frequencies Obtained Using Conventional Formulation and Advanced Formulation for Different Fiber Orientations

Ply groups in the Laminate Configuration	Formulation Method					
	Conventional Formulation			Advanced Formulation		
	Mode No.			Mode No.		
	1	2	3	1	2	3
$[0/90]_s$	648.37	2991.39	7627.84	648.28	2982.95	7540.69
$[\pm 45]_s$	485.23	2235.84	5698.55	485.14	2229.53	5633.21
$[\pm 15]_s$	825.64	3804.35	9696.25	825.48	3793.61	9585.08

4.2.3 The Effect of the Beam Discretization on the Natural Frequencies

In this section, the beam elements will be meshed into four different types. In the first type (Type A) the beam will be divided equally as: $L/3$, $L/3$, and $L/3$. In the second type (Type B) the beam will be divided as: $L/4$, $L/2$, and $L/4$. In the third type (Type C) the beam will be divided as: $L/4$, $L/4$, and $L/2$, and finally in the fourth type (Type D) the beam will be divided as $L/2$, $L/4$, and $L/4$, where L is the total length of the composite

beam and equal to 1.08 m (see Figure 3.10, where l_1 , l_2 , and l_3 in the figure are expressed here as $L/3$, $L/2$...and so on). The beam type of support is fixed-fixed and the laminate configuration is cross-ply.

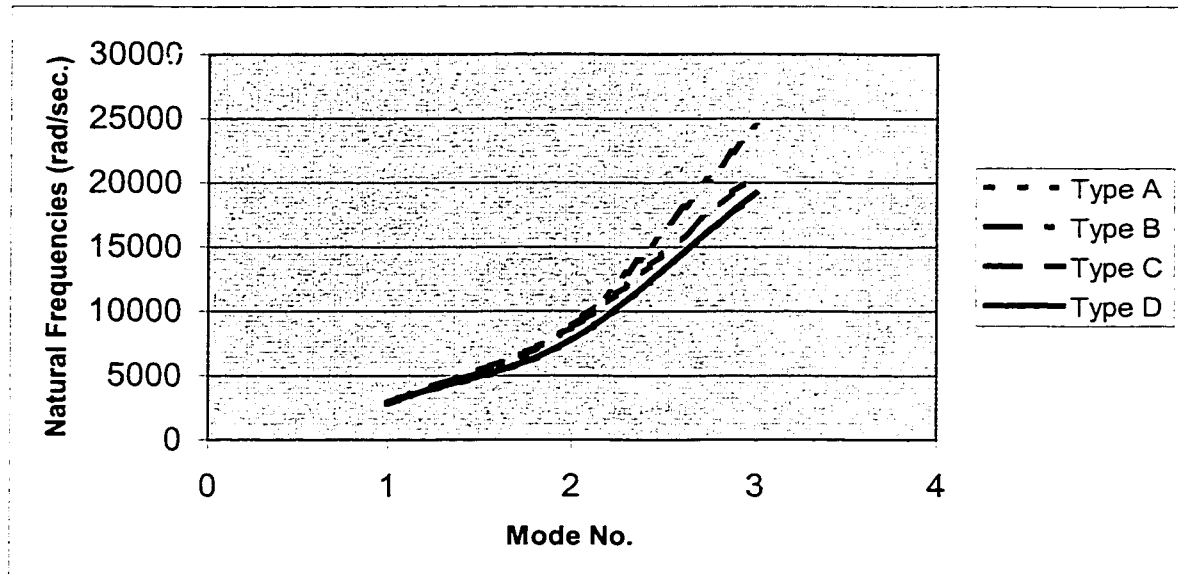


Figure 4.9 The Variations in the Natural Frequencies for Different Meshes of an Externally Tapered Composite Beam Obtained Using Conventional Formulation

First, *using the conventional formulation*, the lowest three natural frequencies for Type A mesh of the beam are obtained to be: 2830.97, 7713.23, and 19075.25 rad./sec., respectively. For Type B mesh of the beam they are: 2945.52, 7773.12, and 19197.41 rad./sec., respectively. For Type C mesh of the beam they are: 2782.52, 8822.17, and 24373.01 rad./sec., respectively. For Type D mesh of the beam they are: 2870.21, 8692.11, and 20753.62 rad./sec., respectively. The results are plotted in Figure 4.9.

As the curves in Figure 4.9 almost coincide, they are re-plotted, each two of them in one figure. Figure 4.10 is for comparison between Type A and Type B meshes, and Figure 4.11 is for comparison between Type C and Type D meshes.

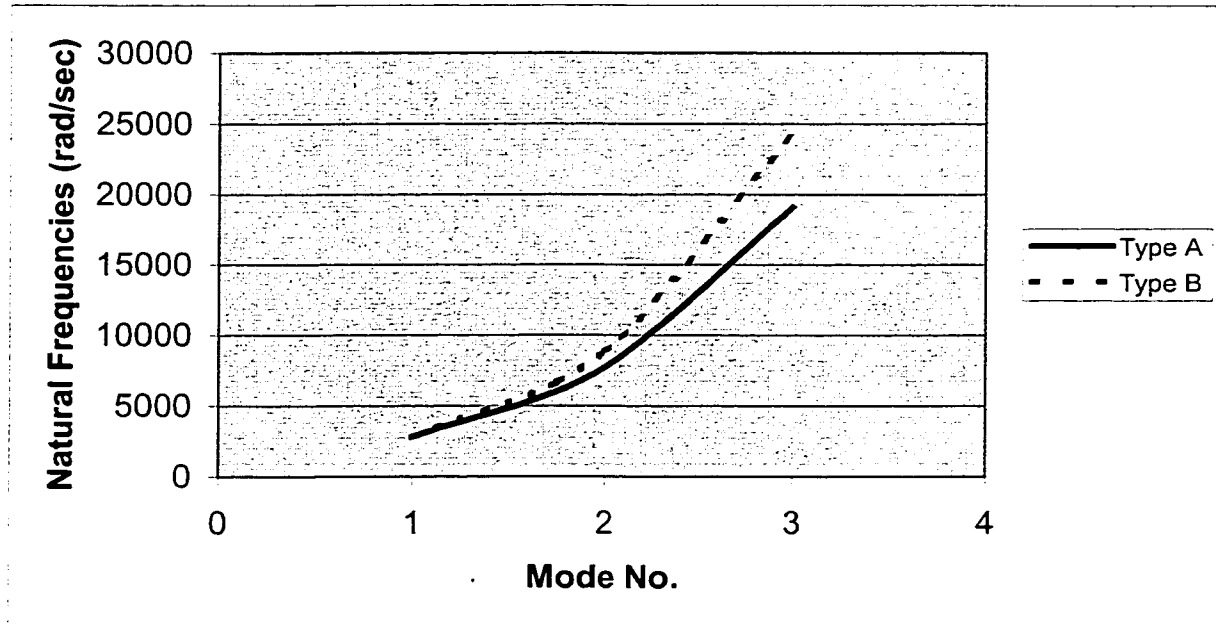


Figure 4.10 The Variations in The Natural Frequencies of Type A and Type B Meshes of An Externally Tapered Composite Beam Obtained Using Conventional Formulation

The first observation is that the results of the natural frequencies exist in a close range, which makes them look almost coinciding, as shown in Figure 4.9.

Dividing the beam with nodes at lengths $L/4$, $L/4$, and $L/2$ gives the lowest value of the natural frequency in the first mode, whereas dividing it with equal length elements gives the lowest values of the natural frequencies in the second and third modes. On the

other hand, the mesh division with nodes at lengths $L/4$, $L/2$, and $L/4$ gives the highest value of the natural frequency in the first mode, and dividing the beam with nodes at lengths $L/4$, $L/4$, and $L/2$ gives the highest values of the natural frequencies in the second and third modes. So, the discretization with nodes at lengths $L/4$, $L/4$, and $L/2$ gives the lowest value of the natural frequency in the first mode, and the highest in the second and third modes. Hence, the equal division of the beam can provide a compromise among all results.

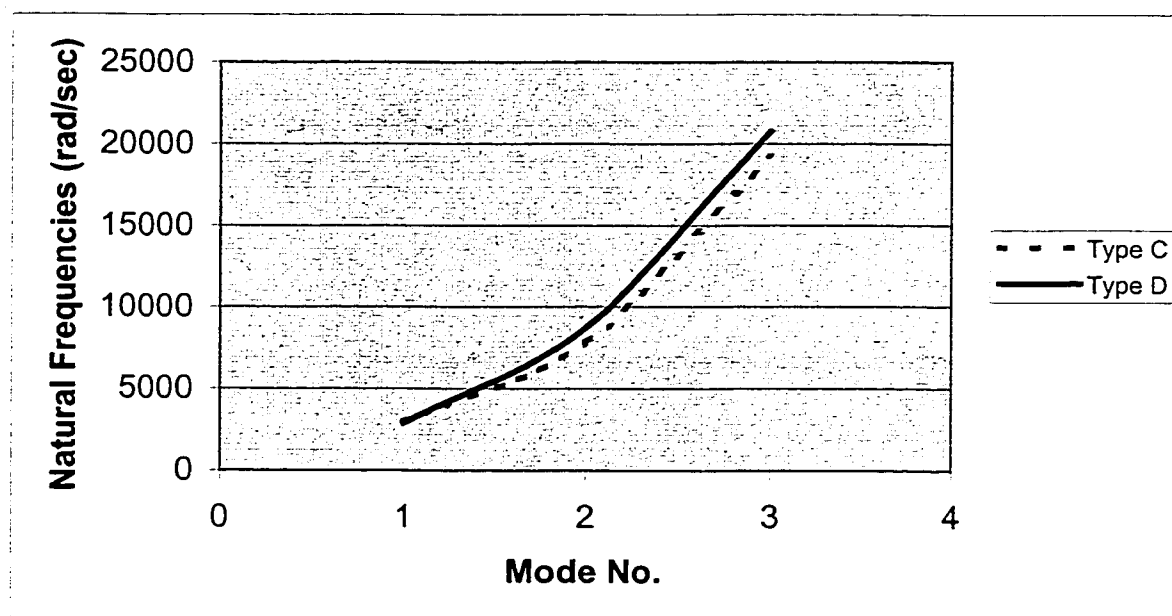


Figure 4.11 The Variations in The Natural Frequencies of Type C and Type D Meshes of An Externally Tapered Composite Beam Obtained Using Conventional Formulation

The beam discretization has no influence on the laminate physical properties. It affects directly on the values of the coefficients of the mass and stiffness matrices only. In the assembled mass and stiffness matrices, these coefficients change due to the

changes happened in the element lengths. Accordingly, this will affect the eigenvalues of the matrices, and this explains the changes in the values of the natural frequencies from certain element discretization to another.

The difference between $L/3$ and $L/4$ is equal to $L/12$. Generally speaking, this difference is not very big, unless the beam span, L , is very long. The chosen beam span is practical and can be found in many applications. In the present case, this difference is equal to 9 cm . As one can see, these changes in the beam discretization lead to minor differences in the values of the coefficients of the mass and stiffness matrices. Hence, their effects on the results of the natural frequencies will be minor too. This may justify the closeness of the values of the natural frequencies.

Using the advanced formulation, the lowest three natural frequencies for Type A mesh of the beam are obtained to be: 2821.75, 7533.17, and 15553.41 rad./sec., respectively. For Type B mesh of the beam they are: 2885.20, 7629.39, and 15031.20 rad./sec., respectively. For Type C mesh of the beam they are: 2740.11, 7404.47, and 13913.72 rad./sec., respectively. For Type D mesh of the beam they are: 2858.61, 8160.80, and 15702.04 rad./sec., respectively. To avoid the indistinctness happened in the conventional formulation results in Figure 4.9, the advanced formulation results are plotted in two figures. Figure 4.12 is to plot the results for Type A and Type D, and Figure 4.13 is to plot the results for Type B and Type C.

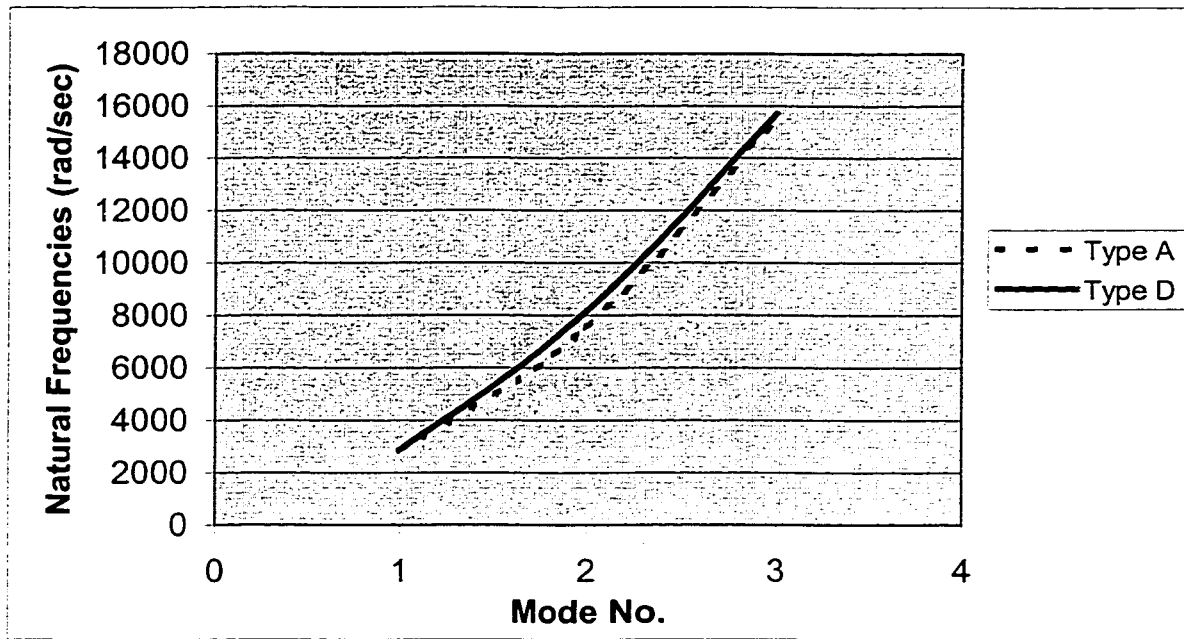


Figure 4.12 The Variations in The Natural Frequencies of Type A and Type B Meshes of An Externally Tapered Composite Beam Obtained Using Advanced Formulation

It is found here in the advanced formulation that dividing the beam with nodes at lengths $L/4$, $L/4$, and $L/2$ gives the lowest values of the natural frequencies in all modes. The equal division comes in the second place. Dividing the beam with nodes at lengths $L/2$, $L/4$, and $L/4$ gives the highest values of the natural frequencies in the first mode, whereas the mesh division with nodes at lengths $L/4$, $L/2$, and $L/4$ does that in the second and third modes.

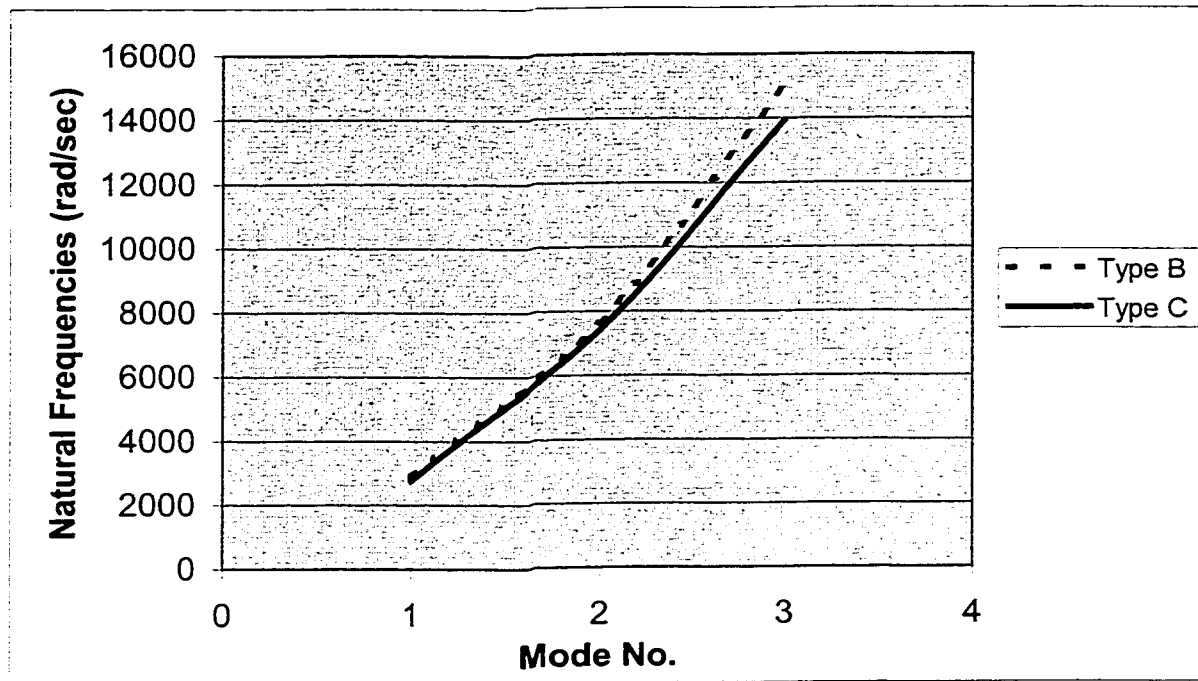


Figure 4.13 The Variations in The Natural Frequencies of Type C and Type D Meshes of An Externally Tapered Composite Beam Obtained Using Advanced Formulation

As it was mentioned before the beam discretization affects directly the mass and stiffness matrices. It can be added here to elaborate on the above-mentioned conclusions that in the assembled mass and stiffness matrices, only the rows and columns that correspond to the existing degrees of freedom stay and the other ones are removed. Due to the changes in the beam discretization, the coefficients of the assembled mass and stiffness matrices will change, which, eventually, will change the eigenvalues of the matrices.

To see the contribution of the advanced finite element formulation, a comparison between the results of the natural frequencies for beam discretization with nodes at

lengths $L/4$, $L/4$, and $L/2$ obtained using both the methods of formulation is introduced, in Figure 4.14. As it might be expected, the values obtained using the advanced formulation are lower by a significant amount.

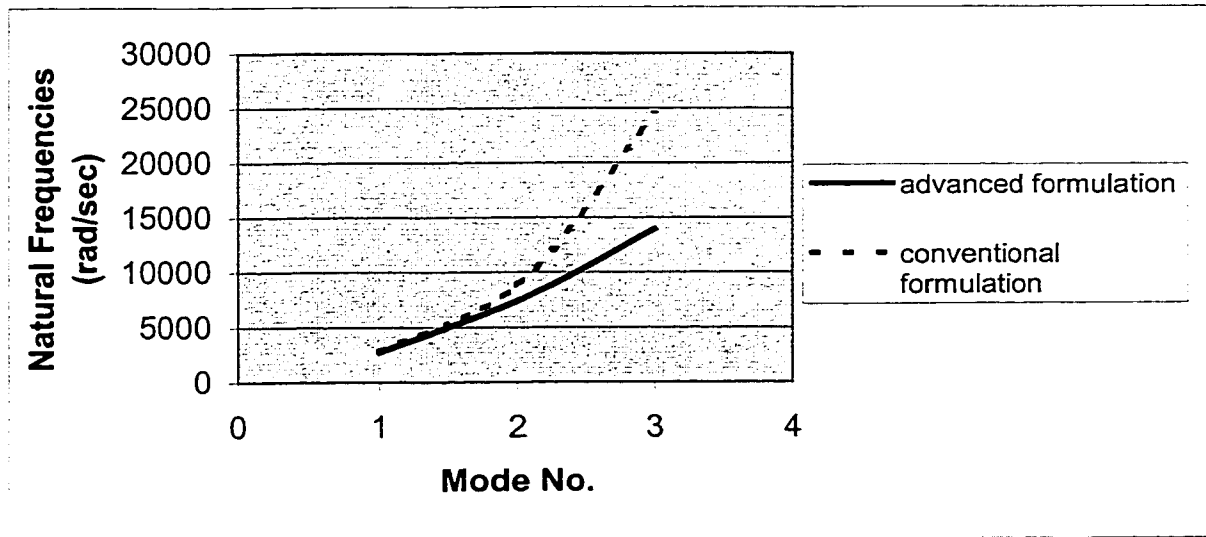


Figure 4.14 A Comparison Between the Natural Frequencies Obtained Using Conventional Formulation and Advanced Formulation for Type A Beam Discretization

Figure 4.14 shows that the values of the natural frequencies obtained using the advanced formulation are remarkably lower. It shows also that the jump from one mode to another is much smoother than its counterpart in the conventional formulation.

Adding the bending moment as a degree of freedom in the advanced formulation gives some kind of balance and organization in the values of the natural frequencies. This appears on the gradual change between the modes. It was mentioned in the conclusions on the conventional formulation that it is needed to choose the kind of

discretization that gives the lowest natural frequencies. On the contrary, this compromise is not needed with the advanced formulation, as it tells, right away, that the beam discretization with nodes at lengths $L/4$, $L/4$, and $L/2$ gives the lowest values. It is believed that this is due to the stability in the results of the advanced formulation. Consequently, this encourages continuing the work about adding the shear force as a degree of freedom in the MATLAB[®] program. Table 4.3 is given below to summarize the above-mentioned results.

Table 4.3 Comparison Between the Natural Frequencies Obtained Using Conventional and Advanced Formulations For Different Element Discretizations

Discretization Type	Formulation Method					
	Conventional Formulation			Advanced Formulation		
	Mode No.			Mode No.		
	1	2	3	1	2	3
Type A	2830.97	7713.23	19075.25	2821.75	7533.17	15553.41
Type B	2870.21	8692.11	20753.62	2858.61	8160.80	15702.04
Type C	2782.52	8822.17	24373.01	2740.11	7404.47	13913.72
Type D	2945.52	7773.12	19197.41	2885.20	7629.39	15031.20

4.3 Parametric Study on Dynamic Analysis of Mid-Plane Tapered Composite Beams

Problem Description:

A mid-plane tapered composite beam made of the same material used in the last section is considered to determine its natural frequencies for both the conventional and advanced formulations. Also, this is to be done under various changes; changes in the boundary conditions, changes in the fiber orientations, changes in the meshing of the composite beam, and changes in the taper angle. The beam is modeled using three elements, which satisfactorily matches with the geometric nature of the taper (see Figure 2.7). The beam is equally divided ($l_1 = l_2 = l_3 = 0.36 \text{ m}$), the taper angle is -6° , and the laminate configuration is cross-ply. The number of plies in each element is 100, 80, and 60, respectively. The total length of the beam is 1.08 m.

4.3.1 The Effect of the Boundary Conditions on the Natural Frequencies

First the conventional formulation is considered. The data of the problem were inputted into the MATLAB[®] program, and the results of the lowest three natural frequencies for the fixed-fixed type of support are obtained as: 1862.15, 6770.05, and 19758.82 rad./sec., respectively. For hinged-roller support the results are: 708.18, 2908.72, and 7495.74 rad./sec., respectively. For fixed-free support the results are:

280.28, 1571.24, and 4391.50 rad./sec., respectively, and for free-fixed support the results are: 244.80, 1908.60, and 6732.69 rad./sec. respectively. These results are plotted in Figure 4.15.

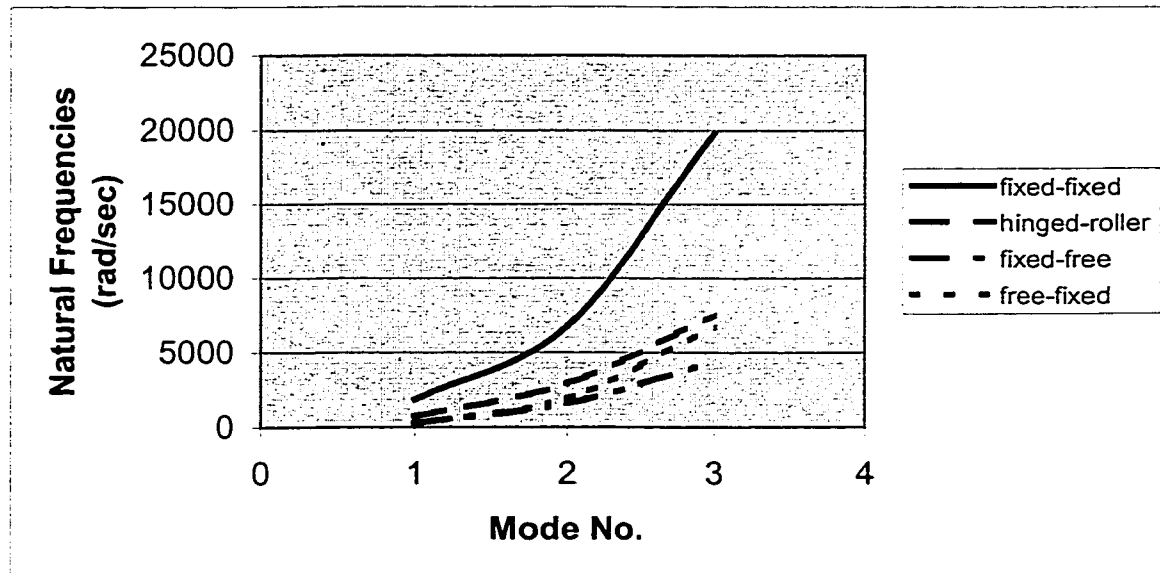


Figure 4.15 The Variations of the Natural Frequencies with Different Boundary Conditions Obtained Using the Conventional Formulation

As shown in Figure 4.15, the fixed-fixed type of support gives the highest values of the natural frequencies. The free-fixed support gives the lowest value in the first mode, whereas the fixed-free support does that in the second and third modes.

As it was mentioned before, the change in the boundary conditions leads to various changes in the number of degrees of freedom, and their distribution over the nodes (what degrees of freedom on what node).

Using the advanced formulation the results of the lowest three natural frequencies for the fixed-fixed type of support are calculated to be: 2693.05, 8742.81, and 16986.51 rad./sec., respectively. For hinged-roller support the results are: 1061.44, 4180.90, and 8425.47 rad./sec., respectively. For fixed-free support the results are: 448.02, 2463.51, and 6772.01 rad./sec., respectively, and for free-fixed support the results are: 261.42, 2603.54, and 8491.27 rad./sec. respectively. These results are plotted in Figure 4.16.

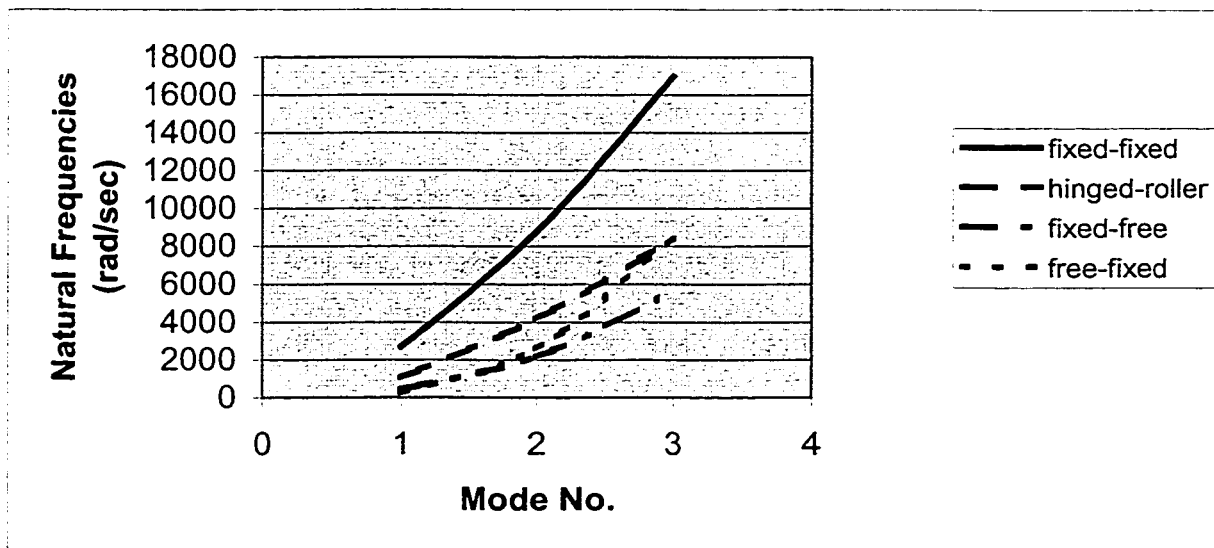


Figure 4.16 The Variations of the Natural Frequencies with Different Boundary Conditions Obtained Using the Advanced Formulation

As one can see from Figure 4.16, fixed-fixed type of support still gives the highest values of the natural frequencies, and hinged-roller support seconds it. Fixed-free support gives the lowest values in the second and third modes, whereas the free-fixed support has the lowest value in the first mode.

Despite that the number of degrees of freedom in both types of supports, fixed-fixed and hinged-roller are the same, that is eight, the values of the natural frequencies in the fixed-fixed support are almost two times the values in the case of hinged-roller support. This is to confirm the importance of the distribution of the degrees of freedom and their entities. The degrees of freedom go with the fixed-fixed support as one (bending moment), three, three, and one (bending moment), where they go with the hinged-roller support as: one (slope), three, three, and one (slope). Since the number of degrees of freedom goes up to nine with the cases of fixed-free and free-fixed supports, the values of the natural frequencies start to reduce.

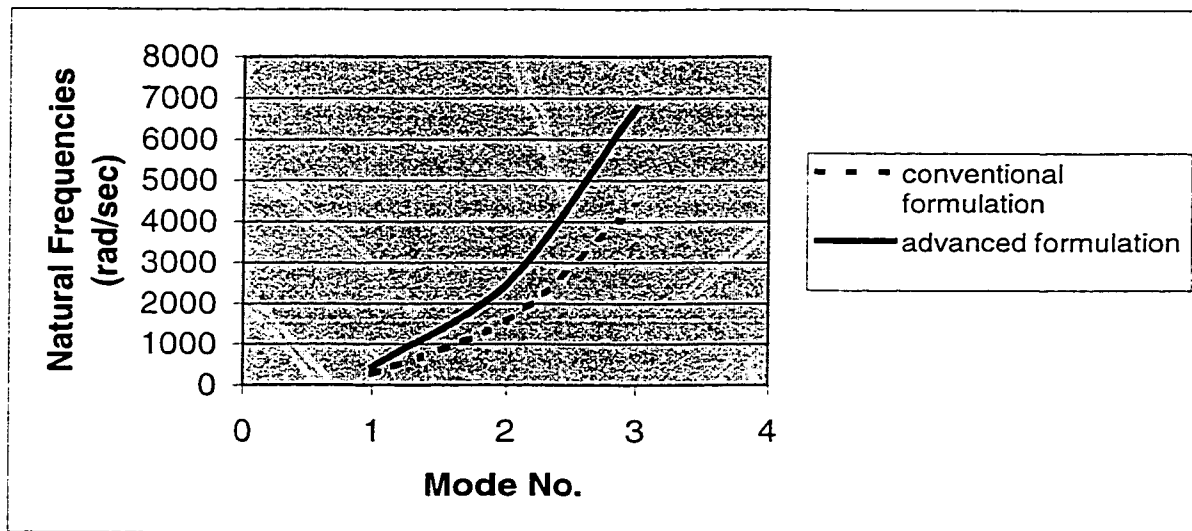


Figure 4.17 Comparison Between the Natural Frequencies Obtained Using Conventional and Advanced Formulations for Mid-Plane Tapered Fixed-Free Composite Beam

Then a comparison between the results of the natural frequencies obtained using both the methods of formulation has to be done. The type of support chosen is fixed-free, and the results are shown in Figure 4.17.

For mid-plane tapered composite beams the natural frequencies obtained using the advanced formulation are higher than the results obtained using the conventional formulation. The output of the MATLAB[®] program was verified carefully, starting from the input data, the distribution of the degrees of freedom, and the calculations of the laminate stiffness (\overline{Q}_{II}). It may be noted here that the processing of the stiffness and mass matrices has been performed as follows. Because of the huge size of these matrices, as it was mentioned before in the last chapter, the coefficients were calculated numerically in the Maple software. For example, the equations 3.47 and 3.49 were integrated numerically within the limits 0 to 0.36 (the beam element length), and not symbolically within the limits 0 to l , as it was done in the conventional formulation. Hence, the stiffness and mass matrices were inputted as numbers into the MATLAB software, and not in symbolic form as in the conventional formulation. In addition, even within the Maple software itself, the mass matrix was calculated using commands that are different from the commands used to get the stiffness matrix. Hence, the methods employed for integration and differentiation would be different from one software to another. Moreover, it is recalled from chapter 2, section 2.7.2.1.2 that the problem was solved using both the software MATLAB[®] and ANSYS[®]. The percentage of error in the first mode when MATLAB[®] was employed was 0.13, and when ANSYS[®] was employed was -0.13. This means that the solution by the MATLAB[®] program yields values that are higher than the exact solution within a certain value, and the solution by the ANSYS[®] program yields values that are lower than the exact solution within the same value. This can be seen from the different signs of the error values. The same remark can be applied in the present case. So if it is assumed that the exact solution for the fixed-free case is

something around 300 rad./sec., one can find that the percentages of error that correspond to the conventional and advanced formulation will be equal in magnitude and opposite in sign. This can be verified by noticing the values of the natural frequencies obtained using both the methods of formulation. It is found that the values obtained using the advanced formulation are almost two times the values obtained using the conventional formulation. So it can be said that each set of the results is on equal distance from the assumed exact solution.

Table 4.4 Comparison Between the Natural Frequencies That Correspond to Different Boundary Conditions and for Different Formulations

Type of Support	Formulation Method					
	Conventional Formulation			Advanced Formulation		
	Mode No.			Mode No.		
	1	2	3	1	2	3
Fixed-Fixed	1862.15	6770.05	19758.82	2693.05	8742.81	16986.51
Hinged-Roller	708.18	2908.72	7495.74	1061.44	4180.90	8425.47
Fixed-Free	280.28	1571.24	4391.50	448.02	2463.51	6772.01
Free-Fixed	244.80	1908.60	6732.69	261.42	2603.54	8491.27

It was found that the free-fixed support gives the lowest value of the natural frequency in the first mode, whilst the fixed-free support does that in the second and third modes in the conventional formulation. This is exactly what is observed from the results

obtained using the advanced formulation. Table 4.4 above shows the values of the natural frequencies in rad./sec. for different types of supports that are obtained using both the methods of formulation.

4.3.2 The Effect of Fiber Orientations on the Natural Frequencies

The same input data of the last sub-section are used, except that the type of support here is set to be fixed-free. The lowest three natural frequencies are to be determined for the laminates with the following ply groups: $[0/90]_s$, $[\pm 45]_s$, and $[\pm 15]_s$, and using both the methods of formulation, conventional and advanced.

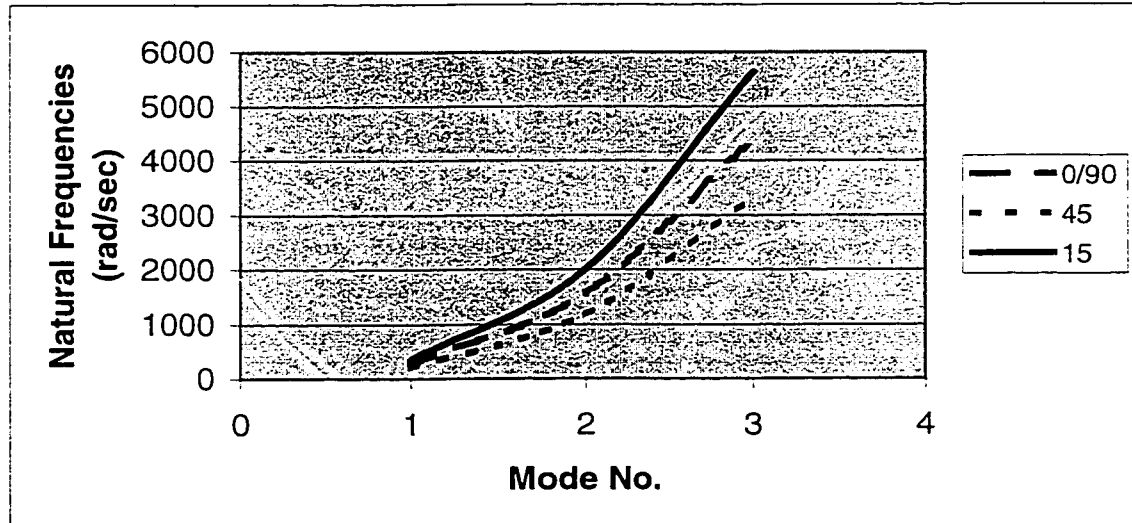


Figure 4.18 The Lowest Three Natural Frequencies for Different Laminate Configurations of a Mid-plane Tapered Composite Beam Based on the Conventional Formulation

First, *using the conventional formulation*, the lowest three natural frequencies for the configuration with $[0/90]_s$ ply groups are obtained as: 280.28, 1571.24, and 4391.50 rad./sec., respectively. For the laminate configuration with $[\pm 45]_s$ ply groups, they are: 211.24, 1184.21, and 3309.78 rad./sec., respectively. For the laminate configuration with $[\pm 15]_s$ ply groups, they are: 359.43, 2014.97, and 5631.69 rad./sec., respectively. These results are shown in Figure 4.18.

As shown in Figure 4.18, the laminate configuration with $[\pm 45]_s$ ply groups gives the lowest values of the natural frequencies among the three laminate configurations. The $[0/90]_s$ type comes in the second place, and the $[\pm 15]_s$ configuration gives the highest values. As it was observed in the external type of taper, the change in the inclination angles has its direct effect on the flexural rigidity of the laminate, bD_{II} (check Figure 4.7).

Using the advanced formulation, the lowest three natural frequencies for $[0/90]_s$ configuration are obtained to be: 448.02, 2463.51, and 6772.01 rad./sec., respectively. For the laminate configuration with $[\pm 45]_s$ ply groups they are: 337.66, 1856.69, and 5103.91 rad./sec., respectively, and for the laminate configuration with $[\pm 15]_s$ ply groups they are: 574.54, 3159.21, and 8684.46 rad./sec., respectively. These results are shown in Figure 4.19.

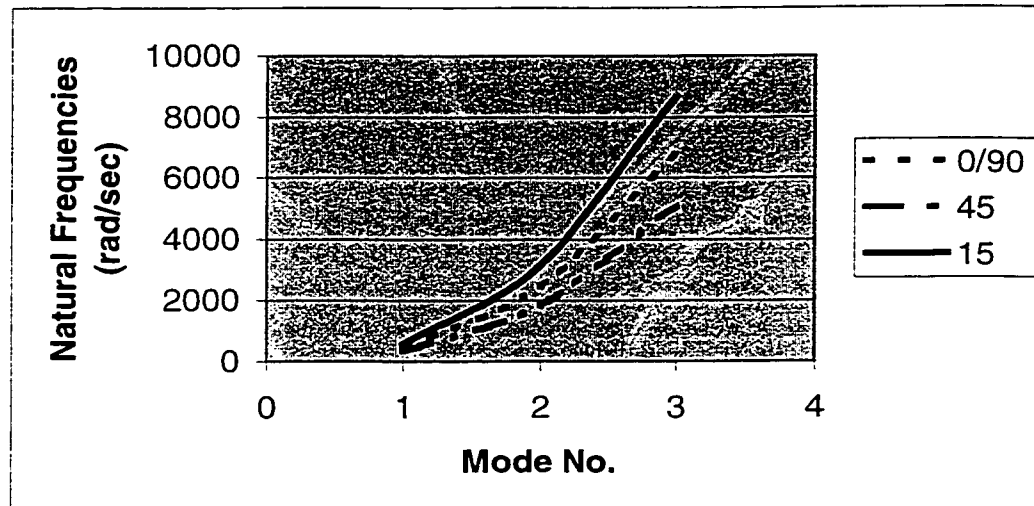


Figure 4.19 The Lowest Three Natural Frequencies for Different Laminate Configurations of a Mid-plane Tapered Composite Beam Obtained Using the Advanced Formulation

Figure 4.19 shows that the laminate configuration with $[\pm 45]_s$ ply groups gives the lowest values of the natural frequencies in all modes, then the cross-ply type, and the $[\pm 15]_s$ configuration gives the highest values, which is related to the flexural rigidity of the laminate, bD_{II} , as it was explained before.

The comparison between the results obtained using the conventional formulation and the advanced formulation is shown below in Figure 4.20.

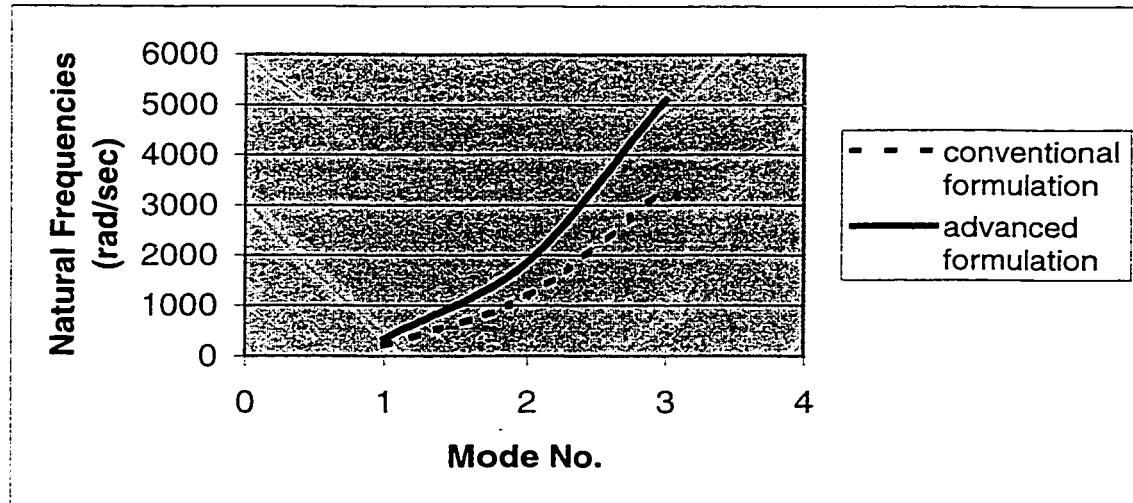


Figure 4.20 Comparison Between the Natural Frequencies Obtained Using Conventional and Advanced Formulations for Mid-Plane Tapered Composite Beam with $[\pm 45]_s$ Ply Groups

As it was observed in the previous case, i.e. the case of change of the boundary conditions, still the values of the natural frequencies obtained using the advanced formulation are higher than the corresponding values obtained using the conventional formulation. Anyhow, this is expected because the change in the fiber orientation angles affects the flexural rigidity of the laminate, and it was said in the last sub-section that this difference in the results comes from the calculated stiffness and mass matrices in Maple software. In any case, the results obtained using the advanced formulation are still reliable, since they exhibit the same effect of the laminate configuration on the natural frequencies (for example, the laminate configuration with $[\pm 45]_s$ ply groups gives the lowest values of the natural frequencies in all modes in both the methods of formulation).

Table 4.5 below shows how the natural frequencies for a mid-plane tapered composite beam are significantly affected by different laminate configurations in both the methods of formulation.

Table 4.5 Comparison Between the Natural Frequencies for Different Fiber Orientations Obtained Using the Conventional and Advanced Formulations

Ply group	Formulation Method					
	Conventional Formulation			Advanced Formulation		
	Mode No.			Mode No.		
	1	2	3	1	2	3
$[0/90]_s$	280.28	1571.24	4391.50	448.02	2463.51	6772.01
$[\pm 45]_s$	211.24	1184.21	3309.78	337.66	1856.69	5103.91
$[\pm 15]_s$	359.43	2014.97	5631.69	574.54	3159.21	8684.46

4.3.3 The Effect of the Taper Angle on the Natural Frequencies

The problem undertaken now is to determine the natural frequencies for mid-plane tapered composite beam with the fixed-free support using different taper angles, 6, 2, and 10 degrees. First, *using the conventional formulation*, the results for the lowest three natural frequencies for the beam with a taper angle of 6 degrees are calculated to be:

280.27, 1571.24, and 4391.50 rad./sec., respectively. For the beam with the taper angle of two degrees they are: 93.19, 522.43, and 1460.14 rad./sec., respectively, and finally for the beam with the taper angle of ten degrees, the results are: 470.18, 2635.82, and 7366.93 rad./sec., respectively. The results are plotted in Figure 4.21 below.

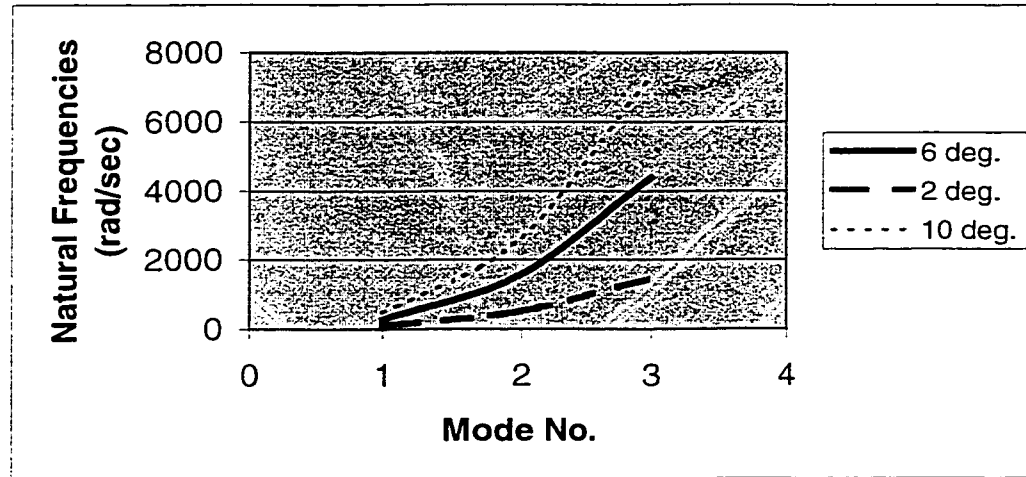


Figure 4.21 The Variations of the Natural Frequencies of a Mid-Plane Tapered Composite Beam with Different Taper Angles Obtained Using the Conventional Formulation

As might be expected, the taper angle of two degrees gives the lowest values of the natural frequencies. The taper angles of six degrees, and ten degrees give the successively higher values.

The change in the taper angle affects directly the entries of the element stiffness matrix. Generally speaking, the higher the taper angle is, the higher the values of the natural frequencies are. It is recalled from equations 2.45-2.48 that the stiffness matrix is

a function of (the slope) the taper, and they are in direct proportions (check equation 2.48). Hence, higher taper angle leads to a stiffer laminate, which eventually leads to higher values of the natural frequencies (the mass matrix is not mentioned here because its coefficients are not function of the taper angle in the conventional formulation). This effect is similar to the effect of the change in the fiber orientations. The change in the fiber orientations affects the flexural rigidity of the laminate, and hence the element stiffness matrix.

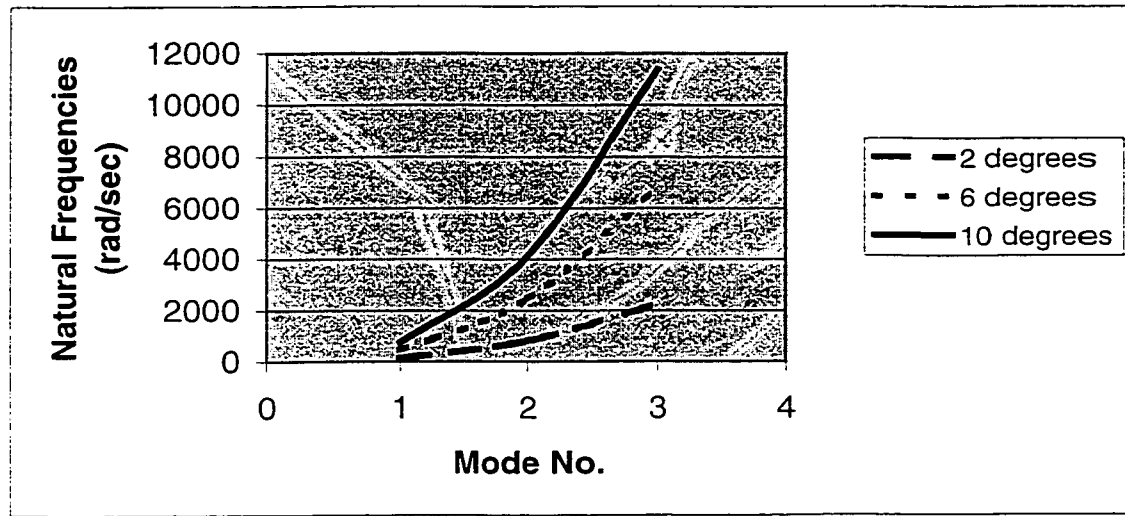


Figure 4.22 The Variations of the Natural Frequencies of a Mid-Plane Tapered Composite Beam with Different Taper Angles Obtained Using the Advanced Formulation

Using the advanced formulation, the results for the lowest three natural frequencies with a taper angle of 6 degrees are obtained to be: 448.02, 2463.51, and 6772.01 rad./sec., respectively. For a taper angle of two degrees they are: 148.00, 815.75, and 2238.35 rad./sec., respectively, and finally for a taper angle of ten degrees

the results are: 752.40, 4135.18, and 11372.17 rad./sec., respectively. The results are plotted in Figure 4.22.

As shown in Figure 4.22, the taper angle of two degrees leads to the lowest values of the natural frequencies, the ten-degree taper angle gives the highest values, and the taper angle of six degrees gives moderate values between that of the other two taper angles.

It was mentioned before that the taper angle affects the calculations of the coefficients of the element stiffness and mass matrices. By examining the stiffness and mass matrices, it is found that the taper angle exists in the numerators and denominators of the coefficients of the matrices, but with different powers. Hence, one cannot establish explicit relationships between the taper angle and the matrices. Nevertheless, the results show that the taper angle is directly proportional to the stiffness matrix and is inversely proportional to the mass matrix. Hence, the higher the taper angle is, the stiffer the laminate becomes, and the smaller the laminate inertia is. It is recalled from vibration analysis that the dynamic matrix $[a]$ is equal to the product of the inverse of the mass matrix and the stiffness matrix. Hence, higher values of these matrices will lead to higher values of the coefficients of the dynamic matrix. Accordingly, this will result in higher eigenvalues, and it is known that the natural frequencies are the square root values of these eigenvalues.

Figure 4.23 is given below to show the comparison between the results obtained using the conventional and advanced formulations.

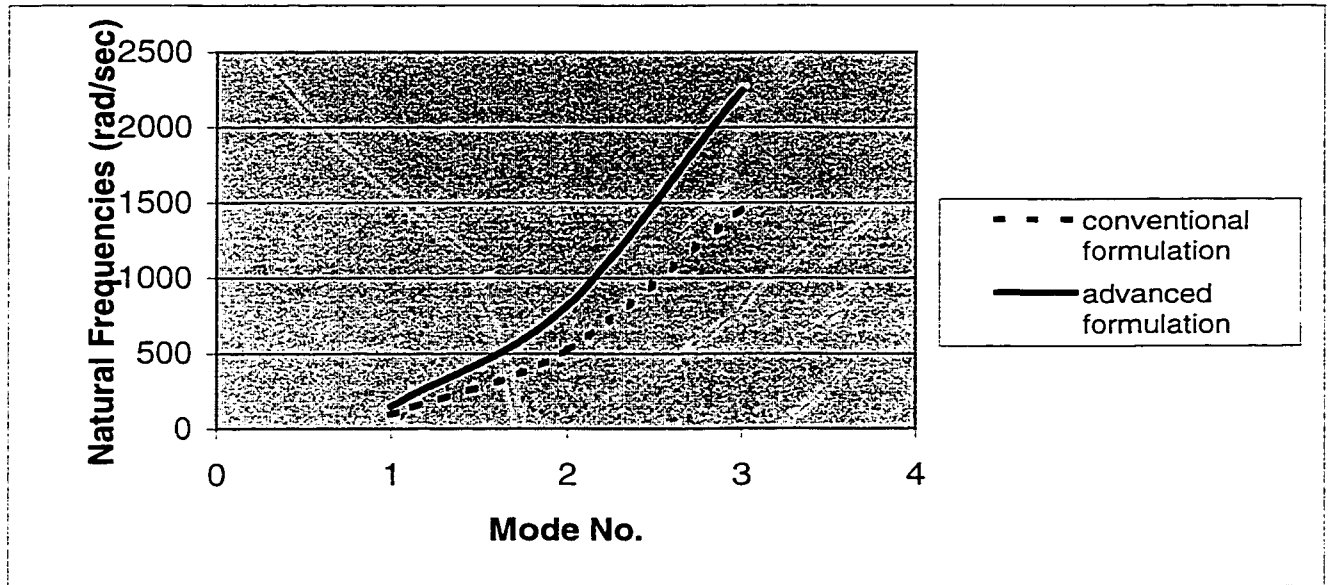


Figure 4.23 Comparison Between the Natural Frequencies Obtained Using Conventional and Advanced Formulations for Mid-Plane Tapered Composite Beam with Two Degrees Taper Angle

Figure 4.23 shows that the values of the natural frequencies obtained using the advanced formulation are higher than the corresponding values obtained using the conventional formulation (almost 1.6 higher). The possibilities of this considerable difference between the two sets of the results were discussed before. In any case, the solution obtained using the advanced formulation is still keeping the inherent relationships between the taper angle and the values of the natural frequencies (that they are in direct proportions).

Table 4.6 Comparison Between the Natural Frequencies for Different Taper Angles for a Fixed-Free Mid-plane Composite Beam Obtained Using the Conventional and Advanced Formulations

Taper Angle (in degrees)	Formulation Method					
	Conventional Formulation			Advanced Formulation		
	Mode No.			Mode No.		
	1	2	3	1	2	3
2	93.19	522.43	1460.14	148.00	815.75	2238.35
6	280.28	1571.24	4391.50	448.02	2463.51	6772.01
10	470.18	2635.82	7366.93	752.40	4135.18	11372.17

It is worth noting that selecting the appropriate value of the taper angle is a challenging task for the finite element analyst. As it can be seen that increasing the taper angle from two degrees to six will triple the values of the natural frequencies, and that increasing the taper angle from six degrees to ten will increase the values of the natural frequencies by almost 67 % in both methods of formulation. The last two observations show consistency of the solutions obtained using both the methods of formulation, which is verification in itself. Table 4.6 above summarizes the results mentioned in this section.

4.3.4 The Effect of Different Discretizations on the Natural Frequencies Obtained Using Conventional Formulation

The beam elements will be meshed into four different types, A, B, C, and D as it was done in section 4.2.3. Also, the beam type of support is fixed-free and the laminate configuration is cross-ply.

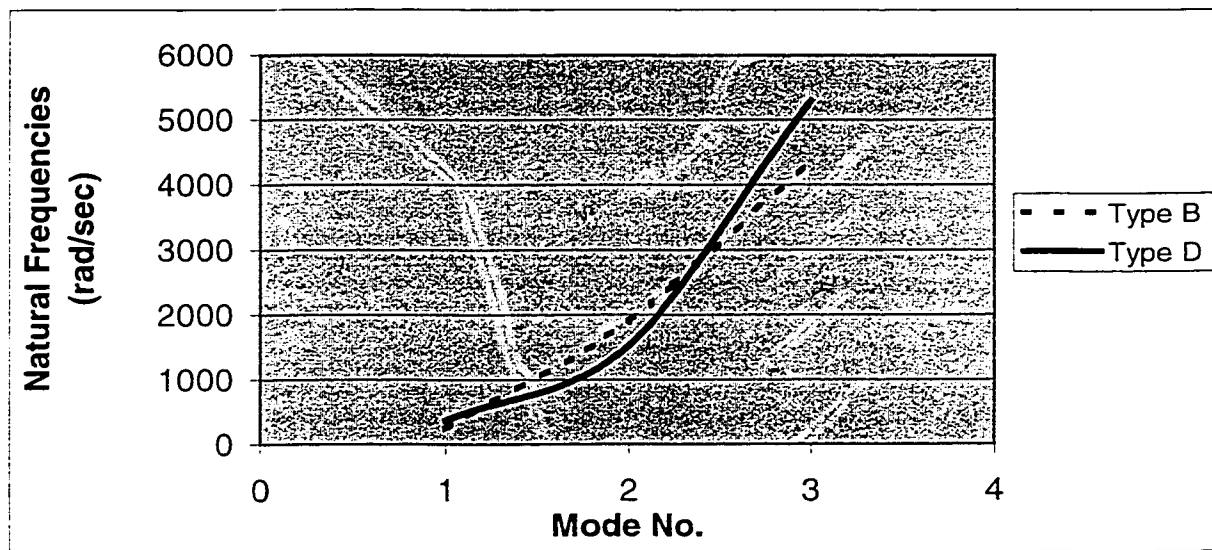


Figure 4.24 The Variations in the Natural Frequencies for Beam Meshes Type B and Type D of a Mid-plane Tapered Composite Beam Obtained Using Conventional Formulation

First, *using the conventional formulation*, the lowest three natural frequencies for Type A mesh of the beam ($L/3$, $L/3$, and $L/3$) are obtained as: 280.28, 1571.24, and 4391.50 rad./sec., respectively. For Type B mesh of the beam ($L/4$, $L/2$, and $L/4$) they are: 241.37, 1907.42, and 4353.84 rad./sec., respectively. For Type C mesh of the beam

($L/4$, $L/4$, and $L/2$) they are: 222.80, 1493.03, and 4476.80 rad./sec., respectively, and for Type D mesh of the beam ($L/2$, $L/4$, and $L/4$) they are: 369.26, 1526.39, and 5290.78 rad./sec., respectively. The results for Type B and Type D meshes are plotted in Figure 4.24, and plotted in Figure 4.25 for Type A and Type C meshes.

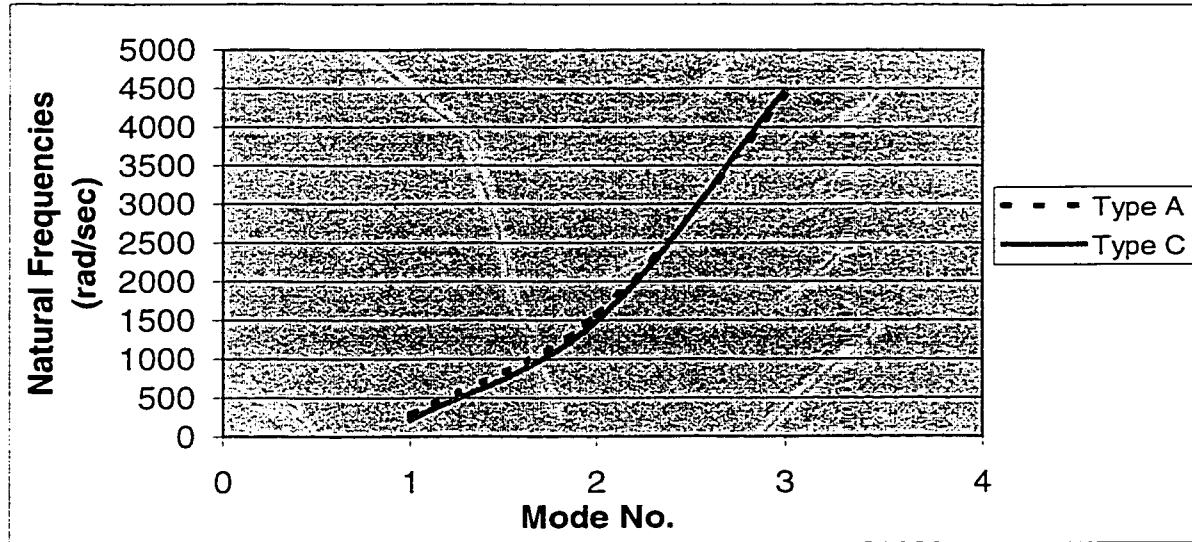


Figure 4.25 The Variations in the Natural Frequencies for Beam Meshes Type A and Type C of a Mid-plane Tapered Composite Beam Obtained Using Conventional Formulation

The beam division with nodes at lengths $L/4$, $L/4$, and $L/2$ gives the lowest values of the natural frequencies in the first and second modes, whereas dividing the beam with nodes at lengths $L/4$, $L/2$, and $L/4$ has the lowest value in the third mode.

The beam discretization has its direct effect on the coefficients of the element mass and stiffness matrices, as it was explained in section 4.2.3. Its direct effect on the

coefficients of the element matrices is same as in the case of the taper angle (check section 4.3.3).

Table 4.7 The Natural Frequencies for Different Beam Meshes Obtained Using Conventional Formulation

Discretization type	Conventional Formulation		
	Mode No.		
	1	2	3
Type A	280.28	1571.24	4391.50
Type B	241.37	1907.42	4353.84
Type C	222.80	1493.03	4476.80
Type D	369.26	1526.39	5290.78

Due to the huge volume of the stiffness and mass matrices, it is difficult to endeavor different beam discretizations. It was relatively easy to work out the previous changes in the last three sub-sections because the beam element length was fixed at 0.36 m . This simplified the size of the matrices significantly in the Maple software, which made it possible to process it in the MATLAB environment. Accordingly, Table 4.7 above shows the change of the values of the natural frequencies for a mid-plane fixed-free composite beam with a taper angle of 6 degrees using the conventional formulation only.

4.4 Parametric Study on the Buckling of Externally Tapered Composite beams

A externally tapered simply supported composite beam with the same mechanical properties and geometric description given in section 4.2 is considered and its critical buckling loads (the buckling load is equal to the lowest eigenvalue) for different fiber orientations are determined. The procedures employed to obtain this eigenvalue are well explained in chapter 2 section 2.7.1.3. The critical buckling load will be obtained using both the methods of formulation, conventional and advanced.

First, *using the conventional formulation*, the critical buckling load for cross-ply laminate with $[0/90]_s$ ply groups is calculated to be 9.02×10^6 N. For the laminate configuration with $[\pm 45]_s$ ply groups it is 5.03×10^6 N, and for the laminate configuration with $[\pm 15]_s$ ply groups, it is 1.46×10^7 N. These results are plotted in Figure 4.26 below (the cross-ply is given number 1 on the abscissa, the laminate configuration with $[\pm 45]_s$ ply groups is given number 2 and the laminate configuration with $[\pm 15]_s$ ply groups is given number 3). As shown in the figure, the laminate configuration with $[\pm 45]_s$ ply groups gives the lowest value of the critical buckling load while the laminate configuration with $[\pm 15]_s$ ply groups gives the highest value.

In buckling analysis, the geometric stiffness matrix affects the whole stiffness of the laminate, as shown in equation 4.3 below:

$$O = [K - n]\{u_i\} \quad (4.3)$$

It is recalled from section 4.2.1.2 that the change in the fiber orientations affects the flexural rigidity (check Figure 4.5), and it is found that the $[\pm 45]_s$ stacking sequence leads to the lowest flexural rigidity whilst the stacking sequence $[\pm 15]_s$ leads to the highest. By examining the geometric stiffness matrix (equation 3.54), one can find that most of its coefficients have the term of the flexural rigidity (bD_{II}) in their denominators (in some of them it is squared). Hence, a higher value of bD_{II} will lead to lower values of the coefficients of the geometric stiffness matrix, i.e. stiffer laminates. Consequently, this reduction in geometric stiffness will result in the highest value of the critical buckling load as obtained in the case of $[\pm 15]_s$ stacking sequence.

Using the advanced formulation, the critical buckling load for cross-ply laminate $[0/90]_s$ is calculated to be 9.00×10^6 N. For the laminate configuration with $[\pm 45]_s$ ply groups it is 5.02×10^6 N, and for the laminate configuration with $[\pm 15]_s$, ply groups it is 1.45×10^7 N. These results are plotted in the same Figure 4.26 below. The figure shows that the laminate configuration with $[\pm 45]_s$ ply groups gives the lowest value of the critical buckling load while the laminate configuration with $[\pm 15]_s$ ply groups gives the highest value as it was the case in the conventional formulation.

The results obtained using the advanced formulation are lower than the results obtained using the conventional formulation, which was proved before in chapter 2. This was considered as an indication of its higher accuracy. As the results are not very clear in Figure 4.13 because the Excel[®] software can not show clearly a difference in this order, they are given again in Table 4.8.

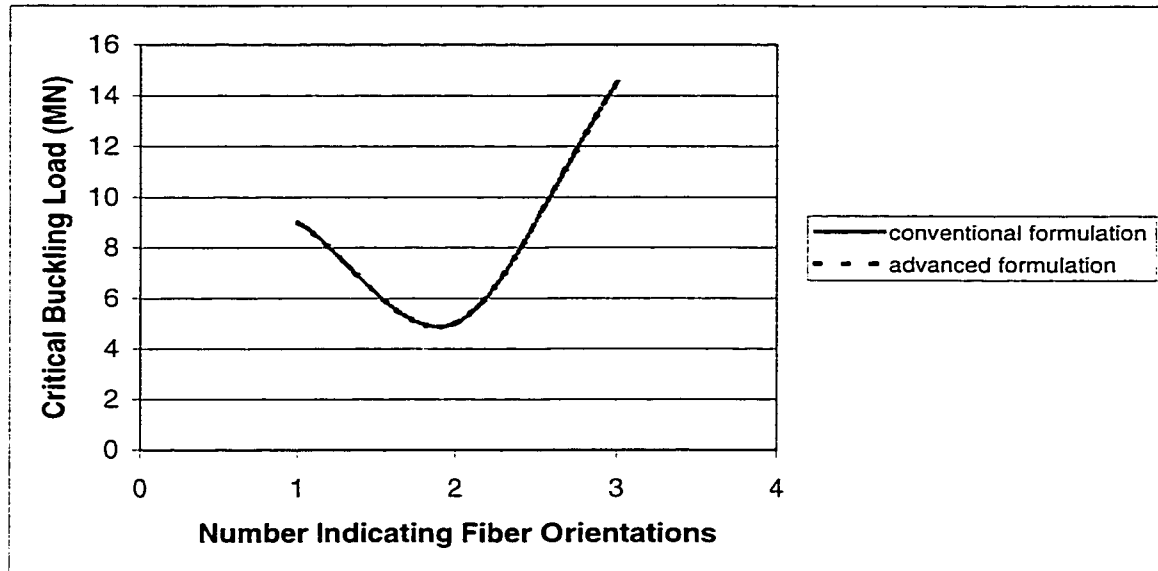


**Figure 4.26 The Critical Buckling Loads for Different Fiber Orientations
Obtained Using the Conventional and Advanced Formulations**

**Table 4.8 The Critical Buckling Load for an Externally Tapered Composite
Beam for Different Fiber Orientations Obtained Using Conventional and Advanced
Formulations**

Formulation Method	Critical Buckling Load in MN		
	$[0/90]_s$ ply groups	$[\pm 45]_s$ ply groups	$[\pm 15]_s$ ply groups
Conventional Formulation	9.02	5.03	14.55
Advanced Formulation	9.00	5.02	14.52

4.5 Overall Conclusions and Discussion

In this sub-section, a comparative study on both types of taper is to be introduced as a guide for the designer to see how the type of taper and the different changes on each of them can contribute in the dynamic analysis.

In Figure 4.27 below is a comparison between the two types of taper for the same boundary condition (fixed-free), the same laminate configuration (cross-ply), and the same beam discretization (elements with equal lengths) using the conventional formulation. In other words, the only difference is the type of taper.

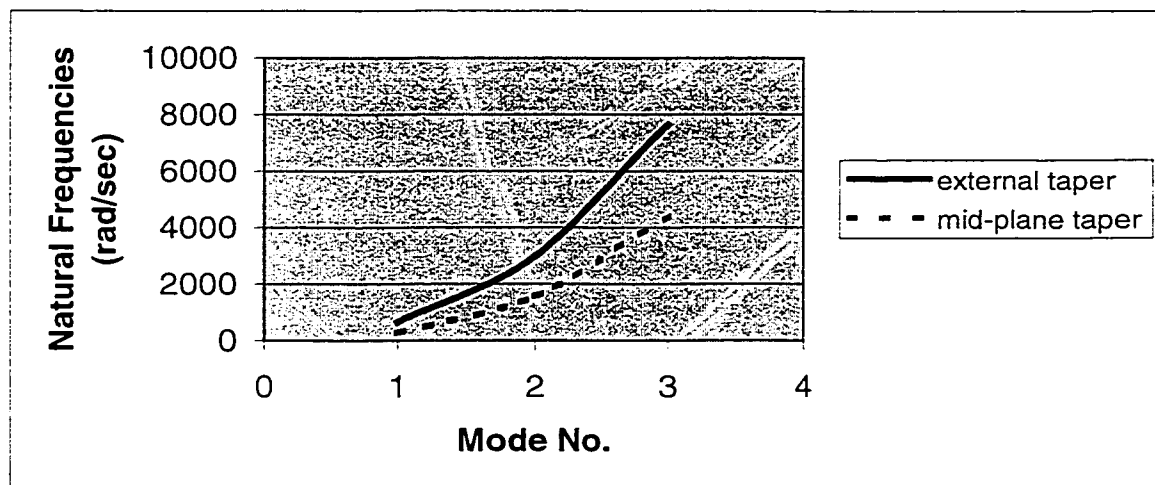


Figure 4.27 The Variations in the Natural Frequencies for External and Mid-Plane Tapered Composite Beams Obtained Using Conventional Formulation

As it is shown in Figure 4.27, the mid-plane type of taper gives lower values of the natural frequencies (this is regardless of the type of support or the fiber orientations).

So from the dynamic analysis point of view the mechanical designer will lean to this type of taper, and for the final decision he or she has to consider the stress and manufacturing aspects.

From the last four sections, one can come up with following important conclusions to help the designer and finite element analyst to choose between different methods of formulation, between different types of taper, and among different configurations of the composite beam within the same method of formulation and the same type of taper:

- 1) The advanced formulation developed in this thesis is of higher efficiency than the conventional formulation. In finite element modeling terms, the inclusion of the natural and essential boundary conditions can lead to more accurate solutions, where the eigenvalues obtained converge rapidly to the exact solution. Accordingly, this will save the finite element analyst a lot of time, and hence effort. Generally speaking, more accurate results are obtained using fewer numbers of elements that have more degrees of freedom than using more number of elements that have fewer degrees of freedom.
- 2) Use of fewer elements in the mesh leads to a better continuity of higher-order derivatives of deflection W . This in turn results in a more accurate calculation of stress and strain distributions in the beam cross-section, and in individual plies.
- 3) The results of the natural frequencies for externally tapered composite beams are always higher than their corresponding values for mid-plane tapered composite beams, regardless of the method of formulation applied.

- 4) Regarding the type of support, the free-fixed type gives the lowest values of the natural frequencies, and the fixed-fixed type gives the highest of them for external type of taper. For mid-plane taper, free-fixed type gives the lowest value of the natural frequency in the first mode, whereas the fixed-free type does this in the second and third modes.
- 5) Dividing the beam with nodes at lengths $L/4$, $L/4$, and $L/2$ lowers the values of the natural frequencies in the first mode, whereas the mesh with nodes at lengths $L/4$, $L/2$, and $L/4$ lowers them in the second and third modes, for external type of taper. For the mid-plane type of taper, dividing the beam with nodes at lengths $L/4$, $L/4$, and $L/2$ gives the lowest values of natural frequencies in all modes.
- 6) Regarding the fiber orientations, the laminate configuration with $[\pm 45]_s$ ply groups minimizes the values of the natural frequencies in both types of tapers. This means that the $[\pm 45]_s$ stacking sequence leads to stiffer laminates.
- 7) The higher the taper angle is in the mid-plane type of taper, the higher the values of the natural frequencies are.
- 8) The laminate configuration with $[\pm 15]_s$ ply groups gives the highest value of the critical buckling load, whereas the laminate configuration with $[\pm 45]_s$ ply groups gives the lowest.

4.6 Summary

In this chapter, a thorough parametric study on external and mid-plane tapered composite beams is conducted. The composite beams chosen are practical in terms of mechanical properties and geometric description. All the problems are solved using both the methods of finite element formulation, conventional and advanced.

The external type of taper is examined for all possible changes: changes in the boundary conditions, changes in the stacking sequences, and changes in the beam discretization. For each change, the results for the lowest three natural frequencies are obtained and plotted in figures to elaborate on the interpretations (this is done for free vibration analysis). The externally tapered beams were analyzed for their critical buckling loads for different fiber orientations using both the conventional and advanced formulations. The same changes were done for the mid-plane tapered composite beam, plus the changes in the taper angle. These figures are plotted once for the results obtained using conventional formulation, and again for the results obtained using the advanced formulation. Then concise interpretations are provided to elaborate on the relationships between these changes and the natural frequencies of the composite beams. This explanation covers all aspects in the problem. Also, a comparison between the results obtained using both the methods of formulation is done with the help of the figures. Each sub-section ends by a table that summarizes the results mentioned in it. In the last section overall conclusions are provided that serve for the design aspects.

Chapter 5

Conclusions and Recommendations

In the present thesis a finite element simulation for externally tapered and mid-plane tapered composite beams that can incorporate both of the vibration analysis and the buckling analysis is developed.

The formulation is employing the conventional finite element formulation. In the finite element model, two degrees of freedom per node are considered so as to satisfy the geometric boundary conditions, the displacement and the slope.

A new formulation consisting of a newly developed finite element modeling with efficient higher order basis (interpolation) functions is established. In the finite element model, four degrees of freedom per node are considered so as to satisfy all the boundary conditions, the geometric boundary conditions, the displacement and the slope, and the natural boundary conditions, the bending moment and the shear force. Accordingly, all the stiffness, geometric stiffness, and mass matrices are set up.

The MATLAB[®] program that can endeavor all kinds of problems regarding this concern is developed and explained. At the end of each formulation, a plenty of problems on free and forced vibration, and buckling problems are worked out along with

the validation of their results. The comparison between the conventional and the advanced formulations is inherent with all problems.

To elaborate on the analysis in the present thesis, a parametric study on both types of tapers using both types of formulations is performed.

This parametric study considers various changes in the composite laminates to demonstrate their influences on the natural frequencies and the buckling loads of the beams. These changes include the change in the boundary conditions, the change in the laminate configuration, the change in the element discretization, and the finally the change in the taper angle. The difference in the composite laminates' responses is remarkable for each change within the same type of taper. This difference becomes more obvious by switching to another type of taper.

The parametric study done here in this thesis is of major worth to the mechanical designer, who uses composite structures for designing under dynamic loading. It shows him or her the following important and principal conclusions: -

- 1) A finite element formulation with efficient higher order interpolation functions can satisfy the entire essential and natural boundary conditions of tapered composite beams. Thus, this element adequately represents all the physical interpretation involved in any combination of displacement, slope, bending moment, and shearing force.

- 2) The new method of formulation results in more accurate results using fewer number of elements. In other words, increasing the number of degrees of freedom with efficient higher order basis functions gives higher accuracy than using less number of degrees of freedom with the conventional interpolation functions.
- 3) In this thesis the designer is given the base of the choice of, first the type of taper that can be used. Moreover, within the specific type of taper, which boundary conditions can be applied on the structure, which laminate configuration will minimize the natural frequencies of the structure, which way of discretizing the beam element will affect the natural frequencies the most, and finally for mid-plane tapered composite beams, how one can compromise for the optimum value of the taper angle.
- 4) Above all, the mechanical designer has all the matrices necessary for the finite element formulation, all in symbolic form, well defined, and that hold good for all types of loading. This generalization will give him or her the capacity to apply whatever changes he or she sees more convenient for the application he or she is about to design.

The following recommendations may be considered in the future studies: -

- i) The finite element formulation with higher order basis functions obtained in the present thesis can be extended to the internal type of taper.
- ii) This advanced formulation can be applied to the stress analysis of tapered composite beams and plates.

- iii) The stiffness and mass matrices for mid-plane tapered composite beams obtained using the advanced formulation are huge in volume. So they can be modified to become handier by any suitable mathematical means.
- iv) Including the shear force as a degree of freedom in the interpolation functions is still facing some difficulty in processing it in the MATLAB program. It did not improve the accuracy for uniform beams, metallic and composite.
- v) The work can be extended to be applicable to damped free vibration cases.

References

- [1] Rayleigh, Lord, "*On the Vibration of an Infinite Plate of Homogenous Isotropic Elastic Matters*", Proceedings of London Mathematical Society, Vol. 20, 1889, pp. 225.
- [2] Timoshenko, S.P., "*On the Correction for Shear of the Differential Equation for Transverse Vibrations of Prismatic Bars*", Philosophical Magazine, Vol. 41, 1921, pp. 734-740.
- [3] J. Sutherland and L. Goodman, "*Vibrations of Prismatic Bars Including Rotary Inertia and Shear Corrections*", Illinois Report, Department of Civil Engineering, University of Illinois, Urbana, 1951.
- [4] Mindlin, R.D., "*Influence of Rotary Inertia and Shear on Flexural Motions of Isotropic Elastic Plates*", ASME Journal of Applied Mechanics, Vol. 18, 1951, pp.31-38.
- [5] Mindlin, R.D., "*Waves and Vibration in Isotropic Elastic Plates*", Proceedings of the 1st Symposium of Naval Structural Mechanics, 1960, pp. 199-232.
- [6] Mindlin, R.D., "*An Introduction to the Mathematical Theory of Vibrations of Elastic Plates*", U.S. Army Signal Corps, Fort Montmouth, N.J., 1955.
- [7] Mindlin, R.D., "*High Frequency Vibrations of Crystal Plates*", Quarterly of Applied Mathematics, Vol. 19, 1961, pp. 51-61.
- [8] Hearmon, R.F.S., "*The Frequency of Flexural Vibration of Rectangular Orthotropic Plates with Clamped or Supported Edges*", ASME Journal of Applied Mechanics, Vol. 26, 1959, pp. 536-540.

- [9] Toledane, A. and Murakani, H., "*A Composite Plate Theory for Arbitrary Laminated Configurations*", ASME Journal of Applied Mechanics, Vol. 54, 1987, pp. 181-189.
- [10] Yu, Y.Y., "*A New Theory of Elastic Sandwiches Plates-One-Dimensional Case*", Journal of Applied Mechanics, Vol.26, 1959, pp. 415-421.
- [11] Teoh, L.S. and C.C. Huang, "*The Vibration of Beams of Fiber Reinforced Material*", Journal of Sound and Vibration, Vol. 51, 1977, pp. 467-473.
- [12] Teh, K.K. and C.C. Huang, "*the Vibration of Generally Orthotropic Beams, a Finite Element Approach*", Journal of Sound and Vibration, Vol.62, 1979, pp. 195-206.
- [13] Abarcar, R.B. and P.F. Cunniff," *The Vibration of Cantilevered Beam of Fiber Reinforced Material*", Journal of Composite Materials, Vol. 6, 1972, pp. 504-516.
- [14] Crawely, E.F. and J. Dugundji, "*Frequency Determination and Non-Dimensionalization for Composite Cantilever Plates*", Journal of Sound and Vibration, Vol.72 (1), 1980, pp. 1-10.
- [15] Jensen, D.w. and Crawely, E.F., "*Frequency Determination Techniques for Cantilevered Plates with bending-Torsion Coupling*", AIAA Journal, Vol.22 (3), 1984, pp. 415-420.
- [16] Barbero, E.J. and J.N. Reddy, "*An Application of the Generalized Laminated Plate Theory to Delamination Buckling*", Proc. American Society for Composites, 4th Technical Conference, 1989, pp. 244-251.

- [17] Barbero, E.J. and J.N. Reddy, "*An Accurate Determination of Stresses in Thick Laminates Using A generalized Plate Theory*", Int. J. Numerical Methods in Engineering, Vol. 29, 1990, pp. 502-509.
- [18] Lu, X. and D. Liu, "*An Interlaminar Shear Stress Continuity Theory for Both Thin and Thick Composite Laminates*", J. of Applied Mechanics, Vol. 59, 1992, pp. 502-509.
- [19] Lee, C.Y. and D. Liu, "*An Interlaminar Stress Continuity Theory for Laminated Composite Analysis*", Computers and Structures, Vol. 42 (1), 1992, pp. 9-78.
- [20] Di Sciuva, M., "*Bending, Vibration, and Buckling of Simply Supported Thick Multilayered Orthotropic Plates: An Evaluation of a new Displacement Model*", J. Sound and Vibration, Vol. 105 pp. 425-442.
- [21] Salmon, E.H., "*Columns*", Oxford Technical Publications, London, 1921
- [22] Woinowsky-Krieger, S., "*Buckling Stability of Circular Plates with Circular Cylindrical Aelotropy*", (in German), Ingenieur-Archiv, Vol. 26, 1958, pp. 129-131.
- [23] Patel, S.A., and Broth, F.J., "*Axi-symmetric Buckling of Orthotropic Annular Plates*", AIAA Journal, Vol. 8, 1970, pp. 2102-2104.
- [24] Leissa, A.W., "*Buckling of Laminated Composite Plates and Shell Panels*", Air Force Wright Aeronautical Lab., AFWAL-TR-85-3069, 1985.
- [25] D. G. Liaw and T.Y. Yang, "*Symmetric and Asymmetric Dynamic Buckling of Laminated Thin Shells with the Effect of Imperfection and Damping*", Journal of Composite Materials, Vol. 24, 1990, pp. 188-207.

- [26] R. Courant, “*Variational Methods for the Solution of Problems of Equilibrium and Vibration*”, Bull. Am. Math. Soc., Vol. 49, 1943, pp. 1-43.
- [27] W. Prager and J.L. Synge, “*Approximation in Elasticity Based on the Concept of Function Space*”, Q.J. Applied Math., Vol. 5, 1947, pp. 241-269.
- [28] J. Argyris, “*Energy Theorems and Structural Analysis*”, Aircraft Engineering, Vol. 26, 1954, pp. 410-422.
- [29] M.J. Turner, R.W. Clough, R.W. Martin, and L. Topp, “*Stiffness and Deflection Analysis of Complex Structures*”, Journal of Aeronautical Sciences, Vol. 25, 1956, pp. 805-823.
- [30] J. Thomas, “*Vibration Characteristics of Tapered Cantilever Beams*”, Ph.D. Thesis, University of London, 1968.
- [31] J.S. Amirtharajah, M.A.Sc. Thesis, Concordia University, Montreal, Canada, “*Critical Speeds and Unbalance Response of Cantilever-Sleeve Rotors Using Finite Elements with Efficient Higher Order Basis Functions*”, 1999.
- [32] R.D. Cook, D.s. Malkus and M.E. Plesha, “*Concepts and Applications of Finite Element Analysis*”, 1989, 3rd edition, John Wiley & Sons, New York.
- [33] E.C. Pestel, Proceeding of Conference on matrix methods in structural mechanics, Wright Patterson Air Force Base, Ohio, U.S.A., October 1965.
- [34] I. Fried, “*Discretization and Computational Errors in High-Order Finite Element*”, American Institute of Aeronautics and Astronautics Journal, Vol. 9, 1971, pp. 2071-2073.
- [35] C.T. Sun and S.N. Huang, “*Transverse Impact Problems by High-order Beam Finite Element*”, Vol. 5, 1975, pp. 297-303.

- [36] J. Thomas and E. Dokumaci, "*Improved Finite Elements for Vibration Analysis of Tapered beam*", Aeronautical Quarterly, Vol. 24, 1973, pp. 39-46.
- [37] C.W.S. To, "*Higher Order Tapered beam Finite Elements for Vibration Analysis*", Journal of Sound and Vibration, Vol. 63 (972), 1979, pp. 33-50.
- [38] J. Thomas and B.A.H. Abbas, "*Finite Element Model for Dynamic Analysis of Timoshenko Beam*", Journal of Sound and Vibration, Vol. 41 (3), 1975, pp. 291-299.
- [39] J.E. Akin, "*Application and Implementation of Finite Element Methods*", Academic Press, London, 1982.
- [40] A. Houmat, "*Vibrations of Timoshenko Beams by Variable order Finite Elements*", Journal of Sound and Vibration, Vol. 187, 1995, pp. 841-849.
- [41] Y.C. Hou, C.H. Tseng, and S.F. Ling, "*A New High-Order Non-Uniform Timoshenko Beam Finite Element on Variable Two-Parameter Foundations for Vibration Analysis*", Journal of Sound and Vibration, Vol. 191, 1996, pp. 91-106.
- [42] R. Ganesan, J.A. Selliah, and R.B. Bhat, "Finite Element with Efficient Basis Functions for Vibration Analysis of Structures", 17th Canadian Congress of Applied Mechanics, CANCAM 99, pp. 299-302.
- [43] Yang, T.Y., "*Finite Element Analysis of Structures*", 1st edition, 1985.
- [44] James, M.L., Smith, G.M., Welford, J.C., and Whaley, P.W., "*Vibration of Mechanical and structural systems*", 1989, New York: Harper & Row.
- [45] George J. Simitses, "*An introduction to the elastic stability of structures*", 1976, Englewood Cliffs, N.J. Prince-Hall.

- [46] Rieger, N.F. and McCallion H., "*The Natural Frequency of Portal Frames, I*", International Journal of mechanical Sciences, Vol. 7, 1965, pp. 253-276.
- [47] Timoshenko, S.P., and James M. Gere, "*Theory of Elastic Stability*", 2nd edition, 1961, New York, McGraw-Hill.
- [48] Mario Paz, "*Structural Dynamics, Theory and computation*", 3rd edition, 1991, New York, Van Nostrand Reinhold.
- [49] Klaus-Jürgen Bathe, "*Finite Element Procedures in Engineering Analysis*", c1996, Englewood Cliffs, N.J. Prince-Hall.
- [50] Vinson, J.R. and Sierakowski, R.L., "*The behavior of Structures Composed of Composite Materials*", 1986, The Hague, Boston: M. Nijhoff.
- [51] James M. Whitney, "*Structural Analysis of Laminated Anisotropic Plates*", c1987, Lancaster, Pa., U.S.A.: Technomic Pub. Co.
- [52] Kim, Duk-Hyun, "*Composite Structures for Civil and Architectural Engineering*", 1st edition, 1995, London; New York: E & FN Span.
- [53] Reddy, J.N., "*An Introduction to the Finite Element Method*", 1993, 2nd edition, McGraw-Hill. Inc. New York.
- [54] Reddy, J.N. and Miravete, A., "*Practical Analysis of Composite Laminates*", c1995, Boca Raton, Fla.: CRC Press.
- [55] Clough Penzien, "*Dynamics of Structures*", c1993, 2nd edition, New York, McGraw-Hill.
- [56] K. He, S.V. Hoa, and R. Ganesan, "*The Study of Tapered Laminated Composite Structures: a Review*", Composites Science and Technology (In Press).

- [57] Isaac M. Daniel and Ori Ishai, “*Engineering Mechanics of Composite Materials*”, 1994, New York, Oxford University Press.

APPENDIX I

A PROGRAM FOR FREE-VIBRATION ANALYSIS OF VARIABLE THICKNESS COMPOSITE
BEAMS

```
fprintf(' FIXED-FREE BEAM UNDAMPED FREE VIBRATION CASE FOR EXTERNAL TAPERED  
COMPOSITE STRUCTURE(NCT-301 graphite/epoxy USING SIX DEGREE OF FREEDOM  
MODEL)\n\n\n')
```

```
LMAS=2;  
ICAS=3;  
if ICAS==1  
    fprintf(' THIS DATA IS FOR TRUSS')  
end  
if ICAS==2  
    fprintf(' THIS DATA IS FOR GENERAL FRAME')  
end  
if ICAS==3  
    fprintf(' THIS DATA IS FOR FRAME WITH INFINITE AXIAL STIFFNESS')  
end  
if LMAS==1  
    fprintf(' LUMPED MASS MATRIX,')  
end  
if LMAS==2  
    fprintf(' CONSISTENT MASS MATRIX,')  
end
```

% READING AND PRINTING OF AXIAL FORCE

```
P=0;  
p=0;  
r=0;  
alfa=0;  
s=r/(1+alfa);  
  
if p==0 & P~=0  
    fprintf('\n AND CONSTANT AXIAL FORCE ONLY OF VALUE = %4.1f\n\n',P)  
end  
  
if P==0 & p~=0  
    fprintf('\n AND VARIABLE AXIAL FORCE ONLY OF VALUE = %4.1f\n\n',p)  
end  
if p==0 & P==0  
    fprintf('\n AND NO AXIAL FORCE\n\n')  
end  
if p~=0 & P~=0  
    fprintf('\n ,CONSTANT AXIAL FORCE = %4.1f, AND VARIABLE ONE = %4.1f\n\n',P,p)  
end
```



```

TP=0.0005;
LOB=1.08;
WID=1;
ROW=1480;

% THE MATERIAL PROPERTIES OF THE COMPOSITE BEAM

E1=113.9e9;
E2=7.985e9;
NU12=0.288;
NU21=0.018;
G12=3.137e9;
GG=G12;
Q11=E1/(1-(NU12*NU21));
Q33=GG;
Q12=Q11*NU21;
Q21=(NU12*E2)/(1-(NU12*NU21));
Q22=E2/(1-(NU12*NU21));
Q=[Q11,Q12,0;Q21,Q22,0;0,0,Q33];

% ENTERING THE ORIENTATION AND CALCULATING THE TRANSFORMED STIFFNESS
MATRIX

for II=1:2:100
    J=II+1;
    aTHETA(II)=pi/2;
    aTHETA(J)=0;
end

% ENTERING THE NUMBER OF PLIES FOR EACH ELEMENT

NPP(1)=100;
NPP(2)=80;
NPP(3)=60;

NELE=3;
fprintf('  NUMBER OF ELEMENTS= %1.0f\n',NELE)

NNOD=NELE+1;
fprintf('  NUMBER OF NODES= %1.0f\n',NNOD)

NMOD=3;
fprintf('  NUMBER OF MODES TO BE PRINTED= %1.0f\n\n',NMOD)

% BOUNDARY CONDITION FOR u DISPLACEMENT IN x DIRECTION WHICH THE FIRST
NUMBER IN THE BRACKETS REFERS TO WHAT NODE AND "1" REFERS TO x-DIRECTION

```

```

for I=1:NNOD

IBOU(I,1)=0;
end

% BOUNDARY CONDITION FOR v DISPLACEMENT IN y DIRECTION THE SAME AS FOR THE
PREVIOUS DIRECTION

for I=2: NNOD
    IBOU(I,2)=1;
end
IBOU(1,2)=0;
%IBOU(NNOD,2)=0;
%IBOU(4,2)=1;

% BOUNDARY CONDITION FOR ROTATION "THETA" IN xy PLANE

for I=2: NNOD
    IBOU(I,3)=1;
end
IBOU(1,3)=0;
%IBOU(NNOD,3)=0;
%IBOU(1,3)=0;

% ENTERING THE x COORDINATE FOR EACH NODE

for I=1:NNOD
    XNOD(I)=(LOB/NELE)*(I-1);
end

% ENTERING THE y COORDINATE FOR EACH NODE

for N=1:NNOD;
    YNOD(N)=0;
end

fprintf('  NODE  BOUNDRY CONDITIONS          COORDINATES          MASSES\n')
fprintf('  NO.   1   2   3           X       Y           1       2       3\n')

for I=1:NNOD
    fprintf('      %1.0f      ',I)
    for J=1:3
        fprintf(' %1.0f      ',IBOU(I,J))
    end

    fprintf('      %5.3f      %5.3f      ',XNOD(I),YNOD(I))

% ENTERING THE CONCENTRATED MASSES

for J=1:3
    CMAS(I,J)=0;

```

```

fprintf('%3.1f    ',CMAS(I,J))
    end
fprintf('\n')
end

```

% REDING AND PRINTING OF ELEMENT DATA WHERE THE FIRST NUMBER IN THE BRACKETS OF "NODN" DENOTES THE ELEMENT NO. AND THE SECOND NO. DENOTES WHICH END; "1" FOR FIRST END, AND "2" FOR SECOND ONE

```

for I=1:NELE
    NODN(I,1)=I;
    NODN(I,2)=I+1;
end

```

```

%-----

```

```

%-----

```

% GENERATION OF NUMBERS FOR ASSEMBLING GLOBAL STIFFNESS AND MASS MATRICES

```

ICON=0;
for I=1:NNOD
    for J=1:3
        K=IBOU(I,J);
        if K~=0
            ICON= ICON+1;
            IBOU(I,J)=ICON;
        end
    end
end
NDOF=ICON;
fprintf('\n\n    NUMBER OF DEGREES OF FREEDOM = %1.0f\n\n',NDOF)

```

```

for I=1:NELE
    I1=NODN(I,1);
    I2=NODN(I,2);
    for J=1:3
        ICOR(I,J)=IBOU(I1,J);
        ICOR(I,J+3)=IBOU(I2,J);
    end
end

```

```

fprintf(' ELEMENT    NODAL DEGREES OF FREEDOM\n')

```

```

fprintf(' NUMBER    1    2    3    4    5    6\n\n')

```

```

for I=1: NELE
    fprintf(' %1.0f ',I);

```

```

for J=1:6
fprintf(' %1.0f',ICOR(I,J))
end
fprintf('\n')

end
%fprintf('\n\n ELEMENT   END NODES   AREA   WIDTH   HIEGHT   MASS
DENSITY\n')
%fprintf(' NO.      I      2\n\n')

% INTIALISING GLOBAL STIFFNESS AND MASS MATRICES TO ZERO

SMAS=zeros(NDOF,NDOF);
SYTF=zeros(NDOF,NDOF);

% SUBROUTINE ELEFREX FOR GENERATING TRANSFORMATION STIFFNESS AND MASS
MATRICES

for IE=1:NELE
NP=NPP(IE);
HT=TP;
A=zeros(3,3);
B=zeros(3,3);
D=zeros(3,3);
for I=1:NP
THETA=aTHETA(I);

M=cos(THETA);
N=sin(THETA);

QXX=((cos(THETA))^4*Q11)+((sin(THETA))^4*Q22)+(2*(cos(THETA))^2*(sin(THETA))^2*Q12)+(4
*(cos(THETA))^2*(sin(THETA))^2*Q33);
QYY=(N^4*Q11)+(M^4*Q22)+(2*M^2*N^2*Q12)+(4*M^2*N^2*Q33);
QXY=(M^2*N^2*Q11)+(M^2*N^2*Q22)+((M^4+N^4)*Q12)-(4*M^2*N^2*Q33);
QXS=(M^3*N*Q11)-(M*N^3*Q22)+(((M*N^3)-(M^3*N))*Q12)+(2*((M*N^3)-(M^3*N))*Q33);
QYS=(M*N^3*Q11)-(M^3*N*Q22)+(((M^3*N)-(M*N^3))*Q12)+(2*((M^3*N)-(M*N^3))*Q33);
QSS=(M^2*N^2*Q11)+(M^2*N^2*Q22)-(2*M^2*N^2*Q12)+(((M^2-N^2)^2)*Q33);

QT=[QXX,QXY,2*QXS;QXY,QYY,2*QYS;QXS,QYS,2*QSS];

% ENTERING THE PLY PARAMETERS AND CALCULATING THE LAMINATE STIFFNESS
MATRICES

HB=HT-TP;
A=A+(QT*(HT-HB));
B=B+(0.5*(HT^2-HB^2)*QT);
D=D+((1/3)*(HT^3-HB^3)*QT);
HT=HT+TP;

end

HEI=NP*TP;
FLRI=WID*D(1,1);
AXS=WID*A(1,1);
fprintf('\n\n')

```

```

%fprintf('\n    THE LAMINATE STIFNESSES MATRICES ARE: A B D\n')

%fprintf('\n\n    THE FLEXURAL RIGIDITY OF THE LAMINATE IS: %9.5f\n',FLRI)
%fprintf('\n\n    THE LAMINATE HEIGHT IS: %4.2f AND ITS WIDTH IS: %4.2f\n\n',HEI,WID)

fprintf('\n\n    ELEMENT NO.  NO.OF PLIES  LAM. WIDTH  LAM. THICK.  FLEXURAL
RIGIDITY\n')
fprintf('    %1.0f      %2.0f      %1.0f      %5.2e      %9.2e\n\n',IE,NP,WID,TP,FLRI)


AA=HEI*WID;

% GENERATION OF TRANSFORMATION MATRIX

I1=NODN(IE,1);
I2=NODN(IE,2);
X1=XNOD(I1);
X2=XNOD(I2);
Y1=YNOD(I1);
Y2=YNOD(I2);

% SUBROUTINE TRANMAT TO COMPUTE TRANSFORMATION MATRIX
% AL=LENGTH
% LMBD=COSINE OF THE ANGLE
% MU=SINE OF THE ANGLE

AL=sqrt((X2-X1)^2+(Y2-Y1)^2);
VOL=AA*AL;
LMBD=(X2-X1)/AL;
MU=(Y2-Y1)/AL;
T=zeros(6,6);
T(1,1)=LMBD;
T(2,1)=-MU;
T(1,2)=MU;
T(2,2)=LMBD;
T(3,3)=1.0;
T(4,4)=LMBD;
T(5,4)=-MU;
T(4,5)=MU;
T(5,5)=LMBD;
T(6,6)=1.0;

% GENERATION OF ELEMENT STIFFNESS MATRIX

if ICAS==3
    AXS=AXS*1e6;
end
if ICAS==1
    FLRI=0;
end

```

```
% SUBROUTINE ELESTF FOR ELEMENT STIFFNESS MATRIX
```

```
ESTF=zeros(6,6);
```

```
ESTF(1,1)=AXS/AL;
```

```
n(2,2)=(6*P/(5*AL))+p*(0.6+(s*(1.2-(36/(4+alfa)))+(72/(5+alfa))-(36/(6+alfa))));
```

```
n(5,5)=n(2,2);
```

```
n(5,2)=-n(2,2);
```

```
ESTF(2,2)=(12*FLRI/(AL^3))-n(2,2);
```

```
n(3,2)=(P/10)+p*AL*s*(0.1+(6/(3+alfa))-(30/(4+alfa))+(42/(5+alfa))-(18/(6+alfa)));
```

```
n(5,3)=-n(3,2);
```

```
ESTF(3,2)=(6*FLRI/(AL^2))-n(3,2);
```

```
n(3,3)=(2*P*AL/15)+p*AL^2*(0.1+(s*((2/15)-(1/(2+alfa)))+(8/(3+alfa))-(22/(4+alfa))+(24/(5+alfa))-  
(9/(6+alfa))));
```

```
ESTF(3,3)=(4*FLRI/AL)-n(3,3);
```

```
n(6,3)=(-P*AL/30)-p*AL^2*((1/60)+(s*((1/30)-(2/(3+alfa)))+(11/(4+alfa))-(18/(5+alfa))+(9/(6+alfa))));
```

```
ESTF(6,3)=(2*FLRI/AL)-n(6,3);
```

```
ESTF(4,1)=-ESTF(1,1);
```

```
ESTF(5,2)=-ESTF(2,2)-n(5,2);
```

```
n(6,2)=(P/10)+p*AL*(0.1+(s*(0.1-(12/(4+alfa)))+(30/(5+alfa))-(18/(6+alfa))));
```

```
n(6,5)=-n(6,2);
```

```
ESTF(6,2)=ESTF(3,2)-n(6,2);
```

```
ESTF(5,3)=-ESTF(3,2)-n(5,3);
```

```
ESTF(4,4)=ESTF(1,1);
```

```
ESTF(5,5)=ESTF(2,2)-n(5,5);
```

```
ESTF(6,5)=ESTF(5,3)-n(6,5);
```

```
n(6,6)=(2*P*AL/15)+p*AL^2*((1/30)+(s*((2/15)-(4/(4+alfa)))+(12/(5+alfa))-(9/(6+alfa))));
```

```
ESTF(6,6)=ESTF(3,3)-n(6,6);
```

```
for I=1:6
```

```
    K=I+1;
```

```
for J=K:6
```

```
    ESTF(I,J)= ESTF(J,I);
```

```
end
```

```
end
```

```
% TRANSFORMATION OF ELEMENT STIFFNESS MATRIX TO GLOBAL COORDINATES
```

```
% SUBROUTINE CONTRN FOR CONGRUENT TRANSFORMATION C=(TRANSPOSE A)*B*A
```

```
Z=zeros(6,6);
```

```
Z=Z+ESTF*T;
```

```
ESTT=zeros(6,6);
```

```
ESTT=ESTT+T*Z;
```

```
% COMPUTATION OF ELEMENT MASS MATRIX
```

```
% SUBROUTINE ELEMAS TO COMPUTE LUMPED OR MASS MATRIX OF A BEAM ELEMENT
```

```
EMAS=zeros(6,6);
```

```
if LMAS==2
```

```
    C1=(ROW*VOL)/6;
```

```
    C2=(ROW*VOL)/420;
```

```
    EMAS(1,1)=2*C1;
```

```

EMAS(4,1)=C1;
EMAS(4,4)=EMAS(1,1);
EMAS(2,2)=156*C2;
EMAS(3,2)=22*AL*C2;
EMAS(5,2)=54*C2;
EMAS(6,2)=-13*AL*C2;
EMAS(3,3)=4*C2*(AL^2);
EMAS(5,3)=-EMAS(6,2);
EMAS(6,3)=-3*C2*(AL^2);
EMAS(5,5)=EMAS(2,2);
EMAS(6,5)=-EMAS(3,2);
EMAS(6,6)=EMAS(3,3);
for I=1:6
    K=I+1;
    for J=K:6
        EMAS(I,J)=EMAS(J,I);
    end
end
else
    C1=(ROW*VOL)/2;
    EMAS(1,1)=C1;
    EMAS(2,2)=C1;
    EMAS(4,4)=C1;
    EMAS(5,5)=C1;
end
end

% SUBROUTINE CONTRN FOR CONGRUENT TRANSFORMATION C=(TRANSPOSE A)*B*A

E=zeros(6,6);
E=E+EMAS*T;
EMST=zeros(6,6);
EMST=EMST+T'*E;

% ASSEMBLING THE GLOBAL STIFFNESS AND MASS MATRICES

for I=1:6
    for J=1:6
        K=ICOR(IE,I);
        L=ICOR(IE,J);
        if (K*L)~=0
            SMAS(K,L)=SMAS(K,L)+EMST(I,J);
            SYTF(K,L)=SYTF(K,L)+ESTT(I,J);
        end
    end
end
end

% ADDIND OF NODAL CONCENTRATED MASSES TO GLOBAL MASS MATRIX

for I=1:NNOD
    for J=1:3
        K=IBOU(I,J);
        if K~=0
            SMAS(K,K)=SMAS(K,K)+CMAS(I,J);
        end
    end
end

```

```

end

% SUBROUTINE EIGZF FOR COMPUTATION OF EIGENVALUES AND EIGENVECTORS,
% ARRANGING THEM IN AN ASCENDING ORDER, AND CALCULATING FOR THE CIRCULAR
% FREQUENCIES

AR=inv(SMAS)*SYTF;

[V, Q]=eig(AR);

[LAMBDA,ITEM]=sort(diag(Q));

NEWV=V(:,ITEM);

fprintf(' \n NATURAL FREQUENCIES AND MODES\n\n')

for K=1 : NMOD
    if K<= NDOF

        ALAM=LAMBDA(K);
        OMEGA=sqrt(ALAM);
        FREQ=OMEGA/2*pi;

        fprintf('\n\n  %1.0f EIGENVECTOR AT EIGENVALUE = %9.4f,K,ALAM)
        fprintf(' CIRCULAR FREQUENCY = %7.2f\n\n',OMEGA)
        fprintf('  NODE      X-DISP      Y-DISP      ROTA\n')

        for L=1:NNOD
            fprintf('  %1.0f,L)
            for M=1 : 3
                DISN(M)=0;
                N=IBOU(L,M);
                if N~=0
                    DISN(M)=NEWV(N,K);

                end
                fprintf('      %9.6f,DISN(M))

            end
            fprintf('\n')

        end
    end
end

% SUBROUTINE ELESTF8 FOR ELEMENT STIFFNESS MATRIX IN THE ADVANCED
% FORMULATION

EST=zeros(10,10);

EST(1,1)=AXS/AL;
EST(6,1)=-EST(1,1);
EST(6,6)=EST(1,1);

```



```

EI=FLRI*10^-6;

EST(2,2)=280*EI/(11*AL^3);
EST(3,2)=140*EI/(11*AL^2);
EST(4,2)=1/22;
EST(5,2)=40/(33*AL);
EST(7,2)=-EST(2,2);
EST(8,2)=EST(3,2);
EST(9,2)=EST(4,2);
EST(10,2)=-EST(5,2);

EST(3,3)=600*EI/(77*AL);
EST(4,3)=8*AL/231;
EST(5,3)=379/462;
EST(7,3)=-EST(3,2);
EST(8,3)=380*EI/(77*AL);
EST(9,3)=5*AL/462;
EST(10,3)=-181/462;

EST(4,4)=2*AL^3/(3465*EI);
EST(5,4)=AL^2/(99*EI);
EST(7,4)=-EST(4,2);
EST(8,4)=-EST(9,3);
EST(9,4)=-AL^3/(4620*EI);
EST(10,4)=5*AL^2/(2772*EI);

EST(5,5)=50*AL/(231*EI);
EST(7,5)=-EST(5,2);
EST(8,5)=-EST(10,3);
EST(9,5)=-EST(10,4);
EST(10,5)=-AL/(462*EI);

EST(7,7)=EST(2,2);
EST(8,7)=-EST(3,2);
EST(9,7)=-EST(4,2);
EST(10,7)=EST(5,2);

EST(8,8)=EST(3,3);
EST(9,8)=EST(4,3);
EST(10,8)=-EST(5,3);

EST(9,9)=EST(4,4);
EST(10,9)=EST(4,5);

EST(10,10)=EST(5,5);

for M=1:10
    K=M+1;
    for J=K:10
        EST(M,J)=EST(J,M);
    end
end

% ENTERING THE GEOMETRIC STIFFNESS MATRIX

```



```

n=zeros(10,10);

a1=p*s/((7+f)*(8+f)*(9+f)*(10+f)*(11+f)*(12+f)*(13+f));
a2=p*s*AL*(1084+(1053*f)+(265*f^2)+(20*f^3))/((4+f)*(5+f)*(6+f)*(7+f)*(8+f)*(9+f)*(10+f)*(11+f)*(12+f)*(13+f));
a5=p*s*AL*(-3252+(851*f)+(48*f^2)+f^3)/((7+f)*(8+f)*(9+f)*(10+f)*(11+f)*(12+f)*(13+f));
a3=p*s*AL^3*(3+(4*f))/(EI*(6+f)*(7+f)*(8+f)*(9+f)*(10+f)*(11+f)*(12+f)*(13+f));
a4=p*s*AL^2*((10*f^2)+69+(75*f))/(EI*(5+f)*(6+f)*(7+f)*(8+f)*(9+f)*(10+f)*(11+f)*(12+f)*(13+f));
a6=p*s*AL^3*(f-1)/(EI*(7+f)*(8+f)*(9+f)*(10+f)*(11+f)*(12+f)*(13+f));
a7=p*s*AL^2*((f^2)+(40*f)-69)/(EI*(7+f)*(8+f)*(9+f)*(10+f)*(11+f)*(12+f)*(13+f));
a8=624*f+1200+463*f^2+10*f^4+125*f^3;

n(2,2)=(700*P/(429*AL))+(350*p/429)+(700*p*s/429)-(14112000*a1);
n(2,3)=(271*P/858)+(49*p*AL/429)+(271*p*AL*s/858)-(302400*a2);
n(2,7)=n(2,2);
n(2,8)=(271*P/858)+(173*p*AL/858)+(271*p*s*AL/858)+(840*a3);
n(2,4)=(-5*P*AL^2/(5148*EI))-(5*p*s*AL^3/(5148*EI))+(16800*a4);
n(2,5)=(23*P*AL/(858*EI))+(p*AL^2*(14+(69*s))/(2574*EI))-(100800*a5);
n(2,9)=(-5*P*AL^2/(5148*EI))-(5*p*AL^3*(s+1)/(5148*EI))-(8400*a6);
n(2,10)=(-23*P*AL/(858*EI))-(p*AL^2*(55+(69*s))/(2574*EI))-(3360*a7);

n(3,3)=(300*P*AL/1001)+(61*p*AL^2/286)+(300*p*s*AL^2/1001)-
(259200*p*s*a8*AL^2/((1+f)*(4+f)*(5+f)*(6+f)*(7+f)*(8+f)*(9+f)*(10+f)*(11+f)*(12+f)*(13+f)));
n(3,7)=n(2,3);
n(3,8)=(97*P*AL/6006)+(97*p*AL^2/12012)+(97*p*s*AL^2/6006)+(360*p*s*AL^2*(-46560-
(63720*f)+(15552*f^2)+(11602*f^3)+(1583*f^4)+(62*f^5)+(f^6))/((4+f)*(5+f)*(6+f)*(7+f)*(8+f)*(9+f)*
(10+f)*(11+f)*(12+f)*(13+f)));
n(3,4)=(-25*P*AL^3/(18018*EI))-
(p*AL^4*(301+(500*s))/(360360*EI))+(2880*p*s*AL^4/(EI*(3+f)*(4+f)*(5+f)*(6+f)*(7+f)*(8+f)*(9+f)*
(10+f)*(11+f)*(12+f)*(13+f)));
n(3,5)=(123*P*AL^2/(4004*EI))+(p*AL^3*(238+(369*s))/(EI*12012))-
(21600*p*s*AL^3*((20*f^4)+(1454*f)+(841*f^2)+(235*f^3)+2952)/(EI*(2+f)*(4+f)*(5+f)*(6+f)*(7+f)*(8+f)*(9+f)*(10+f)*(11+f)*(12+f)*(13+f)));
n(3,9)=(5*P*AL^3/(12012*EI))+(p*AL^4*(127+300*s)/(720720*EI))-
(360*p*s*AL^4*a8/(EI*(4+f)*(5+f)*(6+f)*(7+f)*(8+f)*(9+f)*(10+f)*(11+f)*(12+f)*(13+f)));
n(3,10)=(47*P*AL^2/(12012*EI))+(p*AL^3*(52+(141*s))/(36036*EI))-
(360*p*s*AL^3*(11280+(4752*f)+(6521*f^2)+(2148*f^3)+(215*f^4)+(4*f^5))/(EI*(4+f)*(5+f)*(6+f)*(7+f)*(8+f)*(9+f)*(10+f)*(11+f)*(12+f)*(13+f)));

n(4,4)=(P*AL^5/(90090*EI^2))+(p*AL^6*(7+(12*s))/(1081080*EI^2))-
(160*p*s*AL^6*(18+f+(2*f^2))/(EI^2*(5+f)*(6+f)*(7+f)*(8+f)*(9+f)*(10+f)*(11+f)*(12+f)*(13+f)));
n(4,5)=(-37*P*AL^4/(180180*EI^2))-
(p*AL^5*(133+(222*s))/(1081080*EI^2))+(240*p*s*AL^5*(888+(213*f)+(125*f^2)+(20*f^3))/(EI^2*(4+f)*(5+f)*(6+f)*(7+f)*(8+f)*(9+f)*(10+f)*(11+f)*(12+f)*(13+f)));
n(4,7)=n(2,4);
n(4,8)=(5*P*AL^3/(12012*EI))+(p*AL^4*(173+(300*s))/(720720*EI))-
(4*p*s*AL^4*((f^4)+5400+(51*f^3)+(986*f^2)-
(1104*f))/(EI*(6+f)*(7+f)*(8+f)*(9+f)*(10+f)*(11+f)*(12+f)*(13+f)));
n(4,9)=(-P*AL^5/(144144*EI^2))-
(p*AL^6*(1+(2*s))/(288288*EI^2))+(20*p*s*AL^6*((2*f^2)+18+f)/(EI^2*(6+f)*(7+f)*(8+f)*(9+f)*(10+f)*(11+f)*(12+f)*(13+f)));
n(4,10)=(-73*P*AL^4/(720720*EI^2))-
(p*AL^5*(110+(219*s))/(2162160*EI^2))+(4*p*s*AL^5*(1314+(39*f)+(169*f^2)+(4*f^3))/(EI^2*(6+f)*(7+f)*(8+f)*(9+f)*(10+f)*(11+f)*(12+f)*(13+f)));

```

```

n(5,5)=(73*P*AL^3/(18018*EI^2))+(p*AL^4*(91+(146*s))/(36036*EI^2))-
(14400*p*s*AL^4*(219+(49*f)+(35*f^2)+(5*f^3))/(EI^2*(3+f)*(5+f)*(6+f)*(7+f)*(8+f)*(9+f)*(10+f)*(11+f)*(12+f)*(13+f)));
n(5,7)=-n(2,5);
n(5,8)=(-47*P*AL^2/(12012*EI))-(p*AL^3*(89+(141*s))/(36036*EI))+(60*p*s*AL^3*(16920-
(5760*f)+(4959*f^2)+(1295*f^3)+(57*f^4)+(f^5))/(EI*(5+f)*(6+f)*(7+f)*(8+f)*(9+f)*(10+f)*(11+f)*(12+f)*(13+f)));
n(5,9)=(73*P*AL^4/(720720*EI^2))+(p*AL^5*(109+(219*s))/(2162160*EI^2))-
(120*p*s*AL^5*(219+(49*f)+(35*f^2)+(5*f^3))/(EI^2*(5+f)*(6+f)*(7+f)*(8+f)*(9+f)*(10+f)*(11+f)*(12+f)*(13+f)));
n(5,10)=(7*P*AL^3/(5148*EI^2))+(7*p*AL^4*(1+(2*s))/(10296*EI^2))-
(120*p*s*AL^4*(2940+(521*f)+(556*f^2)+(97*f^3)+(2*f^4))/(EI^2*(5+f)*(6+f)*(7+f)*(8+f)*(9+f)*(10+f)*(11+f)*(12+f)*(13+f)));

n(7,7)=n(2,2);
n(7,8)=-n(2,8);
n(7,9)=-n(2,9);
n(7,10)=-n(2,10);

n(8,8)=(300*P*AL/1001)+(173*p*AL^2/2002)+(300*p*s*AL^2/1001)-
(p*s*AL^2*(2592000+(806904*f)+(256966*f^2)+(31323*f^3)+(2017*f^4)+(69*f^5)+(f^6))/((7+f)*(8+f)*
(9+f)*(10+f)*(11+f)*(12+f)*(13+f)));
n(8,9)=(-25*P*AL^3/(18018*EI))-
(p*AL^4*(199+(500*s))/(360360*EI))+(p*s*AL^4*(12000+(1548*f)+(851*f^2)+(48*f^3)+(f^4))/(EI*(7+f)*
(8+f)*(9+f)*(10+f)*(11+f)*(12+f)*(13+f)));
n(8,10)=(-123*P*AL^2/(4004*EI))-
(p*AL^3*(131+(369*s))/(EI*12012))+(p*s*AL^3*((67*f^4)+(54612*f)+(20597*f^2)+(1763*f^3)+26568
0+(f^5))/(EI*(7+f)*(8+f)*(9+f)*(10+f)*(11+f)*(12+f)*(13+f)));

n(9,9)=(P*AL^5/(90090*EI^2))+(p*AL^6*(5+(12*s))/(1081080*EI^2))-
(2*p*s*AL^6*(48+(5*f)+(3*f^2))/(EI^2*(7+f)*(8+f)*(9+f)*(10+f)*(11+f)*(12+f)*(13+f)));
n(9,10)=(37*P*AL^4/(180180*EI^2))+(p*AL^5*(89+(222*s))/(1081080*EI^2))-
(p*s*AL^5*(1776+(233*f)+(116*f^2)+(3*f^3))/(EI^2*(7+f)*(8+f)*(9+f)*(10+f)*(11+f)*(12+f)*(13+f)));

n(10,10)=(73*P*AL^3/(18018*EI^2))+(p*AL^4*(55+(146*s))/(36036*EI^2))-
(2*p*s*AL^4*(17520+(3044*f)+(1211*f^2)+(64*f^3)+(f^4))/(EI^2*(7+f)*(8+f)*(9+f)*(10+f)*(11+f)*(12+f)*(13+f)));

for M=1:10
    K=M+1;
    for J=K:10
        n(J,M)=n(M,J);
    end
end

ESTF=zeros(10,10);
for I=1:10
    for J=1:10
        ESTF(I,J)=EST(I,J)-n(I,J);
    end
end

% TRANSFORMATION OF ELEMENT STIFFNESS MATRIX TO GLOBAL COORDINATES

```

```

% SUBROUTINE CONTRN FOR CONGRUENT TRANSFORMATION C=(TRANSPOSE A)*B*A

DDT=zeros(10,10);
DDT=DDT+ESTF*T;
ESTT=zeros(10,10);
ESTT=ESTT+T*DDT;

% COMPUTATION OF ELEMENT MASS MATRIX

% SUBROUTINE ELEMAS8 TO COMPUTE LUMPED OR MASS MATRIX OF A BEAM ELEMENT

EMAS=zeros(10,10);
if LMAS==2
    C1=(ROW*VOL)/6;
    C2=(ROW*VOL)/420;

EMAS(1,1)=2*C2;
EMAS(6,1)=C2;
EMAS(6,6)=EMAS(1,1);

EMAS(2,2)=72940*C2/429;
EMAS(3,2)=4530*AL*C2/143;
EMAS(7,2)=17150*C2/429;
EMAS(8,2)=-1905*AL*C2/143;
EMAS(4,2)=-383*AL^3*C2/(2574*EI);
EMAS(5,2)=1370*AL^2*C2/(429*EI);
EMAS(9,2)=521*AL^3*C2/(5148*EI);
EMAS(10,2)=775*AL^2*C2/(429*EI);

EMAS(3,3)=100*AL^2*C2/13;
EMAS(7,3)=-EMAS(8,2);
EMAS(8,3)=-1865*AL^2*C2/429;
EMAS(4,3)=-6*AL^4*C2/(143*EI);
EMAS(5,3)=245*AL^3*C2/(286*EI);
EMAS(9,3)=5*C2*AL^4/(156*EI);
EMAS(10,3)=995*C2*AL^3/(1716*EI);

EMAS(4,4)=C2*AL^6/(3861*EI^2);
EMAS(5,4)=-C2*AL^5/(198*EI^2);
EMAS(7,4)=-EMAS(9,2);
EMAS(8,4)=EMAS(9,3);
EMAS(9,4)=-7*C2*AL^6/(30888*EI^2);
EMAS(10,4)=-43*C2*AL^5/(10296*EI^2);

EMAS(5,5)=43*C2*AL^4/(429*EI^2);
EMAS(7,5)=EMAS(10,2);
EMAS(8,5)=-EMAS(10,3);
EMAS(9,5)=-EMAS(10,4);
EMAS(10,5)=131*C2*AL^4/(1716*EI^2);

EMAS(7,7)=EMAS(2,2);
EMAS(8,7)=-EMAS(3,2);
EMAS(9,7)=-EMAS(4,2);

```

```

EMAS(10,7)=EMAS(5,2);

EMAS(8,8)=EMAS(3,3);
EMAS(9,8)=EMAS(4,3);

EMAS(10,8)=-EMAS(5,3);

EMAS(9,9)=EMAS(4,4);
EMAS(10,9)=-EMAS(5,4);

EMAS(10,10)=EMAS(5,5);

for M=1:10
    I=M+1;
    for J=I:10
        EMAS(M,J)=EMAS(J,M);
    end
end
else
    C1=(ROW*VOL)/2;
    EMAS(1,1)=C1;
    EMAS(2,2)=C1;
    EMAS(6,6)=C1;
    EMAS(7,7)=C1;
end

%SUBROUTINE FORVNM FOR DETERMINING THE SYSTEM RESPONSE BY NEWMARK
METHOD

METH=1;
if METH==1
    fprintf('\n\n\n    FINDING THE DYNAMIC RESPONSE USING NEWMARK METHOD\n\n\n')

% ENTERING THE TIME STEP AND INTEGRATION CONSTANTS

DELTA=0.5;
ALFA=0.32;
fprintf('    DELTA = %3.1f\n    ALFA = %4.2f\n\n',DELTA,ALFA)
DT=0.01;
fprintf('\n    TIME STEP OF INTEGRATION = %4.2f\n\n',DT)
AO=1/(ALFA*(DT^2));
A2=1/(ALFA*DT);
A3=(1/(2*ALFA))-1;
A6=DT*(1-DELTA);
A7=DELTA*DT;

% FORMING THE EFFECTIVE STIFFNESS MATRIX

KHAT=SYTF+(AO*SMAS);

% ENTERING THE INITIAL FORCE DISPLACEMENT, VELOCITY VECTORS, AND
CALCULATING THE INITIAL ACCELARATION VECTOR

```

```

IR=[0;0;10000;0;0;0];
IU=zeros(NDOF,1);
IUDOT=zeros(NDOF,1);
EI=IR-(SYTF*IU);
IUDDOT=inv(SMAS)*EI;

% COUNTER FOR THE MATRICES
N=1;

% SETTING UP MATRICES THAT CONTAIN ALL THE VECTORS FOR ALL TIME STEPS

TDIS=zeros(NDOF,20);
TACC=zeros(NDOF,20);
TVEL=zeros(NDOF,20);

fprintf('\n    TIME    FORCING FUNCTION(lb)\n')

% FIXING THE TIME LIMIT FOR INTEGRATION
for TS= DT: DT: 20*DT

% ENTERING THE TOTAL FORCE VECTOR AS A FUNCTION OF TIME

    if TS<= 0.1
        F=10000;
    elseif TS > 0.1 & TS<=0.2
        F=(-100000*TS)+20000;
    else
        F=0;
    end
    if TS==DT | TS==0.09 | TS==20*DT
        fprintf('    %3.1f    %6.1f\n',TS,F)
    end
    plot(TS,F)

R=[0;0;F;0;0;0];

% CALCULATING THE EFFECTIVE LOADS

RHAT=R+(SMAS*((AO*IU)+(A2*IUDOT)+(A3*IUDDOT)));

% SOLVING FOR THE DISPLACEMENT, VELOCITY, AND ACCELERATION VECTORS

DIS=inv(KHAT)*RHAT;

ACC=(AO*(DIS-IU))-(A2*IUDOT)-(A3*IUDDOT);
VEL=IUDOT+(A6*IUDDOT)+(A7*ACC);

for J=1:NDOF
    TDIS(J,N)=DIS(J,1);
    TACC(J,N)=ACC(J,1);
    TVEL(J,N)=VEL(J,1);

```

```

    end
    IU=DIS;
    IUDDOT = ACC;
    IUDOT = VEL;
    N=N+1;
    end
    fprintf('\n\n      MAX DISPLAC.      MAX VELO.      MAX ACCEL.\n\n')

% SETTING UP VECTORS THAT HAVE THE MAXIMUM ABSOLUTE VALUES

MDIS=zeros(NDOF,1);
MACC=zeros(NDOF,1);
MVEL=zeros(NDOF,1);

for L=1:NDOF
    for K=1:20
        if abs(TDIS(L,K)) > MDIS(L,1)
            MDIS(L,1)= abs(TDIS(L,K));
        end

        if abs(TACC(L,K)) > MACC(L,1)
            MACC(L,1)= abs(TACC(L,K));
        end

        if abs(TVEL(L,K)) > MVEL(L,1)
            MVEL(L,1)= abs(TVEL(L,K));
        end
    end
    fprintf('  %lg      %8.4f      %8.4f      %8.4f\n',L,MDIS(L,1),MVEL(L,1),MACC(L,1))
end

else
% SUBROUTINE FORVWT FOR DYNAMIC RESPONSE

    fprintf('\n\n      THE DYNAMIC RESPONSE USING WILSON THETA METHOD\n\n\n')
    THETA=1.4;
    fprintf('      THETA = %3.1f\n',THETA)
    DT=0.01;
    fprintf('\n      TIME STEP OF INTEGRATION = %4.2f\n\n',DT)
    AO=6/(THETA*DT)^2;
    A1=3/(THETA*DT);
    A2=2*A1;
    A4=AO/THETA;
    A5=-A2/THETA;
    A6=1-(3/THETA);
    A7=DT/2;
    A8=(DT^2)/6;
    KHAT=SYTF+AO*SMAS;
    N=1;

% SETTING UP MATRICES THAT CONTAIN ALL THE VECTORS FOR ALL TIME STEPS

TDIS=zeros(NDOF,20);
TACC=zeros(NDOF,20);

```

```

TVEL=zeros(NDOF,20);
IU=zeros(NDOF,1);
IUDOT=zeros(NDOF,1);
IR=[0;0;10000;0;0;0];
EI=IR-(SYTF*IU);
IUDDOT=inv(SMAS)*EI;

fprintf('\n    TIME    FORCING FUNCTION(lb)\n')

    for TS= 0: DT: 20*DT
        M=TS+DT;

% ENTERING THE TOTAL FORCE VECTOR AS A FUNCTION OF TIME
        if TS<= 0.1
            F=10000;
        elseif TS > 0.1 & TS<=0.2
            F=(-100000*TS)+20000;
        else
            F=0;
        end
        if M<= 0.1
            FA=10000;
        elseif M > 0.1 & M<=0.2
            FA=(-100000*M)+20000;
        else
            FA=0;
        end
        if TS==0 | TS==0.1 | TS==0.2
            fprintf('    %3.1f    %6.1f\n',TS,F)
        end

        R=[0;0;F;0;0;0];
        RA=[0;0;FA;0;0;0];

        RHAT=(1-THETA)*R+(THETA*RA)+(SMAS*((AO*IU)+(A2*IUDOT)+(2*IUDDOT)));
        DITH=inv(KHAT)*RHAT;
        ACC=A4*(DITH-IU)+(A5*IUDOT)+(A6*IUDDOT);
        VEL=IUDOT+(A7*(ACC+IUDDOT));
        DIS=IU+(DT*IUDOT)+(A8*(ACC+(2*IUDDOT)));
        for J=1:NDOF
            TDIS(J,N)=DIS(J,1);
            TACC(J,N)=ACC(J,1);
            TVEL(J,N)=VEL(J,1);
        end
        IU=DIS;
        IUDDOT = ACC;
        IUDOT = VEL;
        N=N+1;
    end
    fprintf('\n\n        MAX DISPLAC.    MAX VELO.    MAX ACCEL.\n\n')

% SETTING UP VECTORS THAT HAVE THE MAXIMUM ABSOLUTE VALUES

MDIS=zeros(NDOF,1);

```



```

MACC=zeros(NDOF,1);
MVEL=zeros(NDOF,1);

for L=1:NDOF
    for K=1:20
        if abs(TDIS(L,K)) > MDIS(L,1)
            MDIS(L,1)= abs(TDIS(L,K));
        end

        if abs(TACC(L,K)) > MACC(L,1)
            MACC(L,1)= abs(TACC(L,K));
        end

        if abs(TVEL(L,K)) > MVEL(L,1)
            MVEL(L,1)= abs(TVEL(L,K));
        end
    end
    fprintf(' %1g    %8.4f    %8.4f    %8.4f\n',L,MDIS(L,1),MVEL(L,1),MACC(L,1))
end

end

% END OF THE PROGRAM

```

APPENDIX II

Simplified Derivation of Classical Laminate Theory

Basic Assumptions:

1. Each layer (lamina) of the laminate is quasihomogenous and orthotropic.
2. The laminate is thin with its lateral dimensions much larger than its thickness and is loaded in its plane only, i.e., the laminate and its layers (except for their edges) are in a state of plane stress ($\delta_z = \tau_{xz} = \tau_{yz} = 0$).
3. All displacements are small compared with the thickness of the laminate ($|u|, |v|, |w| \ll h$).
4. Displacements are continuous throughout the laminate.
5. In-plane displacements vary linearly through the thickness of the laminate, i.e., u and v displacements in the x - and y -directions are linear functions of z .
6. Transverse shear strains γ_{xy} and γ_{yz} are negligible. This assumption and the preceding one imply that straight lines normal to the middle surface remain straight and normal to that surface after deformation.
7. Strain-displacement and stress-strain relations are linear.
8. Normal distances from the middle surface remain constant, i.e., the transverse normal strain ϵ_z is negligible (compared with the in-plane strains ϵ_x and ϵ_y).
9. The analysis given here in this appendix is in brief, and is one-dimensional analysis. Ref. [57] has the derivation in detail.

Strain-Displacement Relations:

The xy plane equidistant from the top and bottom surfaces of the laminate and is called the reference plane. The reference plane displacements u_o and v_o in the x - and y -directions and the out-of-plane displacement W in the z -direction are functions of x and y only. For small displacements, the classical strain-displacement relations of elasticity yield:

$$\begin{aligned}\epsilon_x &= \frac{\partial u}{\partial x} = \frac{\partial u_o}{\partial x} - z \frac{\partial^2 W}{\partial x^2} \\ \epsilon_y &= \frac{\partial v}{\partial y} = \frac{\partial v_o}{\partial y} - z \frac{\partial^2 W}{\partial y^2} \\ \gamma_{xy} &= \frac{\partial u}{\partial y} + \frac{\partial v}{\partial x} = \frac{\partial u_o}{\partial y} + \frac{\partial v_o}{\partial x} - 2z \frac{\partial^2 W}{\partial x \partial y}\end{aligned}\tag{a}$$

Noting that the strain components on the reference plane are expressed as:

$$\begin{aligned}\epsilon_x^o &= \frac{\partial u_o}{\partial x} \\ \epsilon_y^o &= \frac{\partial v_o}{\partial y} \\ \gamma_{xy}^o &= \frac{\partial u_o}{\partial y} + \frac{\partial v_o}{\partial x}\end{aligned}\tag{b}$$

and the curvatures of the laminate are expressed as:

$$\begin{aligned}\kappa_x &= -\frac{\partial^2 W}{\partial x^2} \\ \kappa_y &= -\frac{\partial^2 W}{\partial y^2} \\ \kappa_{xy} &= -\frac{2\partial^2 W}{\partial x \partial y}\end{aligned}\tag{c}$$

Stress-Strain Relations of Layer within a Laminate:

Consider an individual layer p in a multidirectional laminate whose mid-plane is at a distance Z_p from the laminate reference plane. The stress-strain relations for this layer referred to the laminate coordinate system are:

$$\begin{bmatrix} \sigma_x \\ \sigma_y \\ \tau_{xy} \end{bmatrix}_p = \begin{bmatrix} Q_{xx} & Q_{xy} & Q_{xs} \\ Q_{xy} & Q_{yy} & Q_{sy} \\ Q_{xs} & Q_{sy} & Q_{ss} \end{bmatrix}_p \begin{bmatrix} \varepsilon_x \\ \varepsilon_y \\ \gamma_{xy} \end{bmatrix}_p\tag{d}$$

Substituting the expressions for the strains from equations (a), (b), and (c) one can get:

$$\begin{bmatrix} \sigma_x \\ \sigma_y \\ \tau_{xy} \end{bmatrix}_p = \begin{bmatrix} Q_{xx} & Q_{xy} & Q_{xs} \\ Q_{xy} & Q_{yy} & Q_{sy} \\ Q_{xs} & Q_{sy} & Q_{ss} \end{bmatrix}_p \begin{bmatrix} \varepsilon_x^0 \\ \varepsilon_y^0 \\ \gamma_{xy} \end{bmatrix}_p + z \begin{bmatrix} Q_{xx} & Q_{xy} & Q_{xs} \\ Q_{xy} & Q_{yy} & Q_{sy} \\ Q_{xs} & Q_{sy} & Q_{ss} \end{bmatrix}_p \begin{bmatrix} \kappa_x \\ \kappa_y \\ \kappa_{xy} \end{bmatrix}\tag{e}$$

Equations (a) and (c) show that the strains vary linearly through the thickness, but the stresses do not. Because of the discontinuous variation of the transformed stiffness matrix $[Q]_{x,y}$ from layer to layer, the stresses may also vary discontinuously from layer to layer. In many applications the stress gradient through the layer thickness is disregarded. The average stresses in each layer are determined by knowing the reference plane strains, ϵ' , the curvatures κ of the laminate, the location of the layer mid-plane Z_p , and its transformed stiffness matrix Q .

Force and Moment Resultants:

The stresses acting on a layer p of a laminate given by equation (e) can be replaced by resultant forces and moments as given below:

$$N_x^p = \int_{-t_p/2}^{t_p/2} \sigma_x dz \quad (f)$$

$$M_x^p = \int_{-t_p/2}^{t_p/2} \sigma_x z dz \quad (g)$$

In the case of a multi-layer laminate the total force and moment resultants are obtained by summing the effects for all layers. Thus, for the n -ply laminate, the force and moment resultants are obtained as:

$$N_x = \sum_{p=1}^n \int_{-t_p/2}^{t_p/2} \sigma_x dz \quad (h)$$

$$M_x = \sum_{p=1}^n \int_{-t_p/2}^{t_p/2} \sigma_x z dz \quad (i)$$

General Load-Deformation Relations: Laminate Stiffnesses:

Substituting equation (e) for the layer stresses in equations (h) and (i) above, one can obtain:

$$N_x = \sum_{p=1}^n \left\{ [Q_{xx}]_p [\epsilon_x''] \int_{h_{p-1}}^{h_p} dz + [Q_{xx}]_p [\kappa_x] \int_{h_{p-1}}^{h_p} z dz \right\} + \dots \quad (j)$$

$$M_x = \sum_{p=1}^n \left\{ [Q_{xx}]_p [\epsilon_x''] \int_{h_{p-1}}^{h_p} z dz + [Q_{xx}]_p [\kappa_x] \int_{h_{p-1}}^{h_p} z^2 dz \right\} + \dots \quad (k)$$

where h_p and h_{p-1} are the heights of the top surface and bottom surface of the ply from the reference plane. In the expressions above, the stiffnesses $[Q]^p$, reference plane strains $[\epsilon'']$, and curvatures $[\kappa'']$ are taken outside the integration operation since they are not functions of z . Of these quantities only the stiffnesses are unique for each layer p , whereas the reference plane strains and curvatures refer to the entire laminate and are the same for all plies. Thus equation (g) can be written as:

$$M_x = [B] \left[\varepsilon'' \right] + [D] [\kappa] \quad (l)$$

where

$$B_{ij} = \frac{I}{2} \sum_{p=1}^n Q^p_{ij} (h^2_p - h^2_{p-1}) \quad (m)$$

$$D_{ij} = \frac{I}{3} \sum_{p=1}^n Q^p_{ij} (h^3_p - h^3_{p-1}) \quad (n)$$

In terms of Z_p (the height of the centerline of a ply from the reference plane) and t_p (the ply thickness), equation (n) can be re-written as (for the entry 11):

$$D_{11} = \sum_{p=1}^n \left[t_p Z_p^2 + \frac{t_p^3}{12} \right] (Q_{11})_p \quad (o)$$